DEVELOPMENT OF A VIDEO-BASED SLURRY SENSOR FOR ON-LINE ASH ANALYSIS

by

Peter L. Dunn

Thesis submitted to the Faculty of the

Virginia Polytechnic Institute and State University

in partial fulfillment of the requirements for the degree of

MASTER OF SCIENCE

in

Mining and Minerals Engineering

APPROVED:

Dr. Gregory T. Adel, Chairman

Dr. Gerald H. Luttrell

Dr. Roe-Hoan Yoon

November, 1996
Blacksburg, Virginia

Key Words: Optical Sensors, Image Analysis, Coal Preparation

DEVELOPMENT OF A VIDEO-BASED SLURRY SENSOR FOR ON-LINE ASH ANALYSIS

by
Peter L. Dunn

Committee Chairman: Dr. Gregory T. Adel

Mining and Minerals Engineering

ABSTRACT

The implementation of process control in fine coal processing operations has traditionally been limited by the lack of adequate on-line ash sensors. Several nuclear-based analyzers are available, yet none have seen widespread acceptance by the coal industry. This is due largely to their high cost, the influences of seam type and pyrite content on accuracy, and the inconvenience of having radioactive sources in a plant. Thus, reliable process control of fine coal circuits is often unobtainable due to the lack of on-line monitoring devices for ash content in process slurry streams.

Recently, a video-based slurry sensor for ash analysis of coal tailings has been developed which provides a low cost, reliable ash-monitoring system suitable for use as a process control sensor. The video-based slurry sensor is mounted in a small sump which is continuously fed with coal tailings. The slurry presentation system uses a pressurized tube to rapidly acquire samples of tailings slurry. The video-based sensor employs a black-and-white television camera to acquire live images of the slurry samples. These images are then processed by the PC-based image analysis system to rapidly determine ash content. An adaptive calibration system is used in conjunction with manual monitoring

and sampling to provide a means for continuous improvement of the measurement accuracy.

Problems with sample illumination and sample presentation have plagued previous developments of on-line optical sensors. The video-based slurry sensor developed in this work uses a unique sample presentation system to provide high-quality slurry images on-line. The possibilities of using this technology in other mineral processing applications are abundant.

ACKNOWLEDGMENTS

Firstly I would like to thank Dr. Greg Adel for his guidance of this project. His continual support was the single most crucial aspect of the completion of this work. He firstly served as primary motivation for my entering the department of Mining and Minerals Engineering, and he later employed me as a lab assistant which certainly helped me get through undergraduate schooling. Dr. Adel then served as an advisor and friend throughout this work, and I consider myself blessed to have worked under him. Thanks to Dr. Gerry Luttrell for his invaluable ideas and input during the course of this work, and thanks to Dr. Yoon for serving on this thesis committee and for his encouragement in my study of mineral processing.

Thanks must be given to the Department of Energy, particularly their University Coal Research program, through which this project was funded under contract number DE-FG22-94PC94226. Also, through the UCR intern program, I was able to work with an excellent student from another university, Gerald Lilly, whose aid in completion of an important aspect of this work was greatly appreciated.

Many thanks to other VPI&SU departmental faculty and students, especially those working at the Plantation Road research facility; for their friendship and support during all phases of this work. Thanks to Eva Cruz for her direct assistance with this project, and the educational opportunity working with her provided. The ideas from Jason Pyecha and Eric Yan and technical support from Wayne and Billy Slusser were invaluable. Alisa Alls

must be thanked for continually arranging for transportation, accommodations, and orders during completion of the work.

Thanks to the operators at the Middlefork and Maple Meadow coal preparation facilities who put up with my burdening presence at their sites, and for their willingness to facilitate the project in any and all ways possible. Thanks to Van Davis and Fred Stanley of Pittston Coal Company for their support of this work at the Middlefork plant.

Special thanks to my wife Michelle for her support, understanding, and motivation throughout this project. Thanks also to my parents for their continual support and guidance throughout both my undergraduate and graduate years.

Lastly and most importantly, I would like to thank God for his love and countless blessings.

TABLE OF CONTENTS

		Page
	Abstract	ii
	Acknowledgments	iv
	Table of Contents	vi
	List of Figures	ix
	List of Tables	xi
1	**Introduction**	1
	1.1 Background	1
	1.1.1 Magnitude of the Industry	2
	1.1.2 Importance of Process Control	3
	1.2 Literature Review	5
	1.2.1 Review of Ash Measurement Techniques	5
	1.2.2 Optical Sensors	10
	1.2.3 Video-Based Image Analysis	14
	1.2.4 Video-Based Sensors in Mineral Processing	17
	1.3 Objective	29
	1.4 Scope	30
2	**Sensor System Development**	32
	2.1 Image Analysis System	32
	2.2 Slurry Sample Presentation System	33
	2.2.1 Prototype 1	35
	2.2.2 Prototype 2	37
	2.2.3 Prototype 3	42
	2.2.4 Further Modifications	47
	2.3 Final Sample Presentation System Design	50

			Page
3	**Testing and Verification**		53
	3.1	Test Sites and Material Description	53
		3.1.1 Middlefork Preparation Facility	53
		3.1.2 Maple Meadow Preparation Facility	58
	3.2	Initial In-Plant Testing	61
		3.2.1 Middlefork Plant Visit One	61
		3.2.2 Middlefork Plant Visit Two	64
	3.3	Parametric Investigations	68
		3.3.1 Gray Level Statistical Parameters	69
		3.3.2 Monochromatic Illumination	70
		3.3.3 Percent Solids	75
		3.3.4 Solids Size Distribution	77
		3.3.5 Light Intensity	79
		3.3.6 Sample Tube Angle	81
		3.3.7 Number of Images per Sample	83
		3.3.8 Sensor Warm-Up	85
	3.4	Continued In-Plant Testing	88
		3.4.1 Middlefork Plant Visit Three	88
		3.4.2 Middlefork Plant Visit Four	91
		3.4.3 Middlefork Plant Visit Five	94
		3.4.4 Comparison of Middlefork Plant Visits Four and Five	98
		3.4.5 Maple Meadow Plant Visit One	101
		3.4.6 Maple Meadow Plant Visit Two	105
		3.4.7 Maple Meadow Plant Visit Three	108
	3.5	Installation of Illumination Standard	111

			Page
4	**On-Line Installation**		115
	4.1	System Arrangement	115
	4.2	Software Development	118
	4.3	On-Line Calibration	120
	4.4	Performance Evaluation	125
5	**Summary and Conclusions**		132
6	**Future Work**		135
	6.1	Long Term Sensor Performance	135
	6.2	Investigation of Alternative Imaging Systems	136
	6.3	Sensor-Based Control System	137
	6.4	Additional Applications	138
References			139
Appendix A	**Sensor Software**		142
Appendix B	**Sensor Log File**		153
Vita			161

LIST OF FIGURES

		Page
1.1	Schematic Diagram of Optical Ore Sorter	12
1.2	Schematic Diagram of Virginia Tech Optical Phosphate Analyzer	19
2.1	Generic Schematic Diagram of Slurry Sensor Image Analysis System	34
2.2	Schematic Diagram of Prototype One Sample Presentation System	36
2.3	Schematic Diagram of Prototype Two Sample Presentation System	38
2.4	Prototype Two Reflected Light Image	41
2.5	Prototype Two Transmitted Light Image	41
2.6	Schematic Diagram of Prototype Three Sample Presentation System	43
2.7	Prototype Three Reflected Light Image	45
2.8	Sample Presentation System Cross-Section Showing the Illumination Standard	49
2.9	Overall Schematic Diagram of Video-Based Slurry Sensor	51
3.1	Percent Ash Versus Time for the Feed, Product, and Tailings Streams from a Middlefork Flotation Column	57
3.2	Coal Recovery and Yield Versus Time for a Middlefork Flotation Column	57
3.3	Mean Gray Level Versus Ash Content for Middlefork Plant Visit One	63
3.4	Mean Gray Level Versus Ash Content for Middlefork Plant Visit Two	67
3.5	Gray Level Histograms Obtained of Multi-Colored Dots with Various Forms of Illumination	73
3.6	Gray Level Histograms of Flotation Tailings Slurry Obtained with Various Forms of Illumination	73
3.7	Mean Gray Level Versus Ash Content for Slurry Samples Illuminated with Various Forms of Light	74
3.8	Effect of Percent Solids on Mean Gray Levels for a 76% Ash Sample	76
3.9	Effect of Light Intensity on Mean Gray Levels for a 76% Ash Sample	80
3.10	Effect of Number of Images Collected Per Sample for a 76% Ash Sample	84

		Page
3.11	Mean Gray Level as a Function of Time For Samples with Similar Ash Content and Percent Solids	87
3.12	Effect of Warm-Up Time on Mean Gray Levels Obtained Using Slurry and Paper	87
3.13	Mean Gray Level Versus Ash Content for Middlefork Plant Visit Three	90
3.14	Mean Gray Level Versus Ash Content for Middlefork Plant Visit Four	93
3.15	Mean Gray Level Versus Ash Content for Middlefork Plant Visit Five	97
3.16	Mean Gray Level Versus Ash Content for Middlefork Plant Visits Four and Five	99
3.17	Mean Gray Level Versus Ash Content for Maple Meadow Plant Visit One	104
3.18	Mean Gray Level Versus Ash Content for Maple Meadow Plant Visit Two	107
3.19	Mean Gray Level Versus Ash Content for Maple Meadow Plant Visit Three	110
3.20	Slurry Gray Level Percent Change Versus Illumination Standard Gray Level Percent Change for Varying Lighting Conditions	114
4.1	Schematic of the Industrially Hardened Video-Based Ash Analyzer	117
4.2	Simplified Flowsheet of Video-Based Ash Analyzer Operation	119
4.3	Mean Gray Level Versus Ash Content for Raw Data and Illumination Standard Corrected Data	122
4.4	Initial On-Line Slurry Ash Analyzer Calibration	124
4.5	Slurry Ash Analyzer Calibration Plotted With a 90% Prediction Interval	126

LIST OF TABLES

		Page
3.1	Typical Ash Content and Percent Solids Ranges for Middlefork Column Feed, Product, and Tailings	54
3.2	Typical Ash Content and Percent Solids Ranges for Maple Meadow Flotation Feed, Product, and Tailings	60
3.3	Results of a Size Distribution-Based Ash Analysis of the Maple Meadow Conventional Flotation Circuit	60
3.4	Ash Content, Percent Solids, and Mean Gray Levels for Samples from Middlefork Plant Visit One	63
3.5	Ash Content, Percent Solids, and Mean Gray Levels for Samples from Middlefork Plant Visit Two	66
3.6	Mean Gray Levels of a 76% Ash Sample for Varying Percent Solids	76
3.7	Size Distributions for Samples 5 and 19 from Middlefork Plant Visit Two	78
3.8	Mean Gray Levels for Varying Light Intensities for a 76% Ash Sample	80
3.9	Mean Gray Levels for Sample Tube Angles for a 76% Ash Sample	82
3.10	Ash Content, Percent Solids, and Mean Gray Levels for Samples from Middlefork Plant Visit Three	90
3.11	Ash Content, Percent Solids, and Mean Gray Levels for Samples from Middlefork Plant Visit Four	92
3.12	Ash Content, Percent Solids, and Mean Gray Levels for Samples from Middlefork Plant Visit Five	96
3.13	Ash Content, Percent Solids, and Mean Gray Levels for Samples from Maple Meadow Visit One	103
3.14	Ash Content, Percent Solids, and Mean Gray Levels for Samples from Maple Meadow Visit Two	106
3.15	Ash Content, Percent Solids, and Mean Gray Levels for Samples from Maple Meadow Visit Three	109
3.16	Slurry Sample and Illumination Standard Percent Gray Level Changes With Varying Lighting Conditions	113

		Page
4.1	Ash Content, Percent Solids, and Mean Gray Levels for Samples from Middlefork Initial On-Line Calibration	121
4.2	Calculated Confidence and Prediction Intervals at 72.7% Ash for Initial and On-Line Sensor Testing	128
4.3	Performance Comparison of Coal Tailings Ash Analyzers	131

CHAPTER 1
INTRODUCTION

1.1 BACKGROUND

The production of coal in this country is an essential part of the maintenance and expansion of society's welfare. Throughout the world, coal is the most widely used source of energy for the generation of electrical power. Metallurgical coking coal is also widely used by the steel industry. Worldwide coal reserves have recently been estimated at 1,039,182 million tons. At the present rate of consumption, these reserves should last for nearly 250 years. United States coal reserves alone account for nearly one quarter of this figure [1].

Recently, increased concern on the quality of emissions from coal fired power plants has prompted legislation regulating the quality of coal burned for the generation of electrical power. Coking coal is also used in a host of metallurgical operations where tight quality restrictions on finished products mandate more effective coal cleaning. As additional quality demands are placed on coal producers, technology must be developed to enable cost-effective clean coal production. Process control technology can help to maximize the efficiency of coal preparation plants provided appropriate sensors are available. Thus, the development of low-cost, reliable and accurate sensors is imperative if the coal industry is to take advantage of modern process control technology and stay competitive in a demanding marketplace.

1.1.1 *Magnitude of the Industry*

The production of coal is an enormous industry, with worldwide production estimated at over 4 billion tons per year. United States coal production alone is estimated at nearly 900 million tons per year. Increasing international competition in existing coal markets and the environmental pressure placed on the industry by the 1990 Amendments to the Clean Air Act, have restricted the grades of coal that can be marketed [1]. Therefore, approximately 50% of the total coal produced in the United States has to undergo some sort of beneficiation to meet product quality specifications. For Appalachian coals this number increases to approximately 80%.

Coal cleaning is carried out by several different processes. Generally, coarser coal is treated by gravity separation methods including dense media vessels and spirals. Finer sized material is cleaned by methods involving particle surface treatment, predominately froth flotation. The cost of cleaning coal may be 15-25 % of the cost of mining, and of this fraction, the cost of cleaning the fine coal may be several times more expensive than the cost of cleaning the coarse coal [2]. These facts readily demonstrate the need for improved, cost-effective control of coal preparation circuits.

1.1.2 *Importance of Process Control*

Automatic process control of coal preparation provides numerous benefits. Through process control, operating costs are reduced, equipment utilization and throughput is maximized, and downtime is minimized [2]. Taken together, these factors allow for the efficient production of clean coal within strict quality specifications. Meeting these coal quality specifications is imperative in order to meet the increasingly tight, market-driven limits on ash and sulfur content of clean coal products. General market practices also mandate production of consistent quality products for maintenance of quality business relationships.

Process monitoring devices are the key to a beneficial control system. Measurement of plant operating parameters such as material flow rates, pump operations, sump levels, reagent addition, and parameters specific to the operation of different pieces of equipment are crucial to a control system. Even more crucial are sensors which monitor the quality of material streams, yielding information such as ash and sulfur content and percent solids.

Automatic process control in the area of fine coal processing has traditionally been limited by the lack of adequate quality sensors. Several nuclear sensors have been developed, and a few have proven applicable for process control of fine coal cleaning circuits, yet none have seen widespread acceptance. This is due mainly to their exorbitant cost and the inconvenience of housing radioactive sources in preparation plants. The measurements of these nuclear devices also tend to vary with changes in seam type and pyrite content. Currently, determination of ash content of coal slurries is normally

performed by labor-intensive laboratory procedures that take at least a day to complete. Coal slurry samples are filtered or otherwise dewatered, then placed in an oven for several hours to further reduce moisture content. The dried samples are then placed in a thermogravimetric ashing furnace where, after several hours, the ash contents of these samples are determined. Although these measurements are very accurate, they are nearly useless in the case of process control due to the lengthy turnaround time between taking the samples and obtaining the ash values.

Thus, it is clear that accurate, reliable and inexpensive on-line instrumentation is needed in order to properly determine the ash content of fine coal slurries for process control purposes. While on-line analysis of coarse coal has now become common place, fine coal slurry analyzers are still lacking in operating coal preparation plants. The following review serves to summarize the state-of-the art in on-line ash analysis of coal and alternative techniques for conducting this type of analysis.

1.2 LITERATURE REVIEW

1.2.1 *Review of Ash Measurement Techniques*

Ash is the material which remains after coal has been combusted. It generally consists of the oxidized forms of the mineral constituents found in coal, including clay material, silica, and pyrite. In the past, measurements of the ash content of coal process streams have mainly been performed using two techniques. The relationship between specific gravity and ash content of coal has been used to indirectly determine ash content on-line. More commonly and effectively, nuclear based sensors have been developed that exploit the difference in effective atomic number between the carbonaceous portion of coal and the minerals which make up the ash fraction.

The first ash analyzers that were developed utilized the relationship between specific gravity and ash content of coal. These density meters were developed in a variety of configurations. They were mainly used to roughly measure ash contents of coarse coal (e.g., greater then 12.7 mm). Representative coal samples were weighed underwater to determine the specific volume, and a correction was normally applied to account for the moisture content of the coal. Using the specific volume measurement, a crude determination of the ash content of the sample could be made knowing the proper specific gravity/ash content relationship for the specific sample. Any change in the size distributions of the samples affected the specific volume and in turn adversely affected the accuracy of the measurement [3]. Although sensors of this type provided quick, rough measurements of ash content of coal samples, they were simply not suitable for accurate on-line use.

In more recent times, more elaborate density-based slurry ash sensors were developed that used gamma density gauges and magnetic flowmeters to determine specific gravity of the solids, subsequently allowing determination of the ash content of coal slurry on-line [3]. One advantage of these sensors was the additional measurements that were obtained such as flowrate and percent solids. These sensors were an improvement over the bulk-volume-type density sensors, yet they still lacked the accuracy necessary to be used effectively as process control tools.

The most common types of on-line ash analyzers used today are nuclear based. Nuclear-based coal analyzers are typically of two types, those that are based on radiation absorption and those that are based on back-scattered radiation. In both cases, the amount of radiation absorbed or scattered is proportional to the effective atomic number of the coal, and thus, the ash content. When nuclear sensors were first introduced, carefully prepared dry coal samples were necessary to ensure relatively accurate ash measurements. Over several decades, continued research and development has improved the ruggedness and accuracy of these devices. In the last 15 years several nuclear based sensors have been developed which are capable of measuring the ash content of coal slurry on-line.

One of the first nuclear-based ash analyzers, the Cendrex, was developed in the nineteen sixties by the Dutch State Mines [3]. With this device, samples were dried and crushed to minus 0.25 mm, spread out into a level bed, and analyzed for ash content based on radiation absorption. The main disadvantages of this and ensuing similar sensors that were developed were the elaborate sample preparation procedures, and the variations in

absorbed and/or back-scattered radiation due to the presence of trace amounts of calcium, sulfur, and chlorine [3]. Continued development of sensors of this type led to several improvements. These improvements included: reduced costs of radioactive sources, deeper bed penetrations, and use of coarser samples. The most significant improvements were those that allowed measurements to be taken directly on conveyor belts, normally after the sample passed under some sort of leveling device [4].

Over the years, research and development continued in the area of nuclear based ash sensors, with the focus on developing sensors that would permit effective on-line quality control through process control schemes. Also, with the increasing amount of fine coal being processed, it was realized that plant operating costs could be greatly reduced and overall plant yields could be maximized by improving fine coal recovery. This growing area of fine coal processing helped lead to the development of on-line ash analyzers for coal slurries.

Nuclear based slurry ash analyzers require at least two measurements, percent solids and ash content of the solids. Gamma density gauges employ radiation absorption techniques, where the loss in intensity of the gamma radiation applied to a sample is related to the material density. Again, the solids ash content measurements are made by either radiation absorption or back-scattering techniques. The effective atomic number of the combustible carbonaceous material on coal is about 6, while the effective atomic number of the ash-forming minerals varies around 10 [5]. Thus, the overall effective atomic number of coal will increase with increased ash content, and the ash content can theoretically be determined by measuring the radiation absorption or scatter. One

advantage of the back-scatter measurement technique is that by analyzing the back-scattered iron peak, corrections can be applied for the amounts of iron-bearing minerals such as pyrite and pyrrhotite that are present in the coal. These minerals have a much larger effective atomic number (i.e., about 20), and can greatly influence the resulting ash measurements.

Several on-line nuclear-based slurry sensors are currently on the market. They vary by the types of radioactive sources that are employed, and by way that ash measurements are performed. Normally these sensors are only suitable for certain process streams, and each has specific ash and percent solids ranges of accurate operation. An in-depth review of the nuclear based on-line ash analyzers can be found in the literature [6]. Very few of these available sensors have made it to commercial applications in the U.S., thus, a fair comparison of the various commercial sensors is nearly impossible.

There are several factors which explain why these nuclear based sensors have not realized widespread acceptance. Due to the necessity of measuring percent solids along with solids ash content, a typical installation for on-line ash analysis of a coal slurry requires either two radioactive sensors (i.e., an ash analyzer and a gamma density gauge) or a single sensor with two radioactive sources. The hassles associated with housing radioactive sources in a plant also play a large role in their non-acceptance. As previously stated, nuclear based sensors can also suffer from inaccuracy when there are variations in the amount of high atomic number minerals (e.g., pyrite) present in the coal. This problem is particularly noticeable when a sensor is installed in a plant which processes multiple seams. The sensors based on back-scattered radiation are sometimes able to compensate

for variations in pyrite content through use of the back-scattered iron peak. In most cases, however, a separate calibration is required for each seam or blend that is analyzed. Another problem is the presence of entrained or entrapped air in the slurry. This air can cause unacceptable noise in the signal from a nuclear ash analyzer. Thus, most nuclear ash analyzer installations also require some form of deaeration system. These deaeration systems, along with the associated sample handling equipment and the radioactive sources, tend to make on-line nuclear slurry analyzers relatively expensive.

1.2.2 *Optical Sensors*

Optical sensing and image analysis are broad subjects that have undergone intense research for many decades. In almost all types of manufacturing and production industries, long before any sort of on-line instrumentation was developed, human operators used visual inspection as a means of evaluating processing operations. It is this trait that is generally exploited by any type of optical sensor. Even today, skilled operators use visual inspection of processing and manufacturing operations for evaluation and control purposes. As a result of this past history, optical sensors based on what a human operator would see and decide during visual inspection of a process, were immediately beneficial. Thus, developments to improve sensing technology and broaden optical sensor applicability have continued to gain momentum in recent years.

In mining and mineral processing operations, human operators were, and in many cases still are, the primary means of identifying mineral compositions, grades, particle sizes, and efficiencies of separation equipment and processes. One of the earliest forms of optical instrumentation used in mineral processing was the optical ore sorter [7]. This device was used economically to sort ore that was liberated at fairly coarse sizes (i.e., greater than 10 mm). Since the display of individual particles was imperative for the proper operation of the ore sorter, particle surfaces were generally washed, and the ore was fed in a monolayer to the sensor. One popular mechanical configuration of this type of sensor was to reflect laser light off the particles as they fell from the end of a belt. An estimation of the material grade was related to the intensity of the reflected light, and gangue (low quality material) was rejected from the material stream by timed air blasts.

Several different optical ore sorters were developed and used in a variety of mineral processing applications. A typical configuration is shown in Figure 1.1. Sorting of coarsely-sized industrial mineral ores was among the most popular of the applications of these early optical sensors. In addition, optical ore sorters found some use in the South African gold industry where they were used to separate light-colored, gold-bearing ore from dark-colored gangue [7]. Likewise, diamond ores have been processed by optical ore sorters, using X-rays to illuminate the mineral surfaces. X-rays cause diamonds to fluoresce, and this fluorescence can be detected by a photomultiplier which activates an air blast diverting the diamonds from the ore stream.

In recent years, an optical device for monitoring the ash content of coal flotation tailings has been developed [8]. This device uses a test-tube-like probe that is inserted into a canister which receives coal flotation tailings. Laser light is transmitted along a fiber optic cable to the probe, and back-scattered light is measured by a photoconductor. The amount of back-scattered light is taken to be proportional to the ash content of the slurry. An ultrasonic transducer is employed to prevent material from collecting on the probe, which hinders both the initial light transmission and the measurement of the reflected light. The sensitivity of this device limits its use to tailings streams. Also, measurement error due to varying percent solids and material collection on the probe have severely hampered the probe's applicability as a process control sensor. As a result, this device has not seen widespread use.

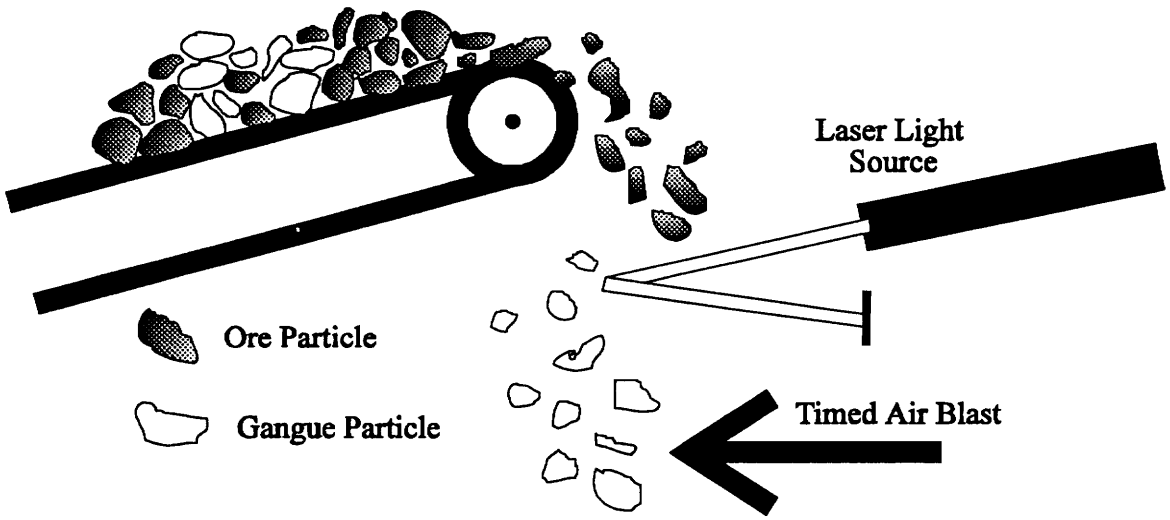

Figure 1.1 Schematic Diagram of Optical Ore Sorter

Optical sensors have proven to be very valuable tools for replacing human operators as visual inspectors across a broad spectrum of industries. The most simple forms of these sensors generally employ some sort of illumination scheme and a way to measure the amount of light that is reflected from an object or surface. The technology is standard and there are many applications of these traditional optical sensors which have yet to be explored. Some examples of present applications include: defect determination on color picture tubes, rapid inspection of bolt heads and threads, verification of the presence and placement of items within packages, and sorting of reject brake shoes [9].

Sensors of this type have seen some use in the mining and mineral processing industry, primarily as ore sorters. However, in most mineral processing applications, the processes being visually monitored are difficult to classify as simply "right" or "wrong". Thus, traditional reflective-light-based optical sensors have seen limited use. In many plants, the operators are still the prevalent "optical sensors" for parameters such as material size, process stream quality, reagent conditions, and percent solids.

1.2.3 *Video-Based Image Analysis*

Video-based image analysis can be used to develop sensors that mimic a human operator's visual observations. These devices can often replace more costly and complex sensors. In the last decade, the cost of desktop computers, image acquisition hardware, and image analysis software has dropped, making the use of computer vision technology remarkably economical.

Traditional image analysis had its origin decades ago when computers were first utilized to analyze two-dimensional scenes in applications that included character recognition, medical diagnosis, and satellite photography [10]. These classical applications required such image analysis techniques as image segmentation, geometric property measurements, and object and boundary recognition. The principles of image acquisition and digitization, and low- and high-level image processing, remain the same as they were with traditional image analysis systems. It is because of the immense technological advancements of the means by which the images are captured, digitized, and analyzed, that video-based image analysis has seen such widespread application over a broad spectrum of industries.

An image analysis system consists of several integral parts. The two main parts of any image analysis system are (i) a means of acquiring and digitizing an image into a computer recognizable format, and (ii) software with which to process the digital images and extract any valuable information. Since this work is focused on video-based image analysis, these types of systems will be discussed.

Images are normally acquired using high-speed television cameras which come in several shapes and sizes with features that vary depending on the application. Proper object or sample illumination is extremely important and should not be overlooked. The type, intensity and geometric orientation of sample illumination is critical, and can drastically affect the consistency and quality of images if not held constant. The high-speed camera is normally linked to a desktop PC that is equipped with some sort of frame-grabber board. These boards also come in a variety of configurations depending on the application. The frame-grabber board accepts the analog signal of the video camera and digitizes or "translates" the signal into an array of 8 bit pieces of information (bytes). These bytes of information are ultimately scaled to decimal values ranging from 0 to 255 [10]. Once an image is acquired and digitized, the live image can be displayed either on a television monitor or, with special equipment, directly on the PC's VGA monitor. This live video image is "frozen" and analyzed using a variety of image processing packages.

There are several analysis methods that are applied to images based on the type of information that is desired. Low-level image processing is occasionally performed in order to improve the image and thereby increase the amount of valuable information that can be extracted. Some examples include noise reduction, image smoothing, and a variety of image enhancing filters. Often, at this level, some intrinsic image parameters are quantifiable such as object orientation, range, and velocity [10]. Once an image has been frozen and enhanced, high-level image processing routines can be carried out. Some commonly sought after image parameters are object geometry, size, orientation, edge/boundary detection, and color or gray level.

Most video-based image analysis systems utilize black and white cameras. During the digitization process, each pixel in an image space is assigned a gray level value ranging from 0-255, with zero being a black pixel and 255 signifying a white pixel. Cumulatively, this pixel-by-pixel gray level information can be viewed in a histogram format, permitting manipulation in a variety of ways to provide quantitative information about the image. It should be noted that color image analysis systems are now available; although many technological barriers still prevent the widespread application of these devices as rapid sensors. Some of these barriers include the necessity for more computing power, intricate optics, and even more sensitive and critical illumination schemes [9]. Some examples of the immense applications of video-based image analysis systems as sensing devices include: inspection of printed circuit boards, shrimp grading, drill bit wear analysis, denim dye streak inspection, citrus fruit grading, poultry grading, solder joint inspection, and inspection of glass objects for cracks, bubbles, and loose slivers [9].

Today, the use of image analysis is relatively common in the mining and mineral processing industries. For example, in the mid to late 1970's, off-line image analysis was introduced as a means of determining mineralogy, size, shape, texture, and degree of liberation of ores. Though this type of analysis requires elaborate sample preparation, it has grown to be quite common and continues to be extremely valuable in understanding minerals and mineral textures. In the last decade, the use of video-based image analysis systems as sensors for mineral processing applications has been explored. The following is a summary of some of the recent research in this area.

1.2.4 *Video-Based Sensors in Mineral Processing*

Research into the use of video-based sensors in mineral processing has become increasingly common in the last decade. The low cost, versatile nature of these types of sensors has helped them gain acceptance in process control applications. Video-based sensors are normally designed to mimic the visual observations of plant operators. Hence, they tend to be more acceptable to plant personnel. Several different applications of video-based image analysis sensors have been researched, and a few have seen successful commercial application.

Phosphate Analysis

One of the first mineral processing applications of video-based image analysis sensors was in the phosphate industry. The initial work leading to the development of the video-based phosphate analyzer was carried out at Virginia Tech in 1988, where samples of phosphate ore from Texasgulf, Inc. were mixed together in various quantities, spread out on white pieces of paper, and placed in front of a television camera [11]. An appropriate gray level was chosen to separate the light gangue minerals from the darker phosphate minerals, and the image was segmented. It was found that the area percent of the dark portion of the sample correlated well with the percent P_2O_5. It was this finding that led to increased research on video-based sensors in the phosphate industry.

In 1990, joint research by the U.S. Bureau of Mines (USBM) and the University of Alabama led to the development of a preliminary system for quantitative identification of the components of phosphate ore [12]. As compared to the earlier work at Virginia Tech which looked at the overall gray level of the phosphate sample, this work focused on

identifying the characteristics of individual mineral grains. The number of pixels associated with specific mineral grains in the sample was related to the total number of pixels in the image. This ratio provided a measurement of the volume percent of a specific mineral in the sample.

In 1992, research conducted at Virginia Tech resulted in the development of a rapid video-based analyzer to determine P_2O_5 content and CaO/P_2O_5 ratio in phosphate ores. A schematic diagram of this optical phosphate analyzer can be seen in Figure 1.2. The system was based around a 25 MHz 386 PC with frame-grabber, a black-and-white CCD television camera, a video monitor, and a gray PVC sample box [13]. The frame-grabber accepts the video-in signal from the camera, and the provides a video-out signal to the video monitor. The line conditioner is used to provide constant voltage to the fiber optic illumination system, which ensures constant uniform sample lighting. The light intensity is monitored by a photocell mounted in the wall of the sample box, and adjustments to the light are made as needed to ensure constant sample illumination.

Dry phosphate flotation concentrate samples are placed in a sample container and positioned in the sample box directly under the television camera. The sample box is closed, the light intensity is adjusted as needed, and an image of the sample is digitized. The resulting gray level information, processed by the computer using the BioScan Inc. Optimas software package, yields measurements of P_2O_5 content and CaO/P_2O_5 ratio.

Optimas is a complete software package for image capture, enhancement, measurement, and analysis. Batch analysis applications were written using the Optimas

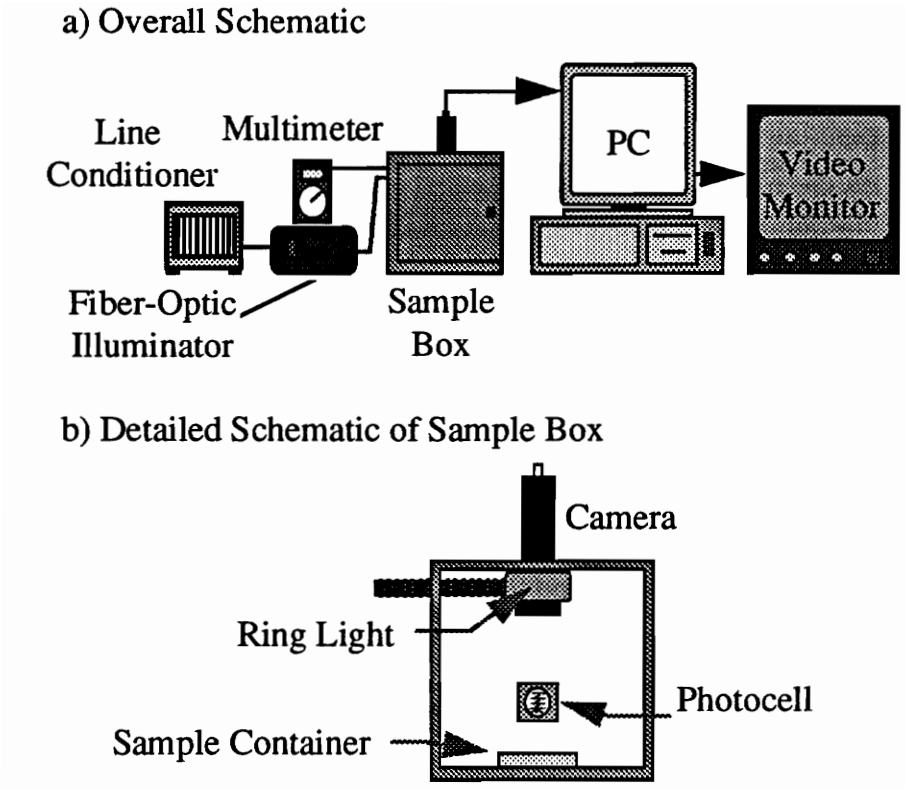

Figure 1.2 Schematic Diagram of Virginia Tech Optical Phosphate Analyzer

environment to provide window-based interfaces for use by plant operators with little knowledge of computers [13]. The analysis program prompts a user to insert a sample into the sample box and to click on the appropriate button to begin analysis. Sample analysis takes approximately fifteen seconds per sample, or under two minutes for an average of five or six samples. P_2O_5 measurements of the fatty acid concentrate stream were found to be accurate to 27.6 ± 0.14 %, while the amine concentrate stream was accurate to 30.3 ± 0.05 %. The accuracy of the CaO/P_2O_5 ratio was reported to be 1.62 ± 0.003 %. These measurements are based on 90% confidence intervals, and are comparable to the results obtained by the time-consuming wet chemical methods that are normally performed. Calibration was found to be difficult on some of the process streams due to color variations in the samples resulting from phosphate staining of the silica and quartz minerals [13]. Overall, however, the Virginia Tech video-based phosphate analyzer has seen excellent success, and two of these devices are now used routinely by Texasgulf (now PCS Phosphate) in their North Carolina phosphate processing facility.

IMC Fertilizer Inc. developed a similar video-based phosphate analyzer in 1993 for use in their Florida phosphate operations [14]. The operating principles behind the image analysis system are very similar to the Virginia Tech optical phosphate analyzer, with a few mechanical differences. Representative samples of process streams are taken and placed in a vibrating pan feeder. The material is then allowed to fall vertically through a light-tight box which houses a horizontally mounted television camera. The light source is flashed synchronous to the image capture rate of the camera in order to "freeze" particle motion and eliminate vertical distortion [14]. Eight images are captured and saved while

the sample is flowing to ensure that a representative portion of the sample has been imaged. Sensor operations are operator controlled using a simple touch screen interface. The captured images are then processed using the same gray level techniques as were used with the Virginia Tech sensor. In the case of the IMC application, however, the amount of insoluble material (i.e., sand) is measured due to the color variations in the phosphate minerals normally found in Florida deposits.

The accuracy of the IMC sensor has been limited for several reasons. The flowing material provides a much more difficult imaging scenario than imaging a static sample. In fact, since the sensor was developed for off-line use, it is questionable as to why the sensor operation involves imaging of a dynamic, free-falling material stream. Also, stream characteristics of the Florida phosphate material change frequently causing considerable difficulty in maintaining a reasonable sensor calibration. It was found in general that this optical phosphate sensor was only slightly more reliable than operator visual estimates. Furthermore, the improvement was not sufficient enough to receive operator support and confidence. Finally, the sensor accuracy was considerably worse than the accuracy of the wet chemical assays, causing additional discontent among plant operators [14]. This work was performed in-house at IMC Fertilizer Inc., and though no further work has been published, it is likely that the system is still under development for remediation of problems associated with the sensor calibration and operator confidence.

Sulfide Mineral Analysis

In recent years, the USBM has investigated the possibility of using image analysis as a means of measuring the specific mineral content of various mineral mixtures and

flotation froths. In this work, a commercial image analysis system was used that employs fiber optic illumination and detection to perform measurements of product color. Material illumination comes from red, amber, and green light-emitting diodes, while measurements are made on the reflected light produced by each of these three sources. An equation relating the three reflective measurements is used to obtain a single value, and this value is correlated to the sample quality [15].

Using this image analysis system, color measurements were made on pure samples of quartz, chalcopyrite, pyrite, and molybdenite. This was done to facilitate the differentiation between these minerals after they were combined in mineral mixtures. Three dry, binary mixtures were then tested including chalcopyrite/quartz, pyrite/chalcopyrite, and chalcopyrite/molybdenite. Each mixture ranged from 0 to 100% of the two constituents. The results of this work were found to be quite encouraging. The ratios of the chalcopyrite/quartz and molybdenite/chalcopyrite mixtures related extremely well with the corresponding color measurements, while the quartz/chalcopyrite ratio showed a slight correlation with the color measurements.

Color measurements of flotation froths were also made and related to the mineral ratios in the froths. Initially measurements were carried out on laboratory flotation cells. Varying amounts of each mineral combination were added to the flotation cells, agitated for one minute, and froth color measurements were then performed. A good correlation between the color measurement and mineral content was seen for flotation froths of pure chalcopyrite. However, as pyrite was added to the cell, a situation was reached where the pyrite/chalcopyrite mixture yielded the same color measurement as a mineral-barren

chalcopyrite froth. This pyrite/chalcopyrite mixture is probably more realistic from an industrial point-of-view. Thus, it was realized that the color measurements were extremely sensitive to the proportions of realistic mineral ratios in the froths [15].

Froth color measurements were also attempted on a commercial molybdenite flotation circuit. Unfortunately, the results obtained from this in-plant testing were quite different from the laboratory tests as a result of variations in such factors as particle size, pulp density, and most significantly, impurity content. The main problems or deviations from the laboratory tests seemed to be a result of the non-binary mineral system experienced in the actual plant operation. Sensor measurements were also affected by the mist produced above the flotation cells as a result of froth breakage [15]. Despite the obvious shortcomings, the in-plant measurements did show a reasonable correlation between froth color and mineral content. In general, this research proved that the use of image analysis as a process monitoring tool in froth flotation could be feasible.

In the most recent continuation of the USBM research presented in 1994, a true color image analysis system, consisting of a 24-bit color television camera and a PC-based color frame-grabber, was employed for the analysis of mineral mixtures, slurries, and flotation froths. The use of commercial television camera color vector angle measurements provided a novel way of measuring color in mineral systems [16]. All experiments were carried out using mixtures of chalcopyrite (yellow) and molybdenite(gray) since these minerals exhibit distinctively different coloring and are commonly mined and processed together by froth flotation. In all of the experiments, careful attention was paid to the camera calibration (white-balancing) and the control of

the light source. From preliminary work it was found that RGB intensities were difficult to correlate with sample composition, and were adversely affected by small variations in the illumination scheme. The color vector angle, on the other hand, which is determined from chrominance red and blue values obtained from empirical equations on the raw RGB intensity measurements [16], proved to be insensitive to drastic light changes, and was shown to correlate with sample composition much more adequately. The color vector angle has traditionally been used as a means of calibrating commercial television cameras.

The experimental work itself was carried out as follows. Dry mixtures of fine material (-325 mesh) were prepared varying from 0 to 100% chalcopyrite with complementary amounts of molybdenite. The mineral mixtures were spread into a shallow pan and images were taken of the samples. The color vector angle was related to the percentage of the two minerals in the dry mixtures, and an excellent power equation fit was shown [16]. Based on the data presented, it appears that estimates of unknown mixtures can be made within 3% of the actual values. Chalcopyrite/molybdenite slurry mixtures were also prepared at 20 wt. % solids in isopropanol. This approach eliminated the problem of the mineral matter adhering to the sides of the sample beakers. The samples were agitated prior to color measurements to ensuring proper mixing, and images were taken of the sides of the glass beakers. Again, the color vector angle correlated well with the varying sample compositions. It should be noted however that these mineral mixtures are not industrially realistic, as the large portion of impurity (non-sulfide mineral) that is normally found in an actual processing plant has been left out of these laboratory test samples. Also, while preparing slurry mixtures in isopropanol does demonstrate that

the slurry color can be related to mineral composition, realistic slurries must be water-based. The associated problems that needed to be addressed concerning this unconventional liquid substitution were seemingly ignored.

Color measurements were also performed on flotation froths generated from commercial chalcopyrite/molybdenite ores. A reasonable correlation between froth color and the percentage of both chalcopyrite and molybdenite in the flotation froth was observed; however, the fit was not as good as that obtained with the dry and slurried mixtures of pure components. In all fairness to the researchers at the USBM, it should be noted that the flotation froth color measurements were considered preliminary in nature, as image analysis of froth surfaces is a much more complex application due to factors such as varying froth texture, loading, and changes in particle size. These parameters were not investigated at that time of this work, however it is believed that they may play a major role in the measurement of froth color [16].

The importance of froth texture in the image analysis of mineral-laden froths was confirmed in 1994, by continuing research being conducted in South Africa. The image analysis equipment used in this work is similar to that which has been described for previous systems. However, in this case, an inexpensive, commercially-available VHS video camera was used along with a spotlight to acquire images of froths. The video-based sensor was tested with a copper flotation froth, in which the copper occurred mainly in the form of chalcopyrite and bornite. It was found that problems with bright spots and shadows in the image could be reduced by ensuring that the camera and light were placed perpendicular to the froth surface [17]. The camera was linked to a PC and a color frame-

grabber was used to digitize the images in 24-bit color. Although color images were acquired, it should be noted that further analysis work with the froth images involved their conversion to 8-bit gray scale format. Thus, froth color (gray level) measurements were performed and gray level histograms generated. Based on these histograms, it was shown that as the copper content of the froth increased, the mode of a small secondary peak in the approximate range of 216-220 gray levels, increased. A normalized measurement relating the major and minor modal frequencies was developed that was found to be less sensitive to differing illumination conditions. This measurement was successfully related to the froth copper content. Although, some work was done to enhance the froth image using edge detection filters, little or no improvement in the froth color/quality correlation was observed [17].

Utilizing the same image acquisition system, work was done in 1995 to develop a system for classifying froths into specific ranges of bubble size distributions. Bubble size distributions in froths are considered to be indicators of important process parameters such as aeration rate, pH, and the type and quantity of minerals that are adhering to bubble surfaces [17]. Four different froth images with varying average bubble size distributions were used to demonstrate the possibility of using video-based sensors to describe such froth conditions. Fast Fourier transforms (FFT) were used to extract features from the images, specifically for determination of ring geometry [17]. This enabled ring counts to be performed on the images, which were shown to correlate extremely well to the increasing average size of bubble distributions in the four images.

Bubble shape is considered an indicator of material grade, entrainment of gangue particles, and froth drainage. Since the presence of elliptical bubbles can indicate a flowing froth, bubble shape can also be used as an indicator of froth rigidity [17]. The FFT power spectra were found to easily extract geometrical bubble features yielding measures of the average bubble shape in the froth. It was shown that these measurements could be related to the flow direction of froth surfaces. Additional work showed that "slow" and "fast" moving froths could successfully be distinguished by using a camera function that would blur images in proportion to the degree of motion that was detected [18]. The use of video-based sensors for classification of several different froth conditions was demonstrated. The combination of the color-based froth quality measurement with the froth classification algorithm shows that video-based sensors in mineral processing could be inexpensive, valuable tools for on-line process control.

Significant research has been performed in the area of video-based sensors in mineral processing. Generally, the low-cost, versatile nature of commercially available image analysis systems has helped them gain acceptance. While several possible applications of these video-based sensors have been demonstrated, few have seen successful implementation in commercial plant environments. Industrial applications of video-based sensors require hardened, robust systems that are able to hold calibration. The sensitivity of the sensors to parameters such as lighting conditions needs to be reduced, and steps need to be taken to test the video-based systems under plant operating conditions. Also, the very important task of obtaining and analyzing images of slurry samples has not yet been successful performed. Although off-line quality measurements of

dry mineral mixtures and on-line measurements of froth quality can provide valuable process information, there will be even wider applications for video analysis systems that can make direct measurements from slurry samples.

1.3 OBJECTIVE

The objective of this research was to develop and validate a video-based slurry sensor for on-line ash analysis of coal slurry. The system was designed and fabricated based on a PC image analysis system using commercially available imaging hardware and software. A slurry sample presentation system was developed which allows high quality images of the slurry to be acquired and digitized by the image analysis system. Software was written to control the operation of the video-based slurry sensor, and the system was tested during several visits to various coal preparation plants. After a reliable calibration of the sensor was obtained, the slurry analyzer was installed on-line at a coal preparation facility and the sensor performance was validated. An adaptive calibration system was used to allow the sensor performance to continuously be improved. Lastly, the industrially-installed system has been monitored over a period of time to validate it's potential use as a reliable, rapid analyzer of the ash content in coal tailings slurry.

1.4 SCOPE

The presentation of this work has been divided into six sections. The first section describes the importance and practicality of this research, and outlines previous work in this research area. Ensuing sections respectively are System Development, Testing and Calibration, Industrial Installation, Summary and Conclusions, and Future Work.

The chapter titled System Development details the equipment used in the video-based image analysis system, including hardware, software, and various sample presentation system designs. Several alternative sample presentation systems were designed and tested, and the performance of each of these systems is discussed in depth. Finally, a detailed description of the final sampling system configuration is given.

The third chapter describes the testing of the sensor. The facilities at the plant site are described and the types of material encountered in the study are characterized. Initial VCR-based testing of the system at the plant site is presented, followed by results from investigations of critical system parameters. Results obtained from testing the entire PC image analysis system at the plant are discussed. Finally a preliminary calibration of the sensor is developed and presented.

The Industrial Installation chapter discusses the work that was done to enable on-line placement of the video-based slurry sensor. Modifications that were made to the imaging system for on-line use and the setup allowing for a continuous flow of sample to the system are detailed. Finally, the validation of the sensor operation, including discussions of the sampling scheme and the implementation of the adaptive calibration system, is presented, and the overall system operation is evaluated.

The fifth chapter presents the pertinent results from Chapter 4 in an abbreviated format. Data supporting the successful installation of the sensor on-line is presented in both tabular and graphical format, and the results are discussed.

The last chapter in this thesis, Future Work, examines the purpose of the work and the direction of future research activities. Some alternatives to the current imaging system are suggested, and commercialization of the sensor is discussed. Lastly, the possible use of this sensor in process control applications is presented.

CHAPTER 2
SENSOR SYSTEM DEVELOPMENT

2.1 IMAGE ANALYSIS SYSTEM

The purpose of this work was to develop a video-based slurry sensor which would be used specifically to monitor the ash content of coal tailings on-line. The novel work performed in this research was the development of the slurry sample presentation system, which permits the acquisition of high quality images of slurry. The equipment used in the image analysis system itself is very similar to the systems that were described in the literature review. The means of presenting slurry samples to the image analysis system was the most important undertaking of this work, and will be discussed in this section.

The image analysis system is based around a 486 DX2-66 personal computer operating in the Microsoft Windows 3.11 environment. A VisionPlus AT frame-grabber board is used to digitize images received from an RS-170 high speed black-and-white television camera. All image operations and analysis were carried out using BioScan's OPTIMAS image analysis software. A Sony video monitor was used to view the ongoing image acquisition processes. It should be noted that with a later imaging system, the live image can be displayed directly on the PC, eliminating the necessity for a second monitor.

These basic image analysis components are used to acquire, digitize, display, and analyze the slurry images. It is commonly known that the performance of video-based sensors is directly related to the quality of the images that are provided to the system. The following section details the various sample presentation systems that were investigated as a means of providing quality slurry images to the assembled image analysis system.

2.2 SLURRY SAMPLE PRESENTATION SYSTEM

Once all the necessary imaging equipment was assembled, work focused on the development of the slurry sample presentation system. A video-based image analysis sensor can only be expected to perform as well as the quality of the images it receives. The lack of previous work in this area readily demonstrates the difficulty of presenting slurry samples on-line to an image analysis system. From careful investigation of related work, some general objectives were identified for the sample presentation system. These objectives included ensuring the reproducibility of images, providing a constant and even illumination scheme, minimizing sample segregation, and eliminating any sort of interface between the camera and the slurry sample. Figure 2.1 below shows a generic schematic of the video-based slurry sensor. Several different sample presentation system prototypes were developed, and were all tested with the assembled image analysis system.

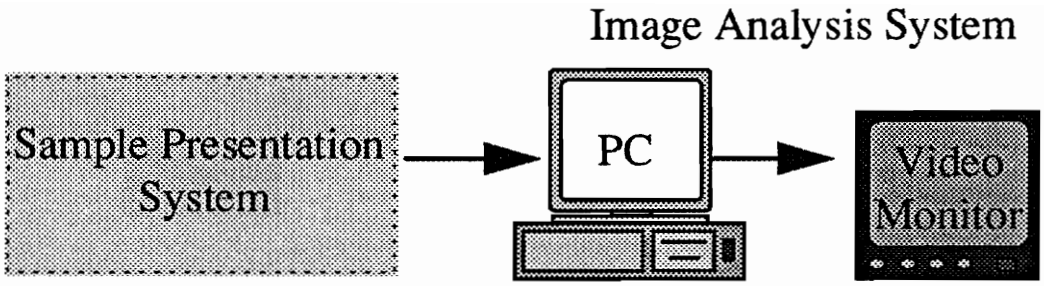

2.1 Generic Schematic Diagram of Slurry Sensor Image Analysis System

2.2.1 *Prototype One*

The initial sample presentation system prototype is shown in Figure 2.2. In this system, slurry is pumped from a sump and fed at an even flow rate to the sample presentation box. The slurry fills the sample box and overflows down the smooth Plexiglas ramp. The overflow material is returned to the sump which allows for closed circuit batch testing. The approximate six inch vertical rise of the slurry in the sample presentation box ensures quiescent overflow conditions across the ramp.

This design had several advantages including the fact that the camera could be mounted in a variety of locations, such as over the ramp, underneath the ramp, over the slurry film as it falls off the ramp, or behind the slurry film. Sample illumination could also be provided using reflected light, transmitted light, or any combination of the two. Unfortunately, preliminary testing of this prototype also revealed several disadvantages. In order to provide an adequately smooth slurry film across the overflow ramp, the flow rate to the sample presentation box had to be relatively low. This allowed suspended particles to settle out and segregate in the box. Increased flow to the sample presentation box eliminated the problem of particles settling out, but at the expense of the even laminar flow across the ramp. In addition, the Plexiglas ramp showed an affinity for the slurry particles. Even at high flow rates, the ramp became dirty and caused the images to darken considerably over time. In order to maintain some of the advantages of this initial prototype while eliminating the disadvantages, a second prototype sample presentation system was developed, and is described in the following section.

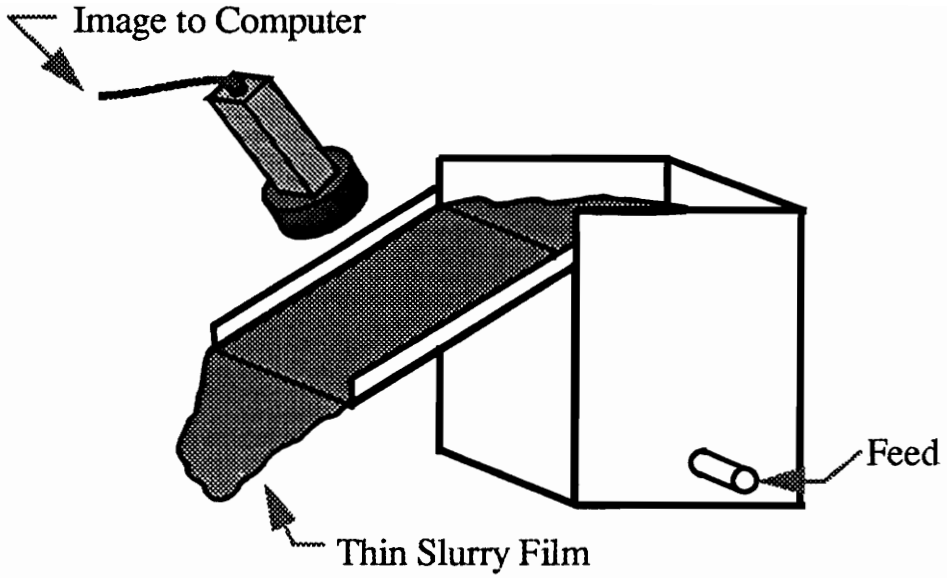

Figure 2.2 Schematic Diagram of Prototype One Sample Presentation System

2.2.2 *Prototype Two*

The second prototype sample presentation system is shown in Figure 2.3. This prototype was designed to take advantage of the smooth slurry film that was seen flowing off the overflow weir of the initial prototype system. This design consisted of three separate, vertically stacked modules, all constructed of opaque PVC material to create a light-free environment. From top to bottom, the first module contains the sample box, the second module houses the camera and lighting systems, and the third module collects material and returns it to the sump.

The first module provides a thin slurry film for viewing by the television. Careful attention was paid to the problems encountered with the initial prototype and this improved design was the result. This module consists of a sample box which receives feed slurry at the top and tapers down to a six inch slot with a 1.8 mm opening. This top to bottom flow scheme eliminated the material settling problem. Furthermore, the vertically falling, unsupported slurry film also eliminates the problem of "support" material getting dirty and darkening images, as was seen with the Plexiglas ramp in the first prototype. This first modules fits tightly into the a slot in the top of the second module.

The second module houses the camera and lighting systems. The television camera, equipped with a 50 mm lens, is mounted on the outside of the second module in an adjustable light-proof enclosure, which also serves as a means of focal adjustment. A ring light is mounted around the camera lens to provide the necessary illumination for reflected light imaging. On the opposite side of the module, a second fiber optic ring light is mounted to provide the necessary illumination for transmitted light imaging. This

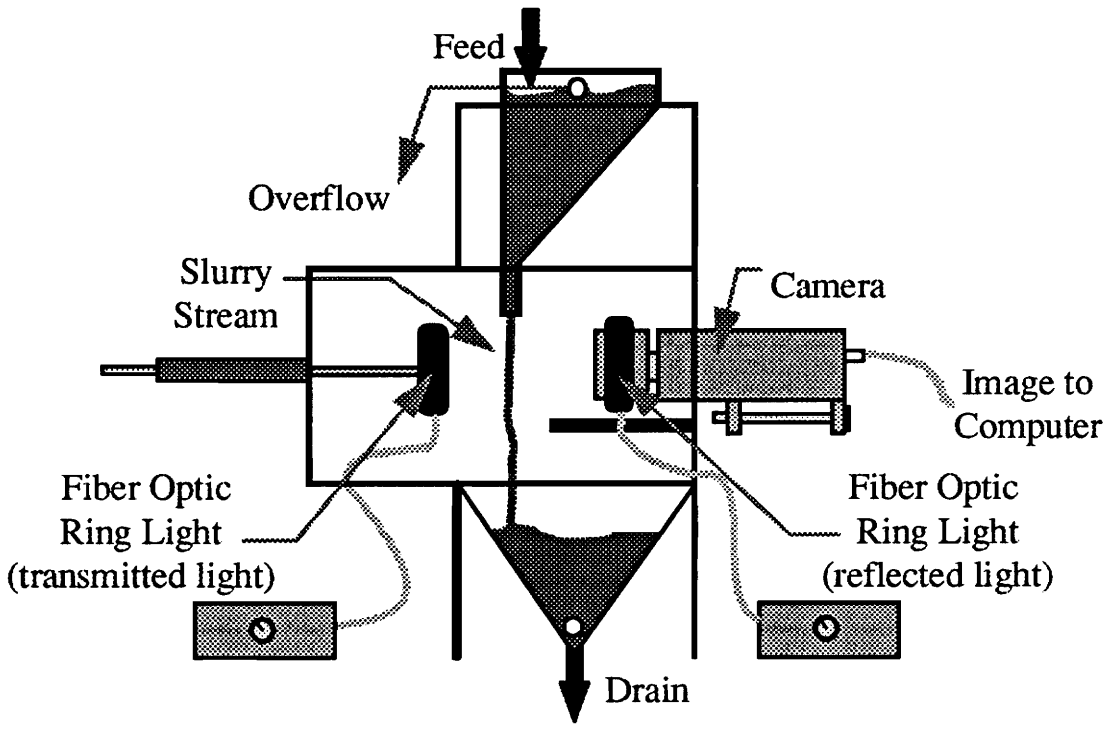

Figure 2.3 Schematic Diagram of Prototype Two Sample Presentation System

second ring light is connected to the side of the module by a light-proof track which allows the illumination distance to be varied. The illumination intensity can also be adjusted by exterior controls on the ring lights.

The third module contains a trough and outlet port which collects the slurry and returns it to the sump. To ensure that slurry does not splash up from the collection system and dirty the camera lens, a splash-guard is installed on the interior beneath the camera, extending out beyond the lens.

Initial tests of the second prototype sample presentation system were carried out using water. From a qualitative perspective, the film appeared to be very smooth as it passed in front of the television camera. However, when coal slurry was added to the system and images were captured by the computer, it became clear that the slurry film contained too many ripples. These images can be seen in Figures 2.4 and 2.5. As shown, the ripples create a form of noise in the image which tends to mask the change in slurry color as a function of ash content, reducing the resolution of the sensor. The ripples in the free falling film can be reduced by decreasing the 1.8 mm slot width in the bottom the sample box; however, this increases the chance of plugging. Typically, an opening of this type should be no less than three particle diameters greater than the maximum particle size in the slurry. Since it was planned that the sensor would have to handle -28 mesh material, the minimum sample box slot width was designed to be 1.8 mm.

Both of the first two prototype sample presentation systems had advantages and disadvantages. While it appeared that both systems might be usable for this video-based slurry sensor, neither showed very positive preliminary results. Because sample

presentation is typically the key to any video-based image analysis systems, a third alternative prototype sample presentation system was investigated.

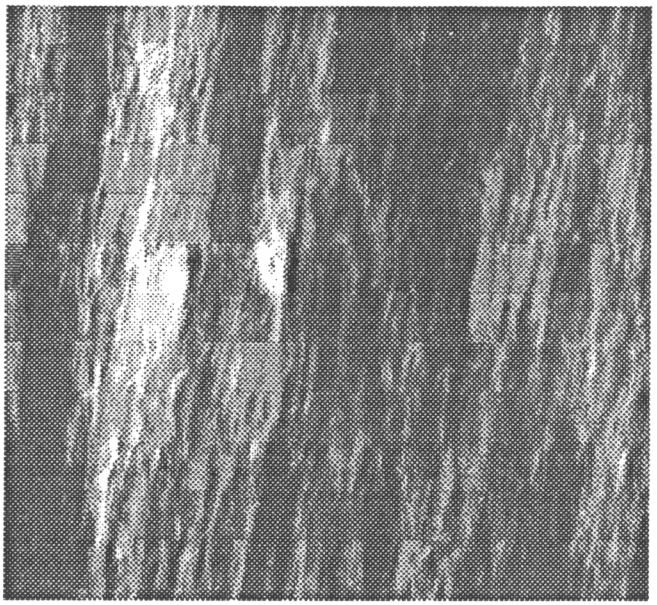

Figure 2.4 Prototype Two Reflected Light Image

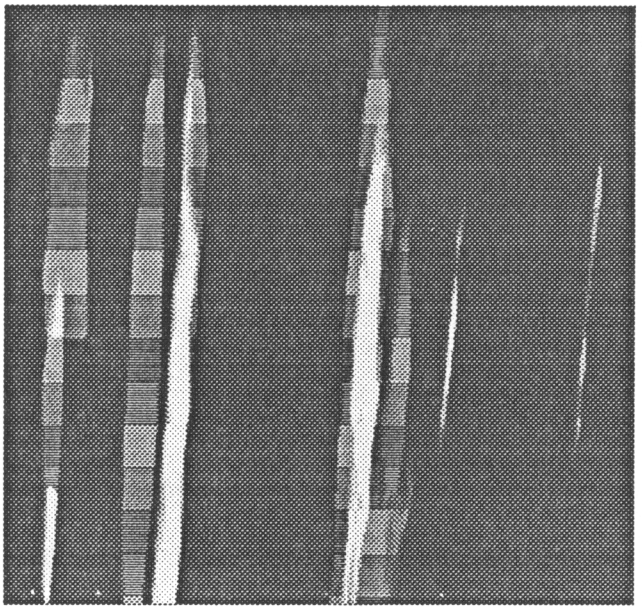

Figure 2.5 Prototype Two Transmitted Light Image

2.2.3 *Prototype Three*

After preliminary tests were performed with the first two prototype sample presentation systems, it was realized that a completely new approach would be necessary in order to present quality slurry images to the sensor system. The third prototype sample presentation system is shown in Figure 2.6.

This prototype consists of a PVC tube approximately 65 cm in length by 9 cm in diameter. The upper portion of the tube houses the camera and ring lighting systems, while the lower portion is the slurry presentation chamber. The upper and lower portions of the tube are bolted together with a Teflon diffusing ring, Plexiglas disk, and rubber gasket material in between the two sections to ensure that an air tight seal is achieved. The camera is held rigidly in place by a threaded PVC cap, with the camera lens placed snugly on the Plexiglas disk. A small cooling fan is mounted on the side of the tube to prevent possible camera overheating. Reflected light illumination is provided to the sample presentation chamber by a fiber optic ring light mounted around the camera lens. The Teflon diffusing ring is placed between the ring light and the Plexiglas disk, serving to "soften" the ring light illumination and eliminate the formation of hot spots. Constant illumination of the slurry sample is maintained by periodically reading the resistance output from the photocell mounted in the sample chamber wall, and making adjustments to the fiber optic illuminator as necessary. The sample presentation system was designed to be easily inserted into a sump or tank, with the level of the slurry within the sample chamber manipulated by controlling the air pressure inside the tube.

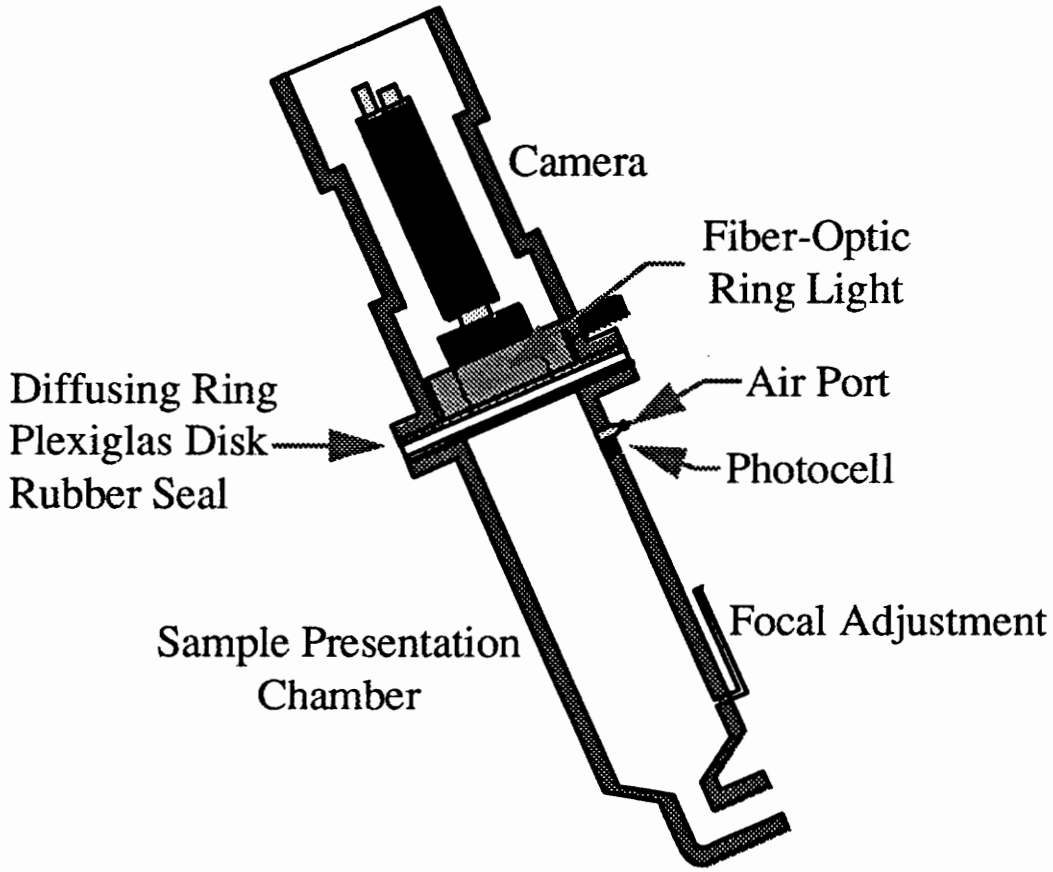

Figure 2.6 Schematic Diagram of Prototype Three Sample Presentation System

The operation of the sample presentation system is as follows. Initially, the sample presentation system chamber is flushed with air by a computer controlled solenoid valve. Once the positive air pressure ceases, slurry fills up the sample tube as air escapes from an adjustable focal level port. The slurry rapidly fills the tube to a preset level within the focal plane of the camera. The slurry sample, illuminated by reflected light, is then imaged and digitized into gray level information by the PC's frame-grabber. This information is then processed to determine the ash content of the sample. Finally, the sample chamber is flushed with air to expel the old sample, and a fresh sample is acquired.

Preliminary tests with this sample presentation system showed that this approach provided excellent image quality, as shown in Figure 2.7. The swirls of dark coal along with the lighter ash and clay minerals are clearly visible in the image. This is a major improvement over the images that were shown in Figures 2.4 and 2.5, acquired using the second prototype sample presentation system. In those images, ripples present in the slurry film created streaks and reflections which obscured the gray level information contained in the image.

The third prototype system solved the problems that had been encountered with previous systems. Very clear images of moving coal slurry were obtained using a system designed for easy insertion into a sump or tank. Furthermore, multiple images could be acquired for a single sample analysis by simply pulsing the air in the sample tube and acquiring fresh samples.

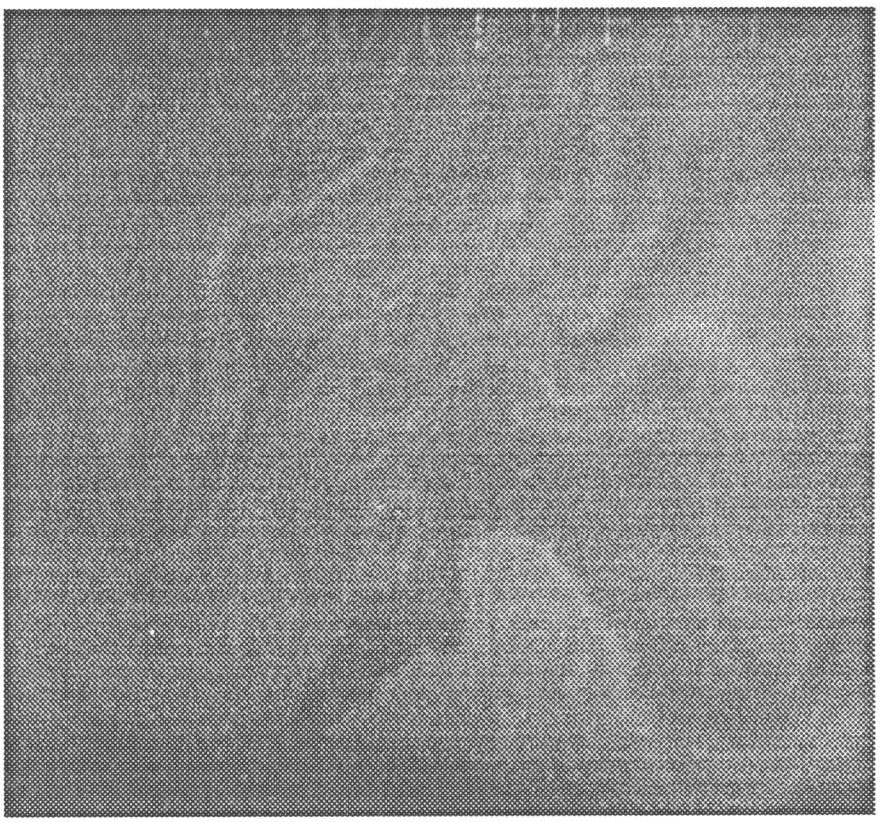

Figure 2.7 Prototype Three Reflected Light Image

As testing of the third prototype sample presentation system continued, it was realized that some modifications would be necessary to ensure optimal performance of the video-based slurry sensor. Different modifications were deemed necessary at different points in time during this work, and are discussed in chronological order in the following section.

2.2.4 *Further Modifications*

During preliminary testing of the sample presentation system, it was found that the angle at which the sample tube was inserted into the sample sump could effect the illumination of the slurry sample. It was found that mounting the sample presentation tube vertically in the sump would cause shimmering effects on the slurry surface, hindering the acquisition of high quality images. If the tube was rotated too near the horizontal, then the sides of the image would become blurred, as the focal plane of the camera shifts when the sample tube is rotated. It was found that mounting the tube fifty degrees from the horizontal eliminated the glare associated with the vertical system, and allowed for the acquisition of clear focused slurry images. This test work is described in further detail in an ensuing chapter of this thesis.

During the fabrication and testing of the sample presentation system, representatives from Pittston Coal Company expressed concern that excess frother in the slurry may cause froth to form inside the sample presentation chamber. This was found to be the case during preliminary in-plant testing of the sensor, and the system was returned to the laboratory where frothing conditions were recreated. It was found that by reducing the size of the opening at the end of the sample presentation chamber, the amount of air entrained in the slurry entering the tube could be reduced. Also, the time that it takes the slurry to rise to the optimal focal plane was greatly reduced, allowing images to be captured before any froth or film could form on the slurry surface. Subsequent testing of the sensor showed that these two minor modifications allowed clear slurry images to be acquired without the formation of froth in the sample presentation chamber.

Towards the completion of the project, consideration was given to the problem of ensuring that the illumination remained even and constant during continuous sensor operation. With other similar sensors, the light had to be checked and manually reset very frequently to ensure constant sample lighting. Since this sensor was developed to operate in a continuous on-line basis, it was desirable that a method of automatically monitoring and correcting for varying lighting conditions be developed. A sealed PVC tube was attached to the inner wall of the sample presentation chamber. A smooth gray disk was placed at the end of the PVC tube in the camera focal plane. Thus, when slurry images are acquired, a portion of the constant illumination standard is imaged along with the slurry. The illumination standard is shown in a cross section view of the sample presentation chamber in Figure 2.8.

Using the image analysis software, image frames can be constructed, allowing the slurry and illumination standard portions of the image to be analyzed separately. The mean gray level of the illumination standard is taken as a measure of the incident light intensity in the sample presentation chamber. The gray level information for the slurry portion of the image is then adjusted according to the measured light intensity of the illumination standard. Variations in sample illumination are caused by a variety of factors including failing illuminator bulbs and varying line voltages.

The addition of the illumination standard has proven to be a very effective way of correcting for small variations in sample lighting, and will be discussed further in a following chapter.

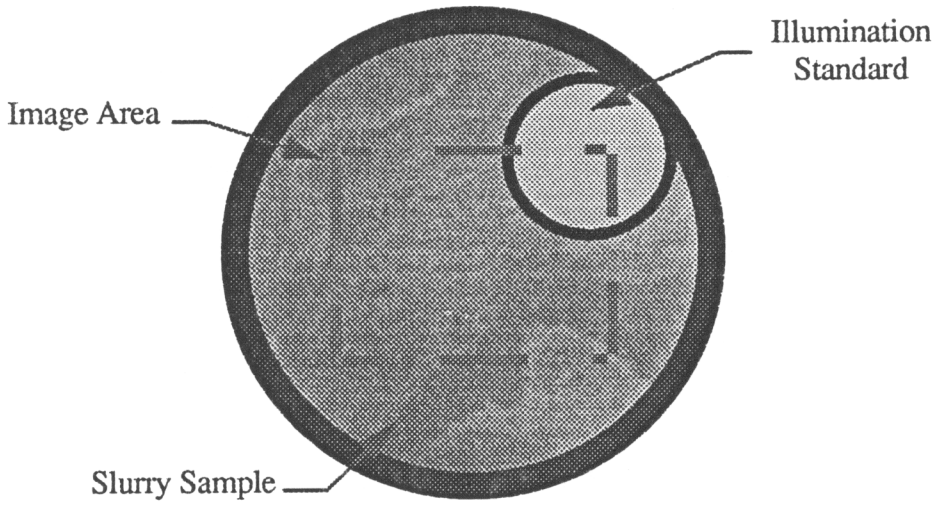

Figure 2.8 Sample Presentation System Cross-Section Showing the Illumination Standard

2.3 FINAL SAMPLE PRESENTATION SYSTEM DESIGN

The third prototype sample presentation system is of a novel design, permitting high quality images of moving slurry material to be acquired on-line. A schematic diagram of the entire slurry sensor system, including the sample presentation and image analysis systems, is shown in Figure 2.9.

A line conditioner is used to minimize fluctuations in the voltage provided to the illuminator. A digital multimeter can be used to measure the resistance of the sample presentation chamber photocell, which is used to set the sensor illumination conditions. Once the light has been initially set, the illumination standard is used as a means of automatically accounting for small variations in sample lighting. Custom-written computer software controls the slurry sensor operations.

The basic operating scenario for the sensor can be described as follows. The solenoid air valve is actuated, permitting the acquisition of fresh slurry sample. The slurry level rises rapidly to the focal plane of the camera, and an image of the slurry surface is captured. The frame-grabber card in the computer digitizes the image into gray-level information and displays the image on the television monitor. The software controlling the sensor operation takes average values obtained from multiple images and performs the necessary calculations that yield slurry ash content. The slurry ash content is then displayed back to the operator in an appropriate format.

The sample presentation system is the key component of the sensor making it possible to take advantage of existing image analysis techniques for analyzing coal slurry

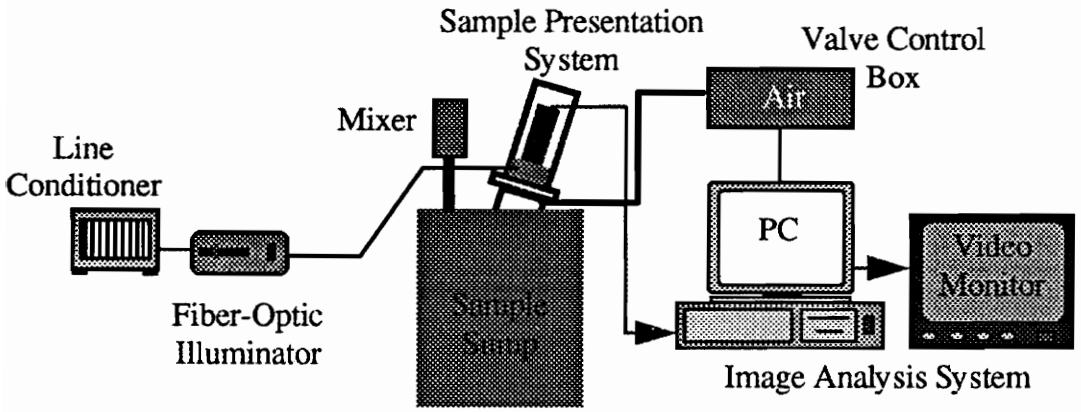

Figure 2.9 Overall Schematic Diagram of Video-Based Slurry Sensor

samples. The following chapter details the testing and analysis work that was conducted using this final sample presentation system design.

CHAPTER 3
TESTING AND CALIBRATION

3.1 TEST SITES AND MATERIAL DESCRIPTION

The video-based slurry analysis system was tested at two different coal preparation facilities. The initial VCR-based testing and the majority of further in-plant testing were carried out at Pittston Coal Company's Middlefork plant site. The samples that were used for the development of the sample presentation system were also obtained from the Middlefork plant. Later, the sensor was calibrated and installed permanently at this site. Some preliminary testing was also carried out at Cyprus-Amax's Maple Meadow plant site.

3.1.1 *Middlefork Preparation Facility*

The Middlefork preparation facility is an extension of Pittston Coal Company's Moss 3 preparation facility and is located near the town of Carbo in southwest Virginia. The Middlefork plant site was built to recover coal from an existing tailings impoundment. During its short life it has proven to be an extremely profitable venture. A dredge is used to provide the plant with feed from the tailings impoundment which is cleaned by a combination of spiral concentrators and column flotation cells. The coarse fraction of the feed material is cleaned by the spiral concentrator circuit, and the finer material (nominally -100 mesh) is cleaned by froth flotation. The Middlefork site operates five three-meter-diameter Microcel flotation columns. Table 3.1 shows typical

Table 3.1 Typical Ash Content and Percent Solids Ranges for Middlefork Column Feed, Product and Tailings

	Percent Ash	Percent Solids
Column Feed	38-50%	5-10%
Column Product	6-7%	15-20%
Column Tailings	65-85%	1-5%

ranges for ash content and percent solids of the column feed, product, and tailings streams.

Figure 3.1 shows percent ash versus time during one of the sampling trips that was made to the Middlefork plant site. The feed, product, and tailings streams for one of the operating column flotation units are represented. The extremely variable nature of the column feed and tailings at the Middlefork plant is clearly shown, demonstrating the need for on-line ash analysis. The abrupt changes seen in the latter part of the plot are due to changes in feed material associated with movement of the dredge which provides feed to the plant. It is shown that although the feed and tailings stream change drastically, the product stream maintains fairly constant throughout the testing. The fact that product quality is not sacrificed is favorable, yet this does not mean that the columns are operating optimally in terms of coal recovery. Figure 3.2 shows the coal recovery and yield for the same column over the same time frame.

The drop off in both coal yield and recovery that is seen in the latter part of the testing is due to relocation of the dredge that provides feed to the plant. The large drop off in coal recovery indicates that recoverable coal is being thrown away, even though the product quality remains essentially constant (Figure 3.1). It should be noted that variations of this nature are typical for the Middlefork plant regardless of the dredge position because of natural variations in the manner in which the impoundment was created over the years.

Preliminary sampling at the Middlefork site and information provided by Pittston personnel revealed that when the column tailings ash drops below 70%, the columns are

generally being overloaded, and coal is being lost from the system via the column tailings. When the ash content of the tailings stream goes above 80%, the columns are being underloaded and are not operating at capacity. Pittston officials would like to ensure that the Middlefork plant maintains a high coal recovery at optimal column performance. Thus, Pittston management were very interested in the testing and installation of the video-based ash analyzer at this site to provide a means of monitoring tailings ash and maximizing coal recovery.

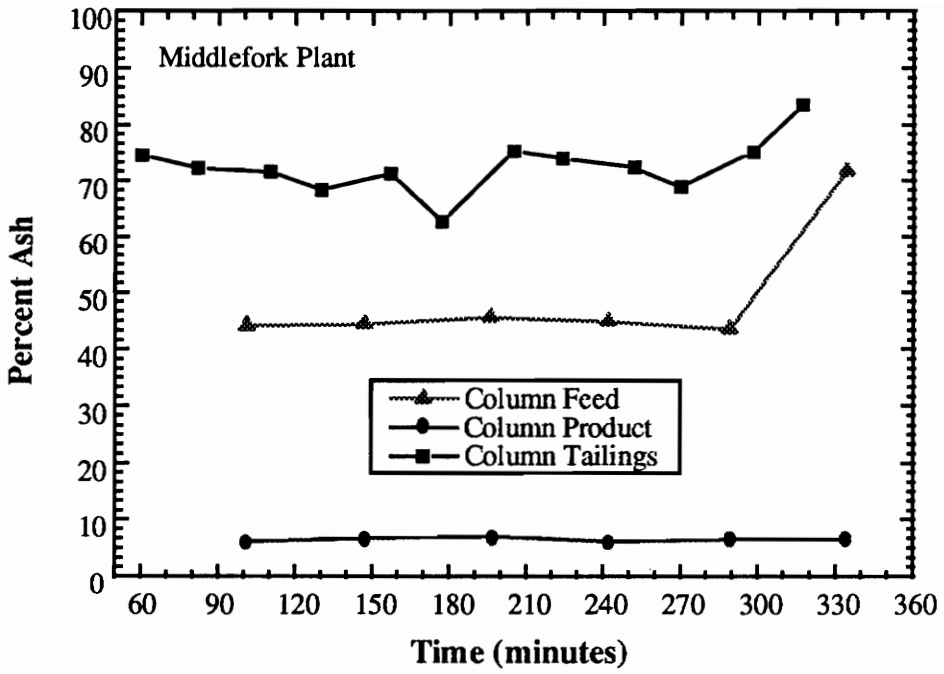

Figure 3.1 Percent Ash Versus Time for the Feed, Product, and Tailings Streams from a Middlefork Flotation Column

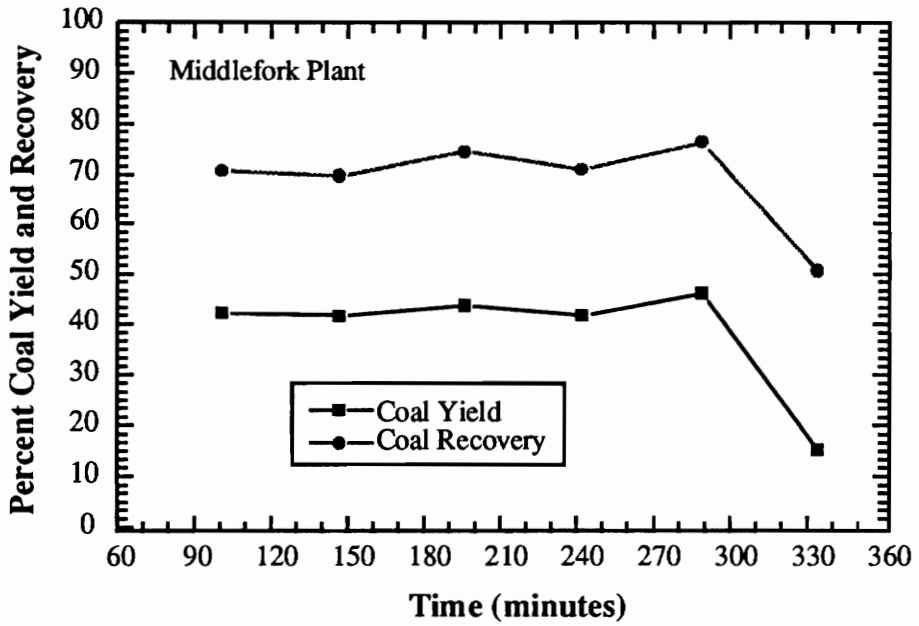

Figure 3.2 Coal Recovery and Yield Versus Time for a Middlefork Flotation Column

3.1.2 *Maple Meadow Preparation Facility*

The video-based ash analyzer was also tested at the Cyprus-Amax Maple Meadow preparation facility, located near Beckley, West Virginia. The preparation facility includes a conventional flotation circuit which produces a high quality metallurgical coal. This preparation facility is very different from the Middlefork facility in a variety of ways. Flotation feed quality at the Maple Meadow site has a much lower ash content and is more stable because the material being cleaned is the -28 mesh run-of-mine fraction. The tailings percent ash therefore is much lower than was seen at the Middlefork site. Table 3.2 shows typical ranges of ash content and percent solids for the conventional flotation circuit feed, product, and tailings.

It can be seen that the circuit feed ash is already low. Thus, flotation is carried out to produce a clean, highly marketable metallurgical coal product. The tailings ash content values would seem to indicate that coal is being lost; however, that is misleading. Due to the low feed ash content and the nature of the coal, the coal yield and recoveries for this circuit are exceptionally high. Table 3.3 shows detailed results of a size distribution-based ash analysis of the feed, product, and tailings streams from the Maple Meadow conventional flotation circuit. The percent coal yield and recovery for each size class is also included.

This in-depth analysis of the Maple Meadow flotation circuit was carried out to quantify circuit operation, and to determine more clearly the nature of the tailings stream on which the ash analyzer was tested. Though the tailings ash value seem low in comparison to the Middlefork site, it is shown that the flotation circuit is operating

efficiently by the favorable values for coal yield and recovery. This testing will be discussed further in a later section.

Table 3.2 Typical Ash Content and Percent Solids Ranges for Maple Meadow Flotation Feed, Product, and Tailings.

	Percent Ash	Percent Solids
Feed	10-15%	10-15%
Product	4-6%	25-30%
Tailings	45-55%	2-5%

Table 3.3 Results of a Size Distribution-Based Ash Analysis of the Maple Meadow Conventional Flotation Circuit

Feed				Product				Tails			
Size (mesh)	Weight (g)	Weight Percent	Percent Ash	Size (mesh)	Weight (g)	Weight Percent	Percent Ash	Size (mesh)	Weight (g)	Weight Percent	Percent Ash
+28	17.1	5.4	8.7	+28	29.0	8.1	2.5	+28	11.1	10.8	41.7
28 x 100	126.5	40.3	7.9	28 x 100	136.0	38.0	3.0	28 x 100	38.6	37.6	50.6
100 x 150	33.8	10.8	8.7	100 x 150	44.0	12.3	3.8	100 x 150	6.8	6.6	54.0
150 x 200	22.2	7.1	9.9	150 x 200	27.3	7.6	3.7	150 x 200	4.9	4.8	50.0
200 x 270	21.1	6.7	11.9	200 x 270	28.0	7.8	5.1	200 x 270	4.5	4.4	49.1
270 x 400	16.5	5.3	10.1	270 x 400	21.4	6.0	4.8	270 x 400	3.6	3.5	44.9
-400	76.7	24.4	20.3	-400	72.3	20.2	9.4	-400	33.2	32.3	56.3
Total	313.9	100.0	11.6	Total	358.0	100.0	4.7	Total	102.7	100.0	51.4

Size (mesh)	% Coal Yield	% Coal Recovery
+28	84.3	90.0
28 x 100	89.8	94.5
100 x 150	90.2	95.1
150 x 200	86.6	92.5
200 x 270	84.5	91.1
270 x 400	86.6	91.8
-400	76.8	87.3
Total	85.2	91.9

3.2 INITIAL IN-PLANT TESTING

Initial testing of the video-based ash analyzer was carried out at the Middlefork plant site. The sample presentation system for the optical analyzer and a Super-VHS video cassette recorder used to save images collected by the system, were taken on-site. The video-taped images were then analyzed at the lab and related to samples that were taken during the on-site analysis. This testing configuration facilitated the in-plant sensor testing, and allowed an abundance of data to be collected over a short period of time.

3.2.1 *Middlefork Plant Visit One*

For the first Middlefork site visit, the VCR-based approach was used. The sample presentation tube was installed in a small sump which was periodically filled with column tailings. Samples were also collected at the same time to be analyzed later for percent solids and ash content. In total, twelve samples were placed in the sample sump, with four images of each slurry sample recorded on video-cassette for later analysis. The samples were acquired from three of the five operating columns in time intervals of approximately twenty minutes. During this trip the preparation plant experienced a lengthy power outage, hampering the collection of images and samples. Also, the video equipment was adversely affected by the loss of power and some image information was corrupted. Thus, in the following analysis, it should be noted that samples 1-7 were collected prior to the power failure and samples 8-12 were collected after power was restored to the plant.

The samples taken for determination of ash content and percent solids were brought back to the lab and analyzed. Table 3.4 shows the percent solids and ash content

along with the corresponding mean gray levels that were determined for the twelve samples.

Figure 3.3 shows the slurry mean gray levels plotted versus ash content for each of the twelve samples. As shown, there is a definite trend indicating an increase in slurry gray level with increasing ash content, however there is appreciable scatter in the data. Closer examination reveals that samples 1-7 fall along one line, while samples 8-12 fall along a second line situated below the first. This has been attributed to a quantifiable sensor system "warm-up" time which will be discussed in detail in a later section.

Though there is a significant amount of data scatter, the data obtained from this first in-plant test of the ash analyzer was viewed as encouraging. Pittston personnel had indicated that a minimum resolution of five percentage points would prove beneficial as far as they were concerned. Even with the appreciable scatter, it appeared that meeting this resolution requirement would be an attainable goal.

Table 3.4 Ash Content, Percent Solids, and Mean Gray Levels for Samples from Middlefork Plant Visit One

Sample Number	Column Number	Percent Solids	Percent Ash	Mean Gray Level
1	1	2.2	80.1	101.5
2	2	2.7	77.3	90.8
3	3	2.9	75.9	91.8
4	1	2.7	77.1	81.8
5	2	2.8	77.7	84.0
6	3	2.9	76.8	85.6
7	1	4.2	71.0	74.7
8	2	4.3	65.1	61.3
9	3	2.7	74.2	67.7
10	1	1.7	80.4	80.4
11	2	1.1	80.8	83.3
12	3	1.7	74.0	70.4

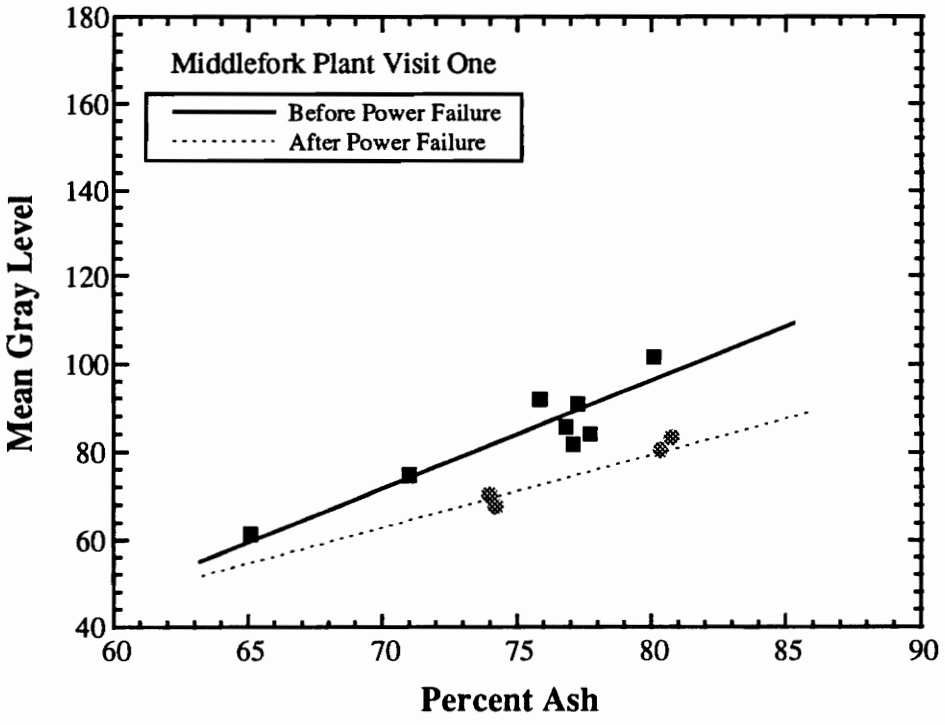

Figure 3.3 Mean Gray Level Versus Ash Content for Middlefork Plant Visit One

3.2.2 *Middlefork Plant Visit Two*

The same testing and sampling configuration that was described for the first Middlefork in-plant test of the video-based ash analyzer was used in the second site visit. In order to reduce the standard deviation for the mean gray levels from each sample and to ensure that representative image information was collected, the number of images recorded per sample was increased from four to ten. Once again, three of the five operating columns were sampled in time intervals of approximately twenty minutes, with a total of 21 samples collected for analysis. At the request of plant personnel, feed and product samples were also collected at the same time as one of the tailings samples for evaluation of flotation column performance. Finally the samples were brought back to the lab and analyzed for ash content and percent solids. The videotaped images were also analyzed to obtain mean gray level values for each sample.

Table 3.5 shows the ash content, percent solids, and mean gray levels for the samples. Several samples have extremely low percent solids and ash content values. These samples are associated with relocation of the dredge that provides feed to the plant. The feed and product ash content and percent solids for sample 20 are also included at the bottom of this table.

The coal yield and recovery for the number two column, as indicated by sample 20, was found to be 36.8% and 66.4% respectively. Though the product ash content was satisfactory, these numbers indicate that the columns should be pulling harder in order to maximize coal recovery. The tailings ash content is nearing the lower limit that Pittston plant operators prefer from the columns, and this again demonstrates the potential

usefulness of the video-based ash analyzer. Figure 3.4 shows the mean gray levels for all 21 samples plotted as a function of slurry ash content.

Once again, as in the first plant visit, there is a definite correlation between the ash content and mean gray level of the samples, although there is appreciable scatter in the data. For some reason, the most significant scatter (upper portion of plot) is associated with the data collected at the end of the sampling campaign. It should be noted that the data shown in Table 3.5 does not seem to indicate any relationship between percent solids and the data scatter. It appears that if the last four sample points could be eliminated that the remaining data would easily fit a reasonable relationship with a percent ash resolution within the desired limit specified by the Pittston Coal Company.

Table 3.5 Ash Content, Percent Solids, and Mean Gray Levels for Samples from Middlefork Plant Visit Two

Sample Number	Column Number	Percent Solids	Percent Ash	Mean Gray Level
1	1	2.0	73.4	102.3
2	2	2.8	70.8	96.1
3	3	4.7	68.7	101.5
4	1	2.8	74.7	108.6
5	2	5.0	65.3	97.8
6	3	5.0	68.1	98.9
7	1	3.6	71.3	106.7
8	2	2.6	73.5	107.8
9	3	3.3	72.5	106.4
10	1	0.5	85.2	160.8
11	2	1.7	69.5	115.9
12	3	3.0	71.6	128.6
13	1	1.6	75.9	125.3
14	2	3.1	70.1	124.3
15	3	2.2	79.1	146.7
16	1	0.6	84.3	171.3
17	2	0.4	82.6	194.0
18	3	0.9	70.7	173.0
19	1	3.4	66.6	189.6
20	2	3.0	72.9	152.2
21	3	2.6	75.9	132.3
20	feed (2)	4.2	49.0	----
20	prod. (2)	12.3	7.9	----

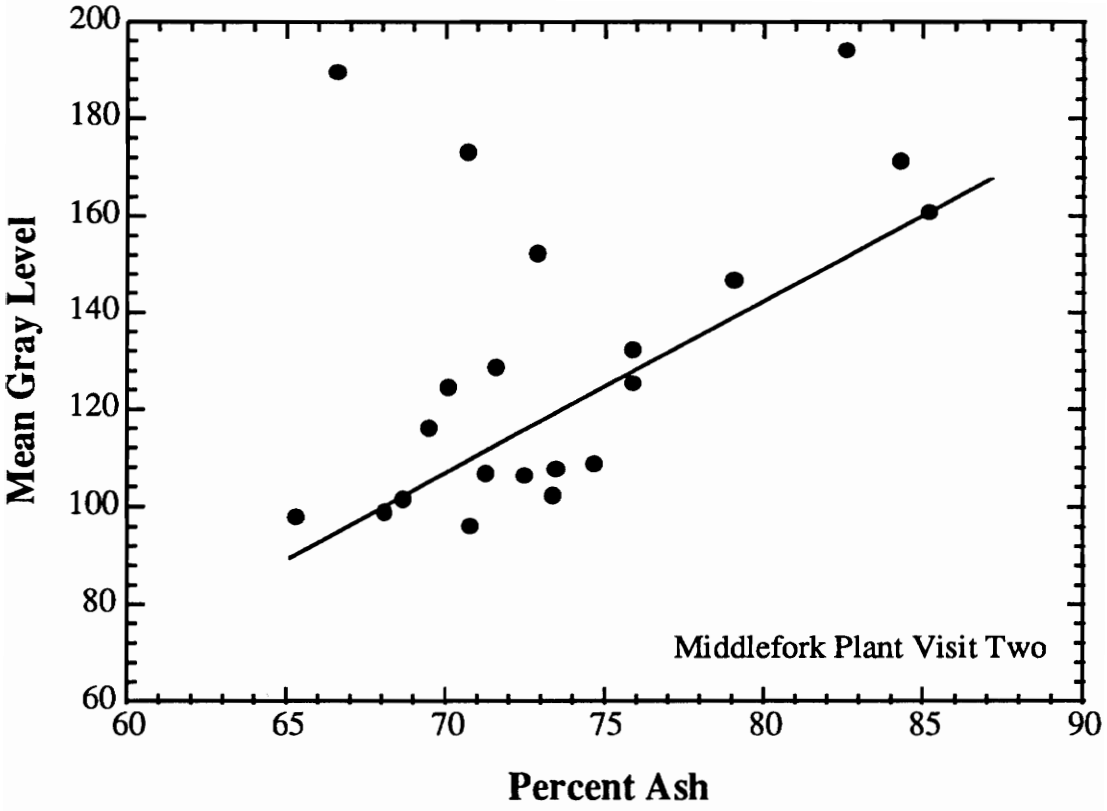

Figure 3.4 Mean Gray Level Versus Ash Content for Middlefork Plant Visit Two

3.3 PARAMETRIC INVESTIGATIONS

A parametric investigation was carried out to further quantify the operation of the video based sensor. The statistical parameters used to quantify the gray level images needed to be investigated. Also, when this work began, it had been planned that monochromatic illumination of the slurry samples would be tested as a means of improving image resolution. Furthermore, based on the results that were obtained from the first two in-plant tests of the video-based ash analyzer at the Middlefork plant, it was felt that a systematic study was in order to identify those parameters that might be responsible for the data scatter. The experience gained with the optical analyzer from the initial plant testing indicated that the parameters most likely to contribute to data scatter were percent solids, solids size distribution, light intensity, sample tube angle, number of images taken per sample, and the sensor system "warm-up" time. The latter parameter was suggested by the fact that there seemed to be a consistent increase in gray level values as a function of time. Slurry samples that were obtained during the second Middlefork plant visit were used in this testing, and the following is a summary of this work.

3.3.1 *Gray Level Statistical Parameters*

The identification of statistical parameters can be summarized as follows. A rectangular image area is characterized by the distribution of the tones of the pixels that form the image. Each of these tones is represented by a value between 0 and 255, which correspond to gray scale values between black (0) and white (255). A frequency distribution of the gray values is calculated and is normally represented in the format of a 255 element vector. The vector elements are the number of image pixels found to have the corresponding gray level. From this distribution several statistical parameters can be calculated and used as a means of extracting information from gray scale images.

For this work, the mean, modal, and median gray values of the gray level histogram were tested to determine which would provide the best correlation with slurry ash content. Also, the skewness and kurtosis of the histograms were investigated. It was determined after preliminary testing of the sensor that the overall mean gray level of the slurry images was the best indicator of slurry ash content.

The slurry mean gray level was therefore used as the statistical parameter with which ash content would be related. This measurement has several advantages, primarily its simplicity and ease of calculation.

3.3.2 *Monochromatic Illumination*

Test work was conducted to evaluate the use of monochromatic light as a means of enhancing the images obtained with the optical analyzer. It was hoped that by filtering out optical noise through the use of monochromatic illumination, a better distinction between ash and coal particles could be obtained.

Initially, a monochromator providing a range of output from near-infrared to near-ultraviolet was employed in this study, however, the intensity of the monochromatic light was insufficient to provide an adequate image. As an alternative, several glass filters were utilized which covered the wavelength range within the visible spectrum from 400 to 700 nm. Although the filters did not provide a continuous variation in wavelength as did the monochromator, they had the advantage that they could be used with the existing sample illumination system. The illuminator was modified slightly to allow the filters to be placed inside the device housing. Since the sensor illuminator utilizes a more powerful light source than the monochromator, and since the glass filters have much larger bandpasses, ample light was able to pass through the filters providing adequate slurry sample illumination. Four filters generating yellow, red, blue, and green light were initially tested. The illuminator output setting that was required to provide sufficient light intensity with the blue and green filters caused the filters to crack due to excessive heat. Therefore, the majority of this work was carried out using the red (600-700 nm) and yellow light filters (535-700 nm) only.

In order to better understand the effects of monochromatic light on reflected gray levels, initial tests were carried out using colored dots on a black background. The results

obtained from these tests served to illustrate the filtering effects of specific wavelength ranges of monochromatic light. Figure 3.5 shows the gray level histograms obtained from yellow, orange, and green dots illuminated by various forms of reflected light.

As shown, under white light, each colored dot produces a peak on the histogram plot. In order from left to right, these peaks are generated by the green dot, the orange dot, and the yellow dot. When the dots are illuminated by yellow light, the yellow dot disappears and the green and orange dots remain; although the orange tends to become red and the green dot tends to become blue as the yellow portion is filtered out. Finally, when the dots are illuminated by red light, the orange dot becomes yellow and combines with the initially yellow dot yielding two distinct peaks, representing green and yellow. In both cases, the use of monochromatic filters was found to eliminate some information, but the remaining gray level histogram peaks were made more distinct.

It was hoped that this type of effect could be achieved when using monochromatic light to filter images obtained from coal slurry. Unfortunately, the color variations in the flotation tailings samples were not as dramatic as the colored dots, and monochromatic illumination was unable to achieve the desired type of effect as shown in Figure 3.6.

As can be seen, the gray level histograms obtained while using white light and the narrow-band red light are nearly identical. It is possible that a detailed search over the entire visible light spectrum might yield some wavelength that would produce the desired filtering effect illustrated in Figure 3.5, however it appears that monochromatic lighting might be more applicable for mineral slurry systems that exhibit a wide color variation such as copper ores.

As a final test of the monochromatic illumination system, five slurry samples were prepared from Middlefork column samples. The samples were all prepared at 4% solids by weight and had ash contents varying from 38% to 72.5%. Each sample was illuminated in turn by white, red, and yellow light, and resulting mean gray level values were plotted as a function of ash content as shown in Figure 3.7.

As shown, although the mean gray values for each of the light sources are different, the curves appear to follow a similar trend. In fact, the white light source appears to provide a curve with a slightly steeper slope in the region of interest (i.e., 55-75% ash) of a typical flotation tailings sample (Middlefork site). This would tend to indicate that the white light source provides a better resolution of ash content than either of the two monochromatic sources. Thus, the use of monochromatic light as a means of filtering out optical noise and enhancing the distinction between ash and coal in slurry samples does not appear viable. All further work used the standard white light illumination.

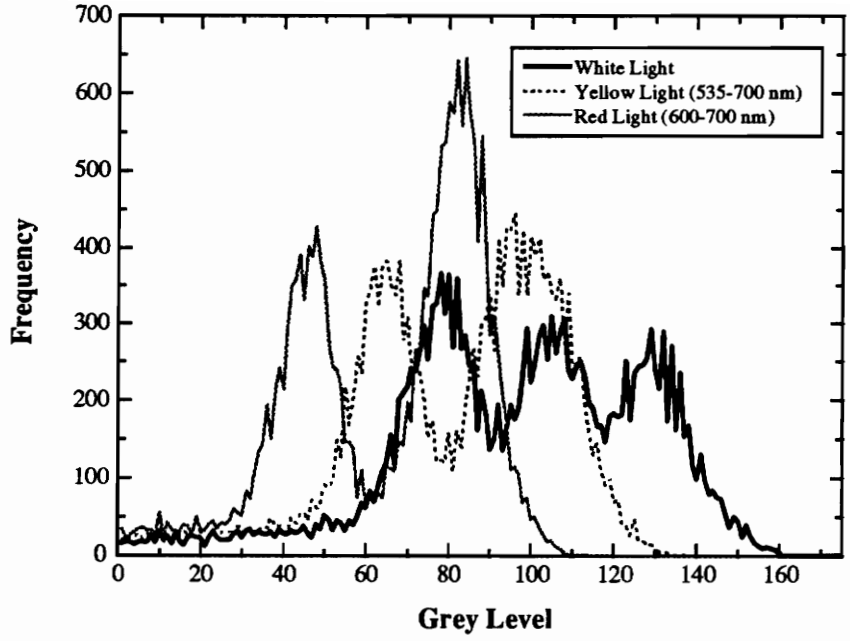

Figure 3.5 Gray Level Histograms Obtained of Multi-Colored Dots with Various Forms of Illumination

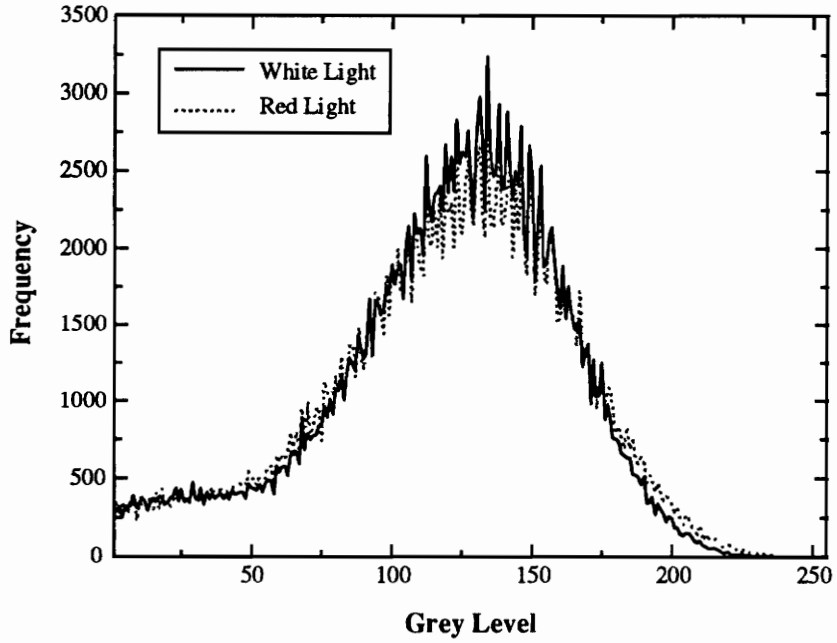

Figure 3.6 Gray Level Histograms of Flotation Tailings Slurry Obtained with Various Forms of Illumination

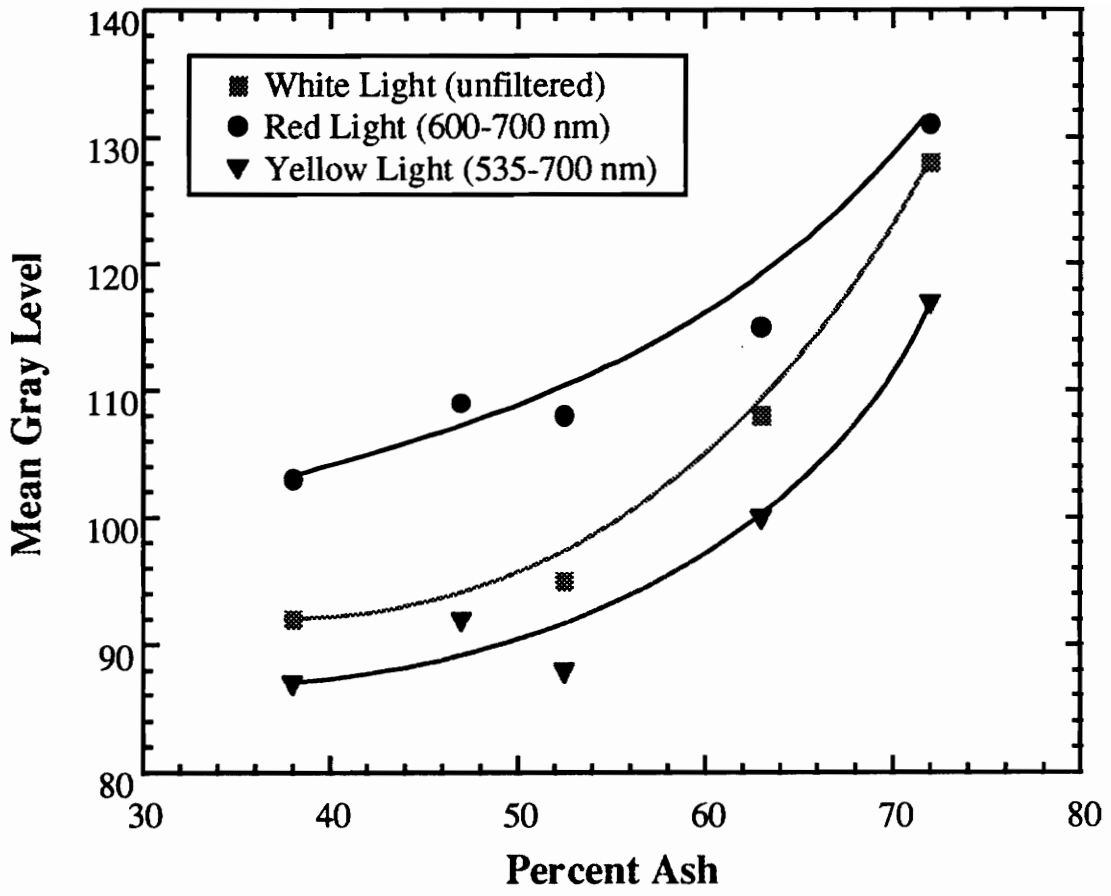

Figure 3.7 Mean Gray Level Versus Ash Content for Slurry Samples Illuminated with Various Forms of Light

3.3.3 *Percent Solids*

The percent solids of the column tailings samples obtained at the Middlefork plant normally vary between 1% and 5% solids by weight. In order to test the effect of percent solids on the gray values of slurry samples, five samples were prepared varying from 1-5% solids from a 76% ash sample acquired during the second visit to the Middlefork plant site. Six images were collected per sample and averaged to obtain the gray level results shown in Table 3.6.

As shown, the overall mean gray level changes by less than three gray level increments over the range of 1-5% solids. Figure 3.8 shows this data plotted on a scale similar to that previously shown for the in-plant testing data (Figures 3.3 and 3.4). It is clear that the effect of percent solids is easily within the statistical "noise" of the sensor. Thus, it was concluded that variations in percent solids were not a contributing factor to the data scatter.

Table 3.6 Mean Gray Levels of a 76% Ash Sample for Varying Percent Solids

Percent Solids	1	2	3	4	5
Mean Gray Level	76.9	76.6	78.9	78.9	79.6

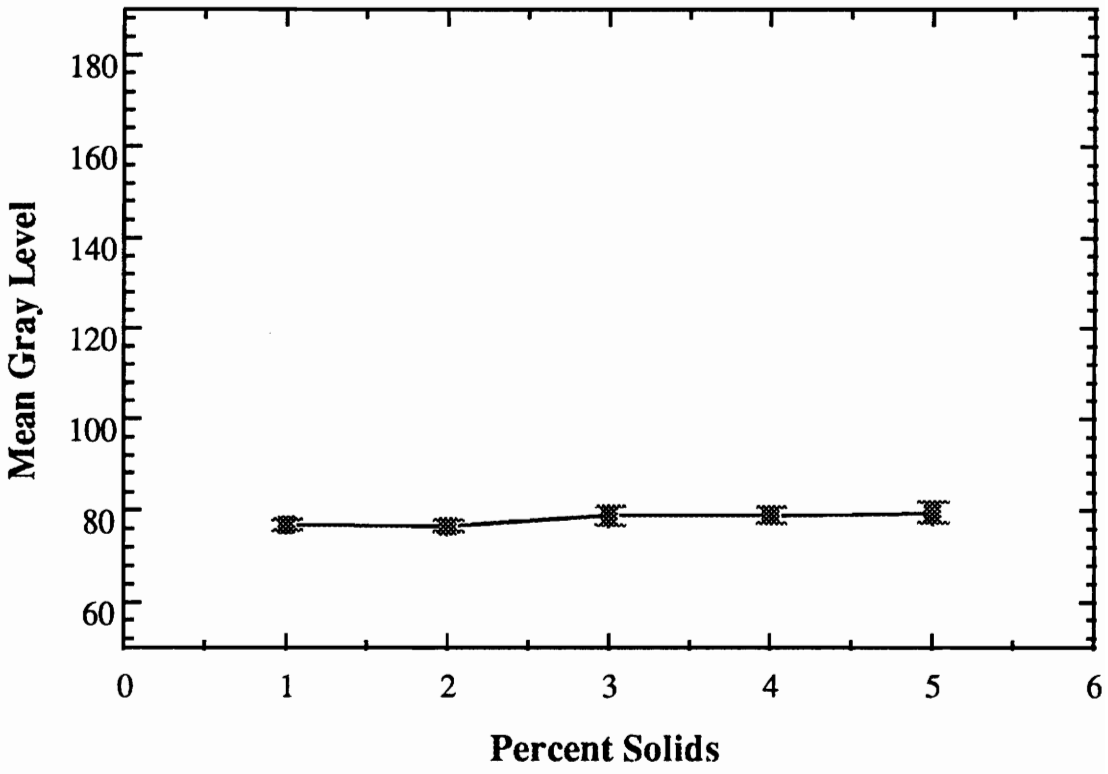

Figure 3.8 Effect of Percent Solids on Mean Gray Levels for a 76% Ash Sample

3.3.4 *Solids Size Distribution*

With percent solids essentially eliminated as a cause of data scatter, it was decided that the size distribution of two samples with similar ash contents, but with widely varying mean gray levels, should be compared. Two samples (5 and 19) from the second Middlefork plant visit were selected for this analysis. These samples are nearly identical in ash content (65.3 and 66.6%, respectively); however, their mean gray levels differ by over 90 gray level increments. The size distributions from these two samples are shown in Table 3.7.

As shown, the size distributions are remarkably similar. Considering that this material is being reclaimed from a tailings impoundment, and that these two samples were collected over four hours apart, the similarity is extraordinary. Thus, it does not appear that variations in particle size distribution are the cause of data scatter in this particular case.

It should be noted that this simple comparison is not a rigorous study of the effects of particle size distributions on slurry gray level measurements. It is expected that a tailings samples containing significant quantities of coarse (+28 mesh) coal would be difficult to analyze using the current methodology, as the coarse coal would settle in the sump and/or the sample tube, and would not be "seen" by the analyzer.

Table 3.7 Size Distributions for Samples 5 and 19 from Middlefork Plant Visit Two

Size (mesh)	Sample 5 Weight %	Sample 19 Weight %
+100	0.4	0.6
100 x 200	3.2	3.1
200 x 400	7.0	6.6
-400	89.4	89.7
Total	100.0	100.0

3.3.5 *Light Intensity*

The effect of incident light intensity was investigated in order to define a relationship between the measured light intensity inside the sample presentation tube and the mean gray values measured for a given slurry sample. In the initial testing of the sensor at the Middlefork plant, the set-point for light intensity was 1.60 kΩ as measured by the photocell mounted in the wall of the sample presentation tube. The light setting was varied from 1.58-1.62 kΩ, and the same slurry sample used to study percent solids was used in this test (76% ash). The results of this test are shown in Table 3.8 and Figure 3.9.

As shown, the relationship between the incident light setting and the mean gray level is nearly linear with a slope of approximately 2.5 gray level increments per 0.01 kΩ of light intensity. Since the built-in light controller easily maintains the light setting to within 0.01 kΩ as measured by the resistance photocell, any variations in light intensity are once again considered to be within the statistical "noise" of the sensor. Therefore, it can be concluded that normal lighting variations are not responsible for data scattering.

Table 3.8 Mean Gray Levels for Varying Light Intensities for a 76% Ash Sample

Light Intensity (kΩ)	Mean Gray Level
1.58	78.3
1.59	75.6
1.60	72.7
1.61	70.0
1.62	68.5

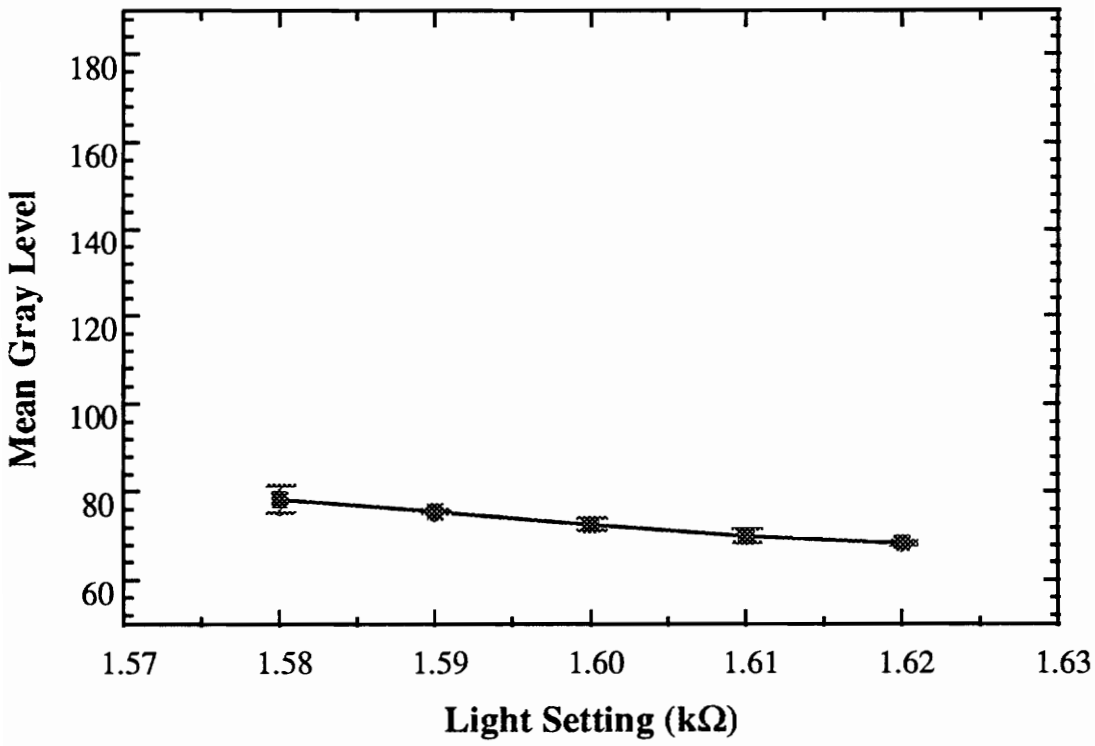

Figure 3.9 Effect of Light Intensity on Mean Gray Levels for a 76% Ash Sample

3.3.6 *Sample Tube Angle*

The sample presentation tube is rigidly mounted to the small sump in which the flotation column tailings are placed for analysis. The tube angle can be varied from 48° to 53° in the sump and is normally placed at an approximate angle of 50° from the horizontal. The tube undergoes some shock when samples are placed in and removed from the sump, as well as when the high pressure air is pulsed through the sample tube permitting acquisition of fresh samples. It was theorized that movement of the tube during the initial in-plant testing of the sensor may have contributed to the data scatter. Therefore, the two extreme sample tube angles were investigated to determine the effect of tube angle on mean gray levels obtained for the same 76% ash sample that was used in the previous tests. Table 3.9 shows the mean gray levels obtained when the tube was placed at the two extreme angles. The minimal difference of 0.3 gray level increments shows that the sample tube angle has an insignificant effect on slurry sample gray level measurements.

Table 3.9 Mean Gray Level as a Function of Sample Tube Angle for a 76% Ash Sample

Sample Tube Angle	Mean Gray Level
48°	77.8
53°	78.1

3.3.7 Number of Images per Sample

A systematic study was conducted to determine the appropriate number of images to collect for each sample in order to minimize the standard deviation from the mean gray level. In this investigation, 40 images were collected from the same 76% ash slurry sample that was used in previous work. Based on the individual mean gray levels for these images, an overall mean gray level was calculated. This made it possible to calculate the deviation of each one of the forty images from the overall mean gray level. In addition a running cumulative mean gray value was determined. These results are shown in Figure 3.10 in which the deviation from the overall mean gray level after 40 images is plotted on a scatter diagram.

As shown, the cumulative mean gray level does not truly represent the ultimate mean gray level of the sample until at least 15 images are included in the overall mean gray level calculation. In fact, the deviation from the true mean gray level of the sample is rather significant for less than 5 images. Thus, it appears that this factor may have played a role in the data scatter exhibited in initial testing of the sensor. In order to ensure that future mean gray levels are truly representative of the slurry being analyzed, it was decided to use a conservative number of 20 images per sample in future analyses. Image capture and subsequent analysis are rapid, and this restriction posed no time constraint for the on-line application of the video-based ash analyzer.

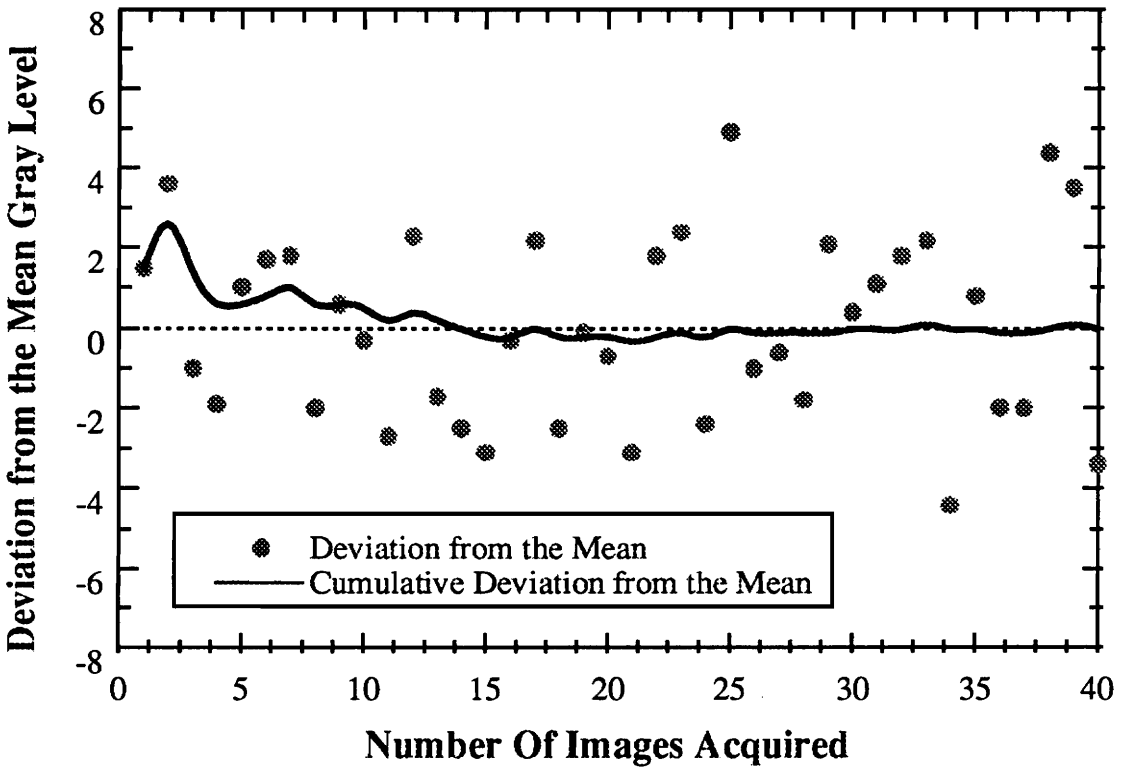

Figure 3.10 Effect of Number of Images Collected Per Sample for a 76% Ash Sample

3.3.8 *Sensor Warm-Up*

As mentioned previously, the data collected from both field tests seemed to show a pattern of increasing gray level as a function of time for slurries with similar ash contents. This pattern can clearly be seen in Figure 3.11 which shows four samples (samples 2, 7, 12, and 14) from Middlefork plant visit two plotted as a function of analysis time. These four samples were chosen because they have nearly identical ash content (70.1-71.6%) and percent solids (2.8-3.6%). As shown, there appears to be a clear upward drift in mean gray level as a function of time.

It was theorized that the phenomenon observed in Figure 3.11 might be due to the "warming-up" of some electrical components in the sensor system. In order to verify this theory, a controlled laboratory test was conducted with the optical analyzer. A 76% ash slurry sample was placed in the sump, and starting with a cold system, multiple images were collected at ten minute intervals over a period of several hours. Since there was some concern that the appearance of the slurry might actually change while it was allowed to mix over several hours, a supporting test was also performed. The system was shut down and was allowed to cool overnight. The following day the same test was carried out with a piece of paper placed inside the sample presentation tube. This was done to ensure that the system was seeing the exact same object in each image.

Figure 3.12 shows the mean gray levels obtained over time for both the slurry and the paper. In order to provide an easier basis for comparison of the two sets of data, the mean gray levels that were obtained for the paper have been scaled to match those plotted for the slurry. It is clear that the overall gray values increase in nearly the exact same

fashion for the slurry and the paper. The optical analyzer appears to reach equilibrium after approximately 2 hours, after which, the resulting gray level remains essentially constant with time.

Thus, there is clearly a system "warm-up" time which must be considered before data collection can begin. This factor, along with the need to include a sufficient number of images per sample for analysis, appear to be the most likely parameters contributing to the data scatter that was seen in initial plant testing of the video-based ash analyzer.

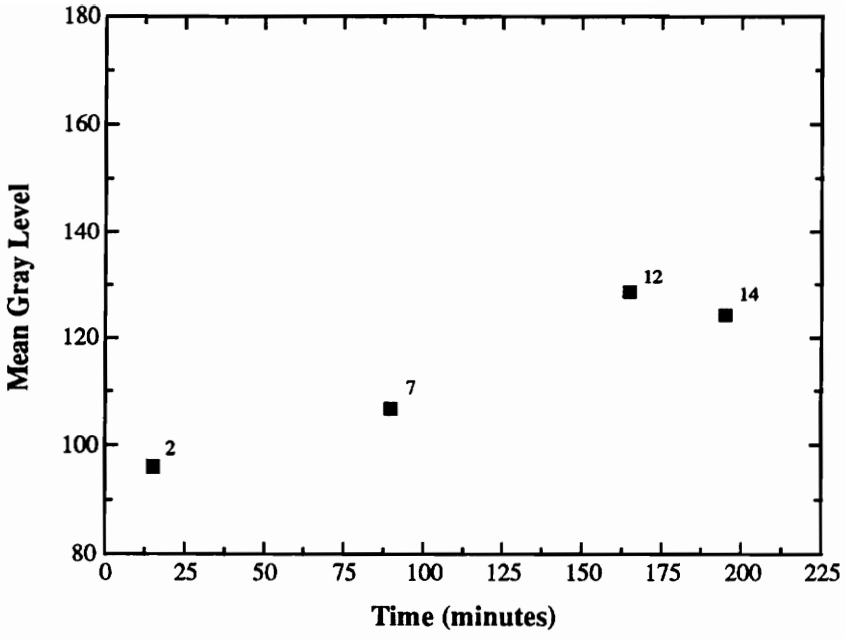

Figure 3.11 Mean Gray Level as a Function of Time For Samples with Similar Ash Content and Percent Solids

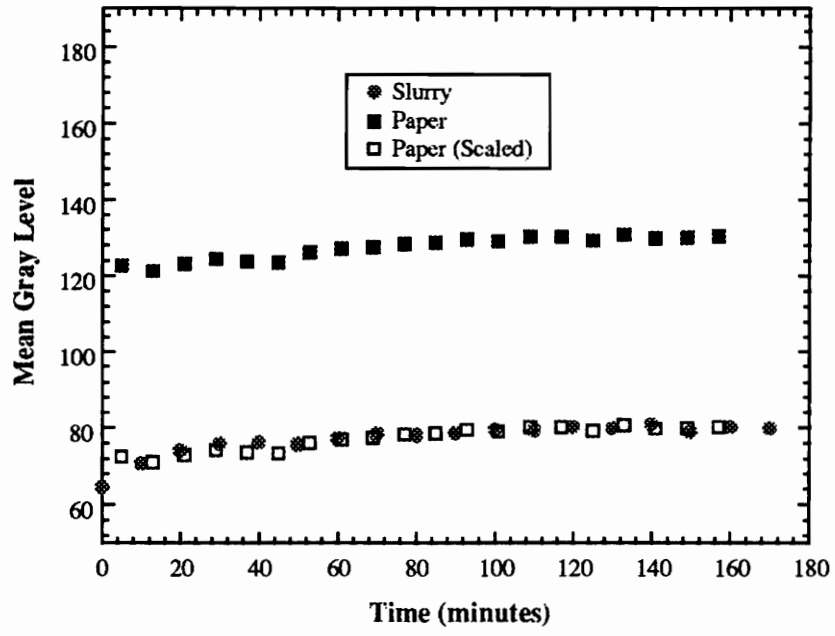

Figure 3.12 Effect of Warm-Up Time on Mean Gray Levels Obtained Using Slurry and Paper

3.4 CONTINUED IN-PLANT TESTING

3.4.1 *Middlefork Plant Visit Three*

For the third in-plant testing trip to the Middlefork plant, it was decided that the entire image analysis system, including the PC with frame grabber board and television monitor, would be taken to the plant site. This was done to eliminate the possibility of any image information loss due to intermediate storage on video-cassette. Based on previous findings, the system was allowed time to adequately warm-up before any images were collected. Once testing began, 20 images per sample were collected for analysis.

After the initial setup and system warm-up, it was found that the Plexiglas disk which fits against the camera lens and is used to create an air-tight seal for pressurizing the sample tube, was fogging due to the extremely cold weather at the plant site. It appeared that the disk, when presented with much warmer slurry from the plant would fog, making it impossible to collect clear images. After repeated attempts to clean the disk and warm the entire sensor system, the in-plant testing effort was abandoned. Instead, samples were collected throughout the day and brought back to the lab for analysis. Results of this test work are shown in Table 3.10 and Figure 3.13.

As shown, the material feeding the plant was much more consistent in terms of ash content. Thus, the samples were not particularly good for determining a calibration trend. However, it is interesting to note that for the five values with ash contents near 73%, the mean gray levels are very consistent. It should also be noted that the two points that are below the line shown are the first two samples that were analyzed and are most likely affected by the previously discussed system warm-up time. Thus, it does appear that the

use of an increased number of images collected per sample and the allowance for instrument warm-up time have substantially helped to reduce the data scatter.

Table 3.10 Ash Content, Percent Solids, and Mean Gray Levels for Samples from Middlefork Plant Visit Three

Sample Number	Column Number	Percent Solids	Percent Ash	Mean Gray Level
1	3	3.5	77.6	73.6
2	2	1.7	72.6	74.7
3	3	5.7	80.6	88.7
4	2	0.9	73.3	83.2
5	3	3.4	72.5	81.3
6	2	2.8	72.7	81.7
7	3	1.4	73.2	84.7

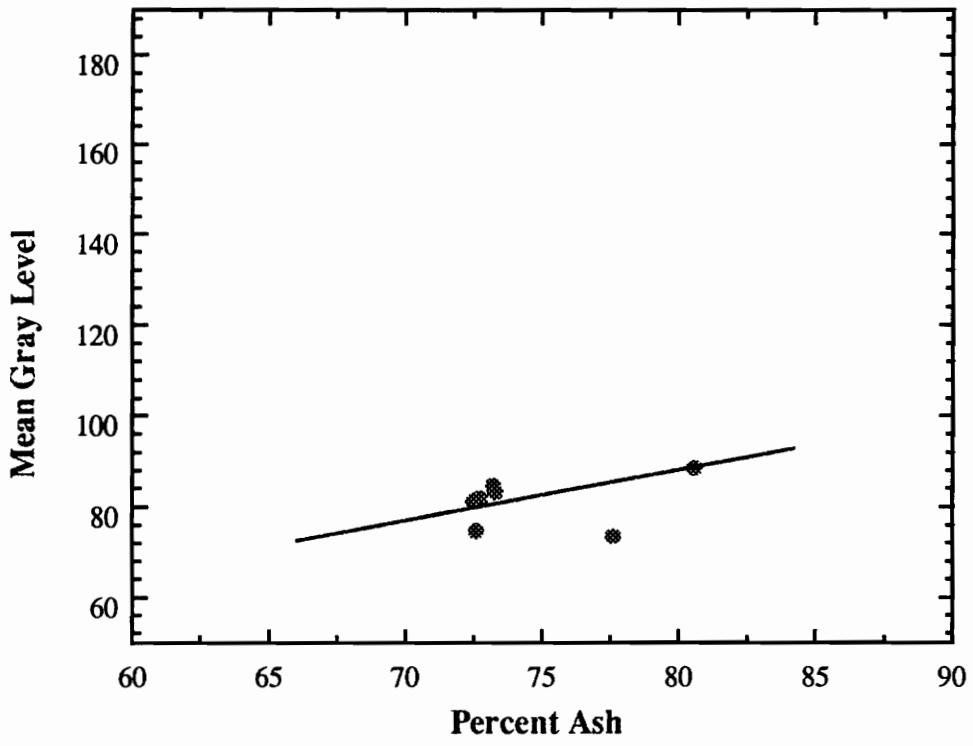

Figure 3.13 Mean Gray Level Versus Ash Content for Middlefork Plant Visit Three

3.4.2 *Middlefork Plant Visit Four*

As before, this test work was conducted by setting up the entire image analysis system at the Middlefork plant site. This was done to eliminate the possibility of information loss due to intermediate storage of images on video-cassette, and to identify and immediately troubleshoot any problems discovered during the test work.

The system was allowed to warm before sample analysis began. In total, twenty-three samples were analyzed by the optical sensor over the course of a day, while simultaneous sample cuts were collected and brought back to the lab for traditional analysis. The samples were collected from two of the five operating flotation columns at time intervals of approximately fifteen minutes. Twenty images were collected per analysis sample to ensure representative gray level measurements. Table 3.11 shows the ash content, percent solids, and mean gray levels for all samples. Some of the last samples collected had extremely low solids content and high ash values related to movement of the dredge that provides feed to the plant.

Figure 3.14 shows the mean gray levels for the 23 samples plotted as a function of ash content. This time an excellent linear correlation was obtained. Furthermore, over 50% of the data points fall within ± 1% of the best fit line, while over 95% of the data points fall within ± 2% of the best fit line. In fact, all of the data points are well within the 5% accuracy limits desired by Pittston. It should be noted that even the samples with low percent solids and high ash contents correlate nicely with the samples in the normal operating range of the plant.

Table 3.11 Ash Content, Percent Solids, and Mean Gray Levels for Samples from Middlefork Plant Visit Four

Sample Number	Column Number	Percent Solids	Percent Ash	Mean Gray Level
1	2	2.9	67.4	55.1
2	3	2.4	70.5	63.2
3	2	3.3	71.5	70.5
4	3	2.8	72.7	70.9
5	2	2.4	70.3	68.8
6	3	2.4	72.6	72.9
7	2	2.6	72.1	69.0
8	3	2.4	73.7	71.4
9	2	3.0	73.7	72.2
10	3	2.7	76.7	76.9
11	2	2.2	77.2	77.0
12	3	2.0	76.1	78.4
13	2	2.4	75.8	77.3
14	3	2.0	79.5	82.2
15	2	1.8	76.3	78.1
16	3	1.4	78.5	84.0
17	2	3.1	70.6	71.7
18	3	2.5	74.6	79.5
19	2	1.9	77.6	82.5
20	3	1.4	80.5	83.8
21	2	0.6	84.3	99.0
22	3	0.4	79.7	85.7
23	2	0.7	77.9	89.6

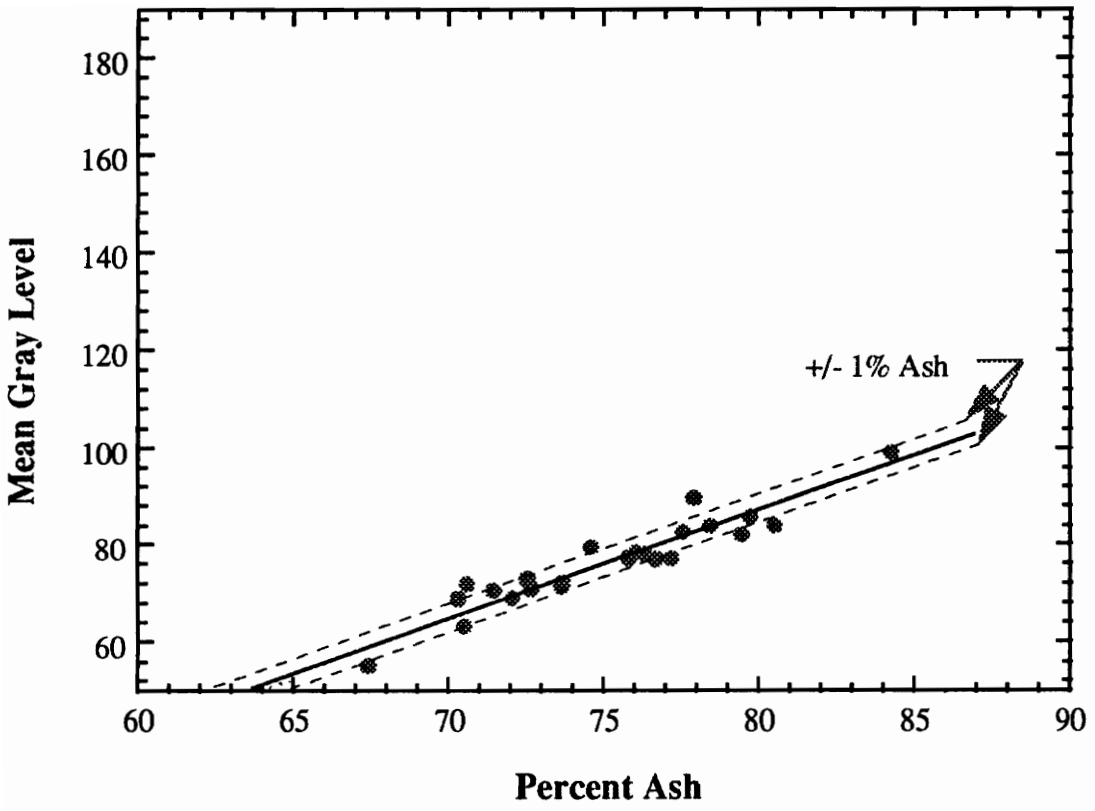

Figure 3.14 Mean Gray Level Versus Ash Content for Middlefork Plant Visit Four

3.4.3 *Middlefork Plant Visit Five*

A fifth extensive sampling trip was made to the Middlefork plant site. The entire image analysis system was again used at the site, while the system warm-up time was reduced from two hours to one to verify some inconsistencies observed in the effect of warm-up time on sensor operation.

During the testing, twenty-four tailings samples were collected from two of the five operating columns and analyzed by the optical ash analyzer. In addition, every fifth sample taken was a sample of the circuit feed. In total, six feed samples were collected throughout the day and analyzed to test the effectiveness of the optical ash analyzer on the darker feed material. At the request of Pittston personnel, flotation concentrate was also sampled whenever a feed sample was collected in order to chart the column performance over the course of a day.

Table 3.12 shows the ash content, percent solids, and mean gray levels for all the feed and tailings samples collected. The product samples that were taken and analyzed for percent solids and ash content are also included in this table. As observed in previous plant tests, some of the samples had extremely low solids content and high ash contents associated with relocation of the dredge that provides feed to the plant. Figure 3.15 shows the mean gray levels for the 24 tailing and 6 feed samples analyzed during this Middlefork plant visit. These values are plotted as a function of slurry ash content.

As shown, an excellent correlation between ash content and the mean gray values of the tailings samples was obtained. The first four tailings samples that were taken within the normal two hour warm-up time of the sensor are shown separately. The effect of the

sensor warm-up time on the mean gray value measurements for the four initial tailings samples can be clearly seen, as these points are well below the mean gray levels of the tailings samples taken during normal sensor operation. It should be noted that the tailings samples with low solids and high ash contents again correlate well with the samples taken during normal operation of the plant.

When the feed samples are added to the video analyzer calibration curve, the sensor appears to be much less effective. In fact, if one assumes that the correlation between ash content and gray level can be extended to the feed samples, the slope of the correlation appears to drop substantially for samples with less than 65% ash, indicating a dramatic drop-off in sensor resolution in terms of percent ash per gray level increment. Furthermore, the scatter in the gray levels obtained for similar feed samples is quite significant. It appears that feed slurry is too dark for the video-based sensor system. Thus, the system is unable to distinguish subtle changes in ash content in these samples. It is interesting to note that the one feed sample which has an ash content above 65% ash seems to fit reasonably well with the calibration data obtained for the tailings samples.

Table 3.12 Ash Content, Percent Solids, and Mean Gray Levels for Samples from Middlefork Plant Visit Five

Sample Number	Column Number	Percent Solids	Percent Ash	Mean Gray Level
1	2	2.18	74.58	85.26
2	3	2.97	74.52	85.45
3	2	2.83	72.34	84.00
4	3	2.09	76.61	87.35
5	2 (feed)	8.51	44.10	74.05
5-P	2 (prod)	16.73	6.38	-----
6	2	3.27	71.67	87.41
7	3	3.80	71.90	88.97
8	2	4.16	68.44	86.71
9	3	4.49	71.65	90.06
10	2 (feed)	1.59	44.39	79.45
10-P	2 (prod)	20.17	6.61	-----
11	2	3.05	71.35	89.32
12	3	4.60	71.09	91.32
13	2	6.00	62.72	88.41
14	3	4.93	73.86	96.65
15	2 (feed)	9.58	45.56	82.71
15-P	2 (prod)	15.71	7.22	-----
16	2	3.15	75.36	97.24
17	3	2.80	76.62	100.88
18	2	2.21	74.00	97.62
19	3	2.26	77.27	102.12
20	2 (feed)	9.01	44.78	87.34
20-P	2 (prod)	17.46	6.25	-----
21	2	2.92	72.41	97.29
22	3	3.55	73.14	99.49
23	2	4.23	68.92	96.16
24	3	3.53	72.90	100.40
25	2 (feed)	9.54	43.45	89.71
25-P	2 (prod)	16.59	6.51	-----
26	2	2.86	75.13	102.84
27	3	1.74	83.75	120.25
28	2	0.98	83.51	118.50
29	3	0.65	87.49	132.45
30	2 (feed)	0.52	71.72	103.86
30-P	2 (prod)	1.00	6.48	-----

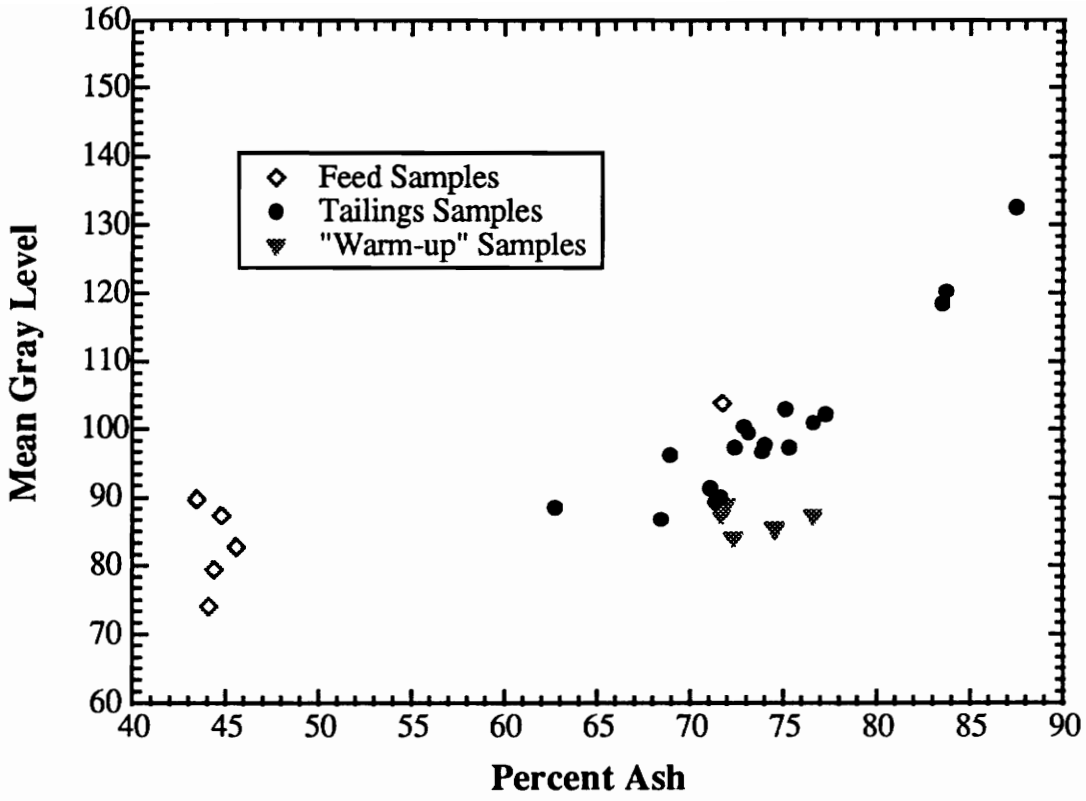

Figure 3.15 Mean Gray Level Versus Ash Content for Middlefork Plant Visit Five

3.4.4 *Comparison of Middlefork Plant Visits Four and Five*

The fourth and fifth visits to the Middlefork preparation plant provided sufficient data to validate the operation of the video-based slurry ash analyzer. Between these two visits to the plant site, some modifications were made to the light intensity monitoring function of the optical ash analyzer. The resistance photocell used to measure the intensity of sample illumination was modified to ensure its accuracy and suitability for rigorous use in the plant environment. The modification resulted in slightly altered measurements of the sample illumination intensity, but was necessary to ensure optimal performance of the optical analyzer in the future. This explains why the data that was shown previously in Figures 3.14 and 3.15 appear to be in separate regions on the gray level axis. Figure 3.16 shows the percent ash versus mean gray level plots for the 23 samples from the fourth plant visit and the 20 tailings samples from the fifth plant visit on the same graph. The four tailings samples that were analyzed within the system warm-up time during the fifth trip to the Middlefork plant site have been excluded.

Though the two sets of data are offset on the mean gray level axis, it is clearly shown that the slopes are identical. This is further demonstrated by the third set of data, which consists of the mean gray levels for plant visit four scaled to bring them in line with the data from the fifth plant visit. Thus, the fact that the calibration slope remains constant for two different incident light settings is a very useful finding. This means that even if the incident light changes over time due to the slow deterioration of the bulb, the calibration can simply be adjusted by changing an offset parameter.

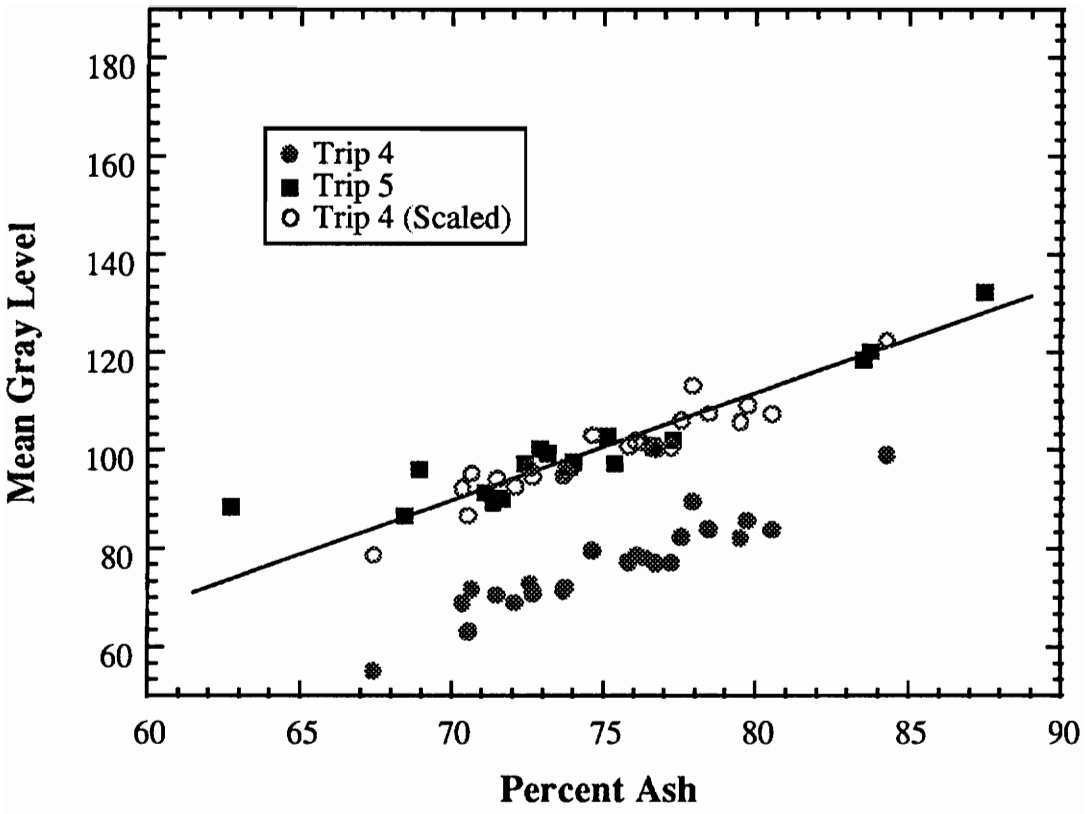

Figure 3.16 Mean Gray Level Versus Ash Content for Middlefork Plant Visits Four and Five

Figure 3.16 shows clearly that operation of the video-based slurry ash analyzer has been validated by collection of numerous samples over several visits to the Middlefork plant site. Once this initial calibration of the optical analyzer had been established, preparations began which would allow the video-based sensor to be installed at the Middlefork site for on-line operation and testing.

3.4.5 *Maple Meadow Plant Visit One*

The video-based slurry ash analyzer was also tested at the Maple Meadow coal preparation facility, which was described in section 3.1.2. The tests that were carried out were performed in the same fashion as the latter tests that were performed and have been previously described at the Middlefork plant. The entire image analysis system was setup at the plant site and twenty images per tailings sample were used to calculate the slurry mean gray level. The system was also allowed to properly warm up before the tailings samples were analyzed. Table 3.13 shows the percent solids, ash content and mean gray level for the eighteen samples that were taken during the first plant test at the Maple Meadow plant site. The mean gray levels for all eighteen samples are plotted as a function of slurry ash content and depicted in Figure 3.17.

As shown, there is a significant amount of scatter in this plot. The majority of the samples are in the range of 47-52% ash, and differences of up to 8 gray level increments are seen with samples that have similar ash contents. Furthermore, the two samples with slightly higher ash content did not show any slurry mean gray level increase. It was theorized that the lack of a correlation between the mean gray level of the slurry samples and the ash content of the samples might be due simply to the fact that the ash content of the samples analyzed was too low to distinguish a difference in slurry color. As shown previously by the series of tests that were carried out at the Middlefork plant site, the video-based analyzer was only suitable for slurry with ash contents greater than 65%. Also, the Maple Meadow flotation circuit is generally much more coarse than the Middlefork circuit, and there was concern that the coarse material was settling out of the

sensor sample tube, affecting the representativeness of the slurry samples and subsequent images.

Table 3.13 Ash Content, Percent Solids, and Mean Gray Levels for Samples from Maple Meadow Plant Visit One

Sample Number	Percent Solids	Percent Ash	Mean Gray Level
1	2.8	33.3	25.3
2	14.1	36.1	23.5
3	5.4	29.0	22.8
4	2.6	51.9	25.3
5	2.5	50.1	27.9
6	3.1	58.9	22.2
7	2.8	51.1	30.7
8	2.5	52.7	30.0
9	2.5	47.2	30.7
10	2.5	51.5	29.9
11	2.4	49.6	28.5
12	2.5	52.1	28.7
13	2.9	57.9	31.1
14	2.8	51.8	31.1
15	2.8	49.7	29.4
16	2.7	48.7	30.4
17	2.5	52.0	31.2
18	2.6	51.1	33.0

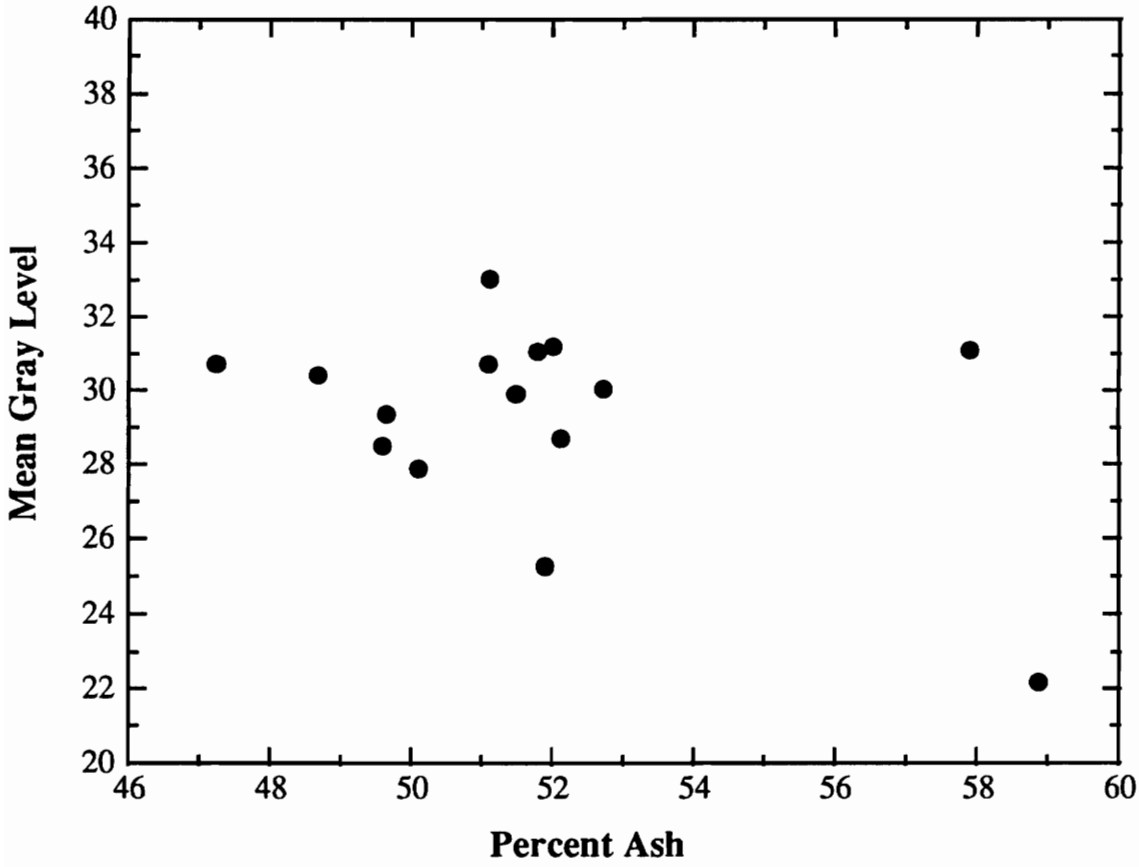

Figure 3.17 Mean Gray Level Versus Ash Content for Maple Meadow Plant Visit One

3.4.6 *Maple Meadow Plant Visit Two*

The testing for the second visit to the Maple Meadow plant site was again carried out in the same fashion as previous plant test work. After reviewing the data from the first trip to this site, it was decided that the sample lighting scheme be optimized to allow for the most appropriate sample illumination. It was hoped that increased slurry sample illumination might provide a means of distinguishing between the subtle changes in ash content for these lower ash samples. Table 3.14 shows the percent solids, ash content, and mean gray levels for the eighteen samples analyzed during this second in-plant test. Figure 3.18 shows the mean gray levels for the eighteen Maple Meadow plant visit two samples plotted as a function of slurry ash content.

As shown, the correlation between mean gray level and ash content of the slurry samples is definitely improved. There is still a large amount of scatter in the data, though overall there does seem to be a vague increase in slurry gray level with ash content. Thus, it appears that increased sample illumination may have improved the ability of the sensor to distinguish between very subtle changes in ash content. At this point it was decided that the size distribution effect on the test work should be investigated.

The results of size-by-size ash analysis of the Maple Meadow flotation circuit were shown previously in Figure 3.3. This test work showed that even if some coarse material settles out of the sample presentation tube and is not seen by the optical ash analyzer, the size fraction that remains in the tube should be sufficiently representative to perform a reasonable measurement of slurry gray level.

Table 3.14 Ash Content, Percent Solids, and Mean Gray Levels for Samples from Maple Meadow Plant Visit Two

Sample Number	Percent Solids	Percent Ash	Mean Gray Level
1	3.0	51.8	82.2
2	3.6	49.8	67.0
3	3.0	53.4	55.7
4	3.3	47.7	54.3
5	2.1	41.5	57.8
6	4.5	48.3	49.2
7	3.8	47.6	65.7
8	3.8	47.7	62.5
9	3.2	48.6	73.8
10	3.0	47.9	52.1
11	3.2	46.4	0.0
12	3.1	47.2	66.2
13	3.0	48.0	66.0
14	3.1	45.0	66.0
15	3.6	46.9	62.9
16	3.0	43.5	65.1
17	2.8	52.0	66.9
18	3.6	52.9	77.1

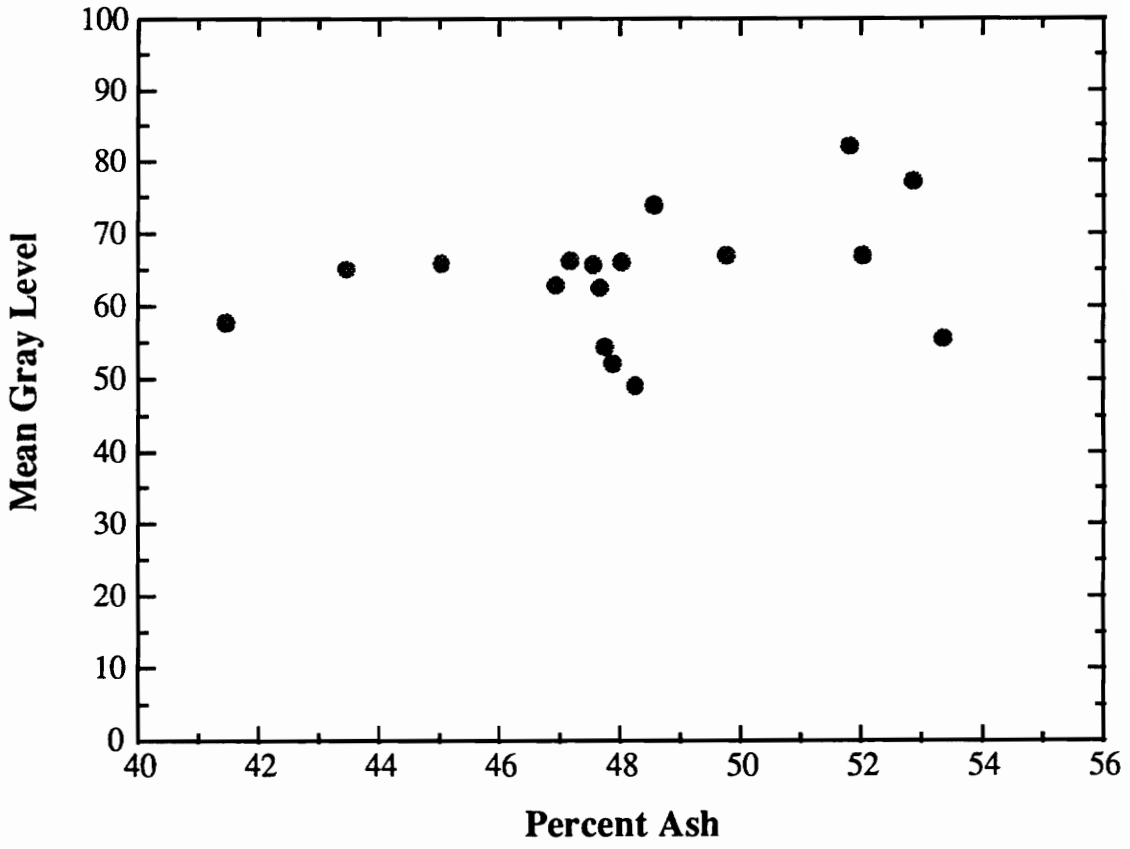

Figure 3.18 Mean Gray Level Versus Ash Content for Maple Meadow Plant Visit Two

3.4.7 *Maple Meadow Plant Visit Three*

One additional plant test of the video-based slurry analyzer was performed. The test work was performed using the same procedure as has been described previously for in-plant testing of the optical ash analyzer. Table 3.15 show the ash content, percent solids, and mean gray levels for the eighteen samples that were analyzed during this in-plant test. Figure 3.19 shows the mean gray level for all 18 samples plotted as a function of slurry ash content.

As shown, a vague correlation exists between the mean gray level of the slurry samples and ash content. There is an upward trend, but the amount of data scatter is too great to permit any calibration of the sensor. It is thought that the main reason for the poor sensor resolution is the low range of ash content that is normally produced in the Maple Meadow plant flotation tailings. The ash range is very low, especially when compared with Middlefork tailings, and does not permit the video-based slurry sensor to distinguish between subtle changes in ash content.

As expected, some correlation was seen with the flotation tailings mean gray level and ash content from samples analyzed during multiple visits to the Maple Meadow preparation facility. The amount of data scatter however, was considered too great to permit the use of the video-based sensor as a process quality measurement tool. Thus, testing of the optical ash analyzer at the Maple Meadow site was abandoned, and work focused completely on the on-line installation of the sensor at the Middlefork preparation facility.

Table 3.15 Ash Content, Percent Solids, and Mean Gray Levels for Samples from Maple Meadow Plant Visit Three

Sample Number	Percent Solids	Percent Ash	Mean Gray Level
1	3.3	45.8	89.2
2	3.9	44.4	88.1
3	4.0	39.4	89.2
4	3.8	41.1	97.1
5	3.9	43.5	111.0
6	3.5	42.0	109.3
7	3.6	48.4	109.6
8	3.2	43.5	109.6
9	3.3	45.0	119.5
10	3.5	47.7	137.8
11	3.5	44.0	160.8
12	3.4	48.0	139.7
13	3.5	50.2	136.4
14	3.6	47.2	137.0
15	3.3	43.4	142.9
16	3.5	49.8	139.3
17	3.4	45.7	137.4
18	3.2	45.1	148.7

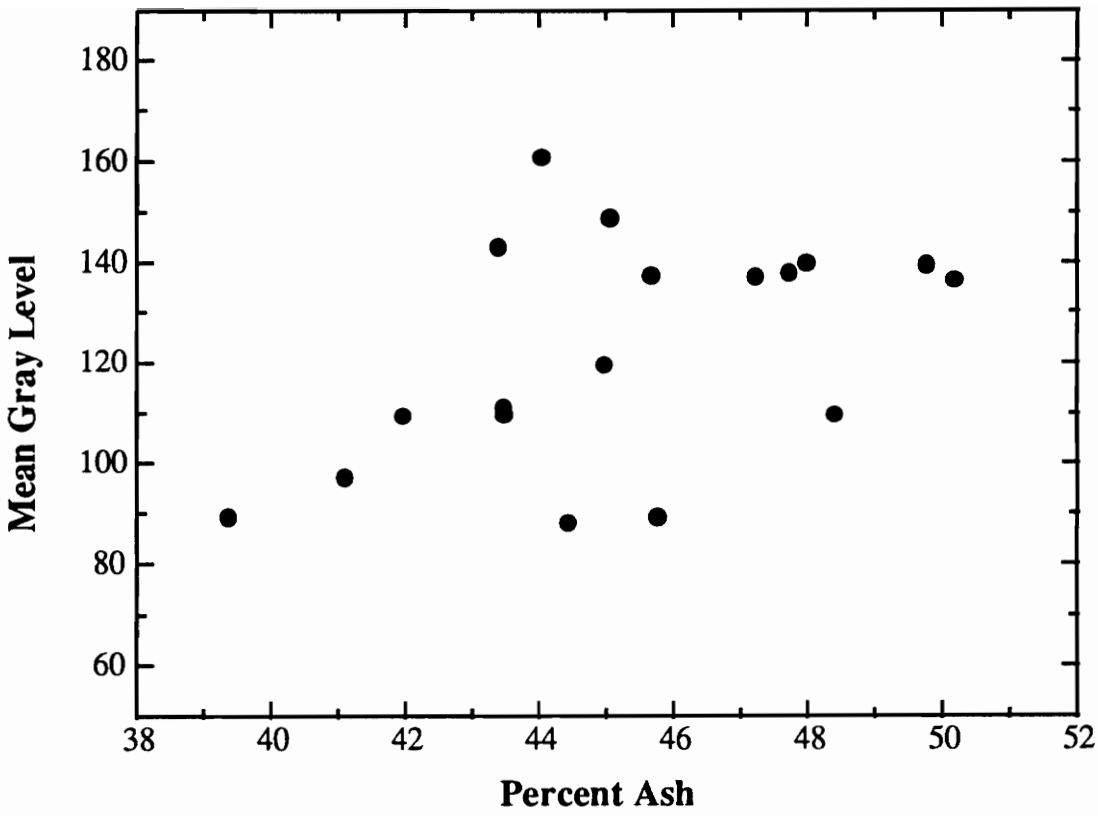

Figure 3.19 Mean Gray Level Versus Ash Content for Maple Meadow Plant Visit Three

3.5 INSTALLATION OF ILLUMINATION STANDARD

Throughout the development of the video ash analyzer, it was noticed that small fluctuations in sample illumination often caused added noise in the data. Although these fluctuations were kept to a minimum, it was felt that an in-situ light standard might provide a means of further minimizing or eliminating these fluctuations. Thus, a method for identifying and automatically correcting for small variations in the sample system illumination was developed and incorporated into the operation of the ash analyzer. The sample presentation tube was modified to include a one-inch diameter sealed PVC tube attached to the inner wall of the sample tube. One end of the one-inch tube was sealed against the Plexiglas disk that separates the camera lens from the sample presentation tube. The other end of the one-inch tube was sealed with a gray disk at the focal length of the camera. This gray disk serves as an illumination standard. It is positioned in such a way that a portion of the disk is always visible in the field of view of the video camera. Figure 2.8 showed a cross-section view of the sample presentation tube, showing the placement of the illumination standard within the effective image area.

Once the illumination standard had been successfully installed in the sample presentation tube, testing was carried out to quantify the relationship between gray level changes of the illumination standard and the slurry samples. A series of samples were analyzed at two lighting conditions each. First, the samples were analyzed at a predetermined optimal illumination condition, and then the same samples were reanalyzed at a slightly different lighting condition. These results are shown in Table 3.16.

The varying lighting conditions for each sample caused differing gray level measurements for the illumination standard and the slurry. The percentage change in the gray levels for both the illumination standard and the slurry were then calculated for each sample. Figure 3.20 shows the percentage change in the slurry sample gray level plotted versus the percentage change in the illumination standard gray level. As shown, there appears to be a fairly good linear relationship between the gray level change in the standard and in the slurry sample with a slope of approximately 2.3. Thus for every one percent gray level change in the illumination standard, the gray level measurement of the slurry should be adjusted by 2.3 % in order to maintain a consistent calibration and a consistent ash measurement regardless of light fluctuations. It is important to note that the scatter in the data appears to increase as the percentage change in the gray level (i.e., the severity of the light fluctuation) increases. However, the data clearly indicated that this type of correction is suitable for the small fluctuations in light intensity normally encountered due to variations in line voltage.

Table 3.16 Slurry Sample and Illumination Standard Percent Gray Level Changes with Varying Lighting Conditions

Sample Number	Percent Solids	Percent Ash	Slurry (I) Gray Level	Standard (I) Gray Level	Slurry (II) Gray Level	Standard (II) Gray Level	% Slurry GL Change	% Standard GL Change
1	3.05	74.05	113.2	199.5	133.1	214.9	17.6	7.7
2	3.12	73.83	111.3	201.8	93.2	186.2	16.3	7.7
3	3.26	74.37	111.5	201.5	127.8	213.5	14.6	6.0
4	3.41	72.59	110.3	201.0	97.0	189.3	12.1	5.8
5	3.17	74.01	111.8	202.8	88.7	181.9	20.7	10.3
6	3.79	70.01	110.9	200.7	131.4	215.2	18.5	7.2
7	3.24	72.01	118.8	201.6	108.0	193.5	9.1	4.0
8	3.44	71.57	121.2	204.7	139.7	218.9	15.3	6.9
9	5.24	64.77	116.1	205.1	104.4	195.1	10.1	4.9
10	3.93	67.04	114.4	203.0	144.4	223.0	26.2	9.9

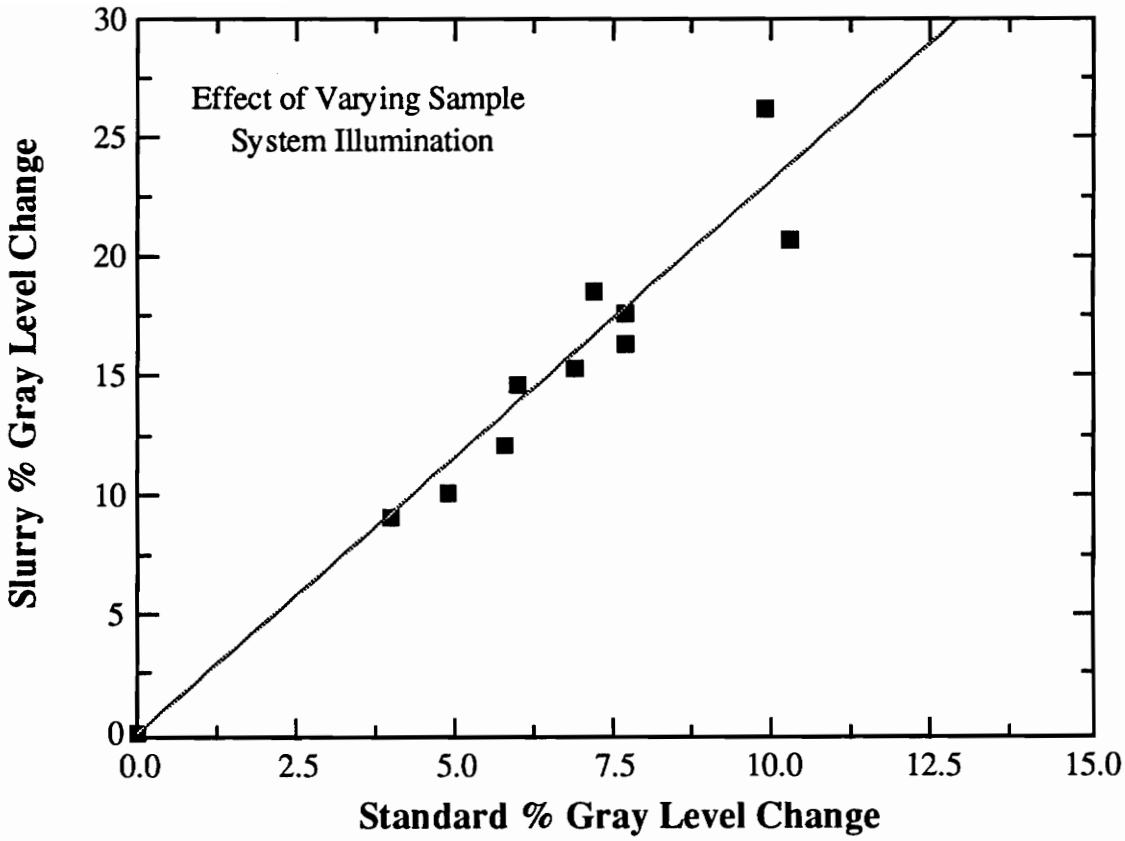

Figure 3.20 Slurry Gray Level Percent Change Versus Illumination Standard Gray Level Percent Change for Varying Lighting Conditions

CHAPTER 4
ON-LINE INSTALLATION

4.1 SYSTEM ARRANGEMENT

Prior to the installation of the video-based ash analyzer at the Middlefork preparation plant, Pittston personnel assisted in preliminary site preparation. This initial work was primarily concerned with the construction of appropriate piping and conduit necessary for providing slurry, air and electricity to the sample presentation system and carrying video and electrical signals from the sensor back to the control room. The details of the sensor installation are described below.

The five operating flotation columns at the Middlefork preparation plant are equipped with a sampling system which allows samples to be taken from each individual column or any combination of columns for each of the three process streams (feed, tailings and clean coal). In preparation for the installation of the video-based ash analyzer, the existing tailings sample lines were modified to provide a continuous flow of tailings slurry to the sample presentation system. Initially the tailings sample presented to the analyzer was a combination of the tailings from all of the columns. It is expected, however, that this configuration may be modified at a later date to allow for tailings ash analysis of any particular column.

In the present configuration of the ash analyzer, slurry is gravity-fed from the sample line to the sample presentation system sump eliminating the need for any intermediate pumping system. In addition, a dedicated 120-volt electrical line has been installed near the sample presentation system to provide power for the light, camera,

solenoid valve and mixer. An air line has also been installed to provide a means of pulsing the slurry in the sample presentation tube.

The PC image analysis system was placed on the top floor of the plant in the operator control room. The sample presentation system was located on the bottom floor of the plant near the existing sampling ports. These two components of the video-based ash analysis system are linked by a video cable and a low voltage signal line. The video cable transmits the live image from the camera to the PC for image analysis and subsequent ash determination. The low voltage signal line provides signals from the PC to the solenoid valve in the sample presentation tube to allow a fresh sample to be acquired from the sump. Currently these lines are temporarily installed. Permanent conduit will be added by Pittston personnel once the final configuration is established.

A heavy duty industrial cabinet is used to house the sample presentation system. It serves to eliminate any problems which may occur due to the harsh environment in which the sensor is operating. The electrical and air lines have been permanently placed on the cabinet wall to provide power and air for the system. The sample sump is bottom-fed through the cabinet wall, and a launder is used to collect the overflowing slurry. Finally, the overflowing slurry exits through the cabinet wall and is discharged into a nearby floor sump. Figure 4.1 shows a schematic of the industrial setup for the ash analyzer.

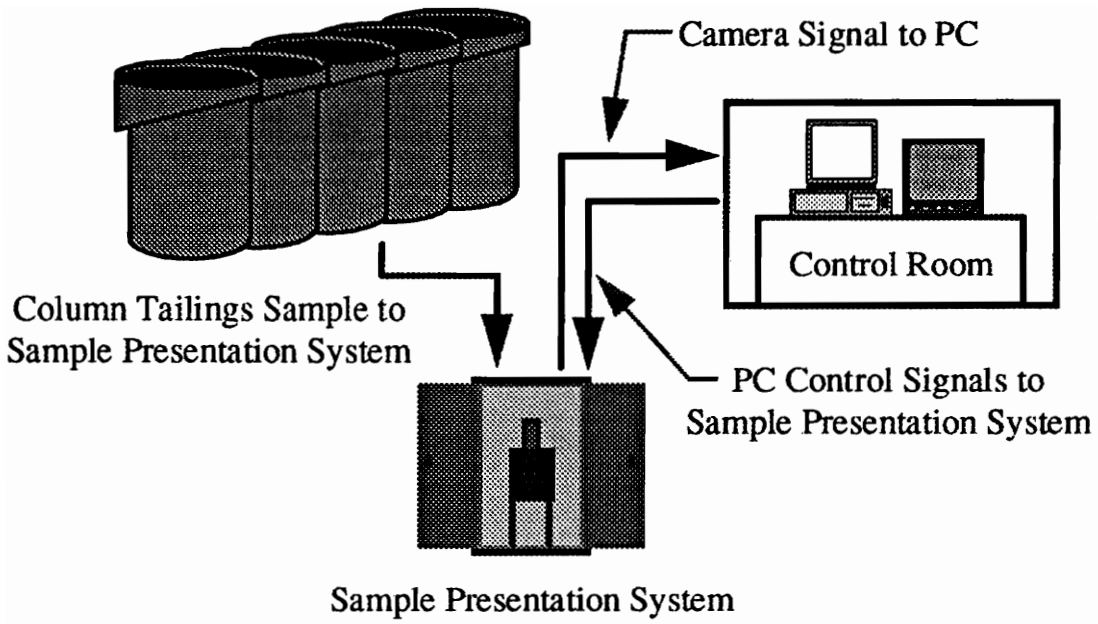

Figure 4.1 Schematic of the Industrially Hardened Video-Based Ash Analyzer

4.2 SOFTWARE DEVELOPMENT

Software for the video-based ash analyzer was developed using the Optimas image processing package. This Windows-based package includes a macro language, ALI (Analytical Language for Images), which can be used to develop application software for specific uses. ALI is a pseudo-"C" code that makes the creation of application-specific image processing routines quick and simple. It is also an interpreted language which saves time over conventional compiled languages during the software development stage.

The software that is currently used to control and operate the video-based ash analyzer at the Middlefork site is a very simplified Windows-based application written in ALI. The macro code for this application is included in Appendix A. Measurement intervals from five minutes up to two hours can be selected, and the user can choose whether or not the sensor information will be logged to a file as measurements are performed. Appendix B shows an excerpt of the sensor measurement log file generated over a period of days during early on-line testing. A user-specified calibration can also be entered by directly providing values for the slope and intercept of a linear calibration between slurry mean gray level and ash content. Figure 4.2 shows a simplified flowsheet of the sensor software.

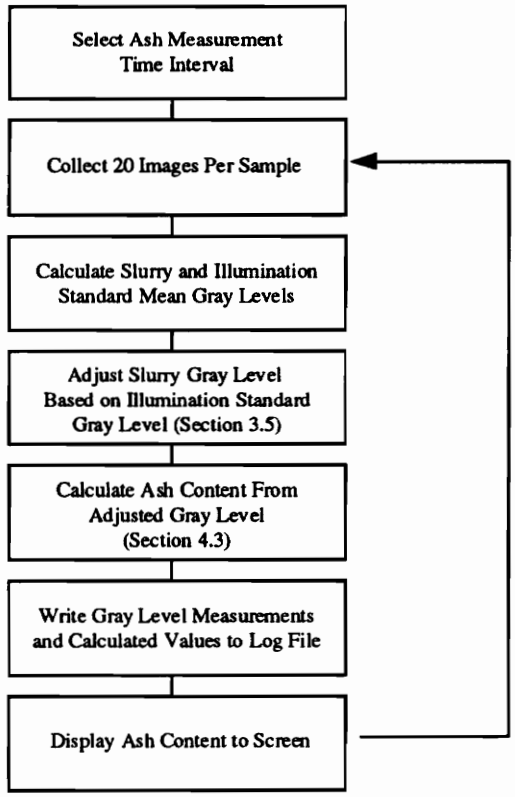

Figure 4.2 Simplified Flowsheet of Video-Based Ash Analyzer

4.3 ON-LINE CALIBRATION

Once the video-based slurry analyzer had been successfully installed at the Middlefork plant site, it was necessary to perform a series of tests to calibrate the sensor. Calibration commenced by initializing the software and setting the system to acquire samples at an interval of five minutes. Representative sample cuts were taken throughout the testing, and these samples were analyzed for percent solids and ash content at Pittston Coal Company's Clinchfield Laboratory. Table 4.1 shows the data collected during the initial on-line calibration of the slurry ash analyzer.

The illumination standard gray level measurement is taken as a measurement of the light intensity inside the sample presentation tube. From previous experience in dealing with the sensor system, it had been observed that optimal slurry images are obtained when the illumination standard mean gray level measures approximately 200. Thus, the percent change of the illumination standard is calculated as a percent deviation from 200. The appropriate percentage adjustment for the slurry mean gray level measurement is calculated by multiplying the illumination standard percent change by 2.3, as determined in Section 3.5, and shown in Figure 3.21. An adjusted, light-corrected slurry mean gray level value is then calculated by applying the slurry percent gray level change to the "raw" slurry gray level value. Figure 4.3 shows the initial slurry gray level measurements and the illumination standard-corrected slurry gray level measurements plotted as a function of ash content. It is shown that the outlying data points fall neatly in line once the measurement values have been corrected by the illumination standard.

Table 4.1 Ash Content, Percent Solids, and Mean Gray Levels for Samples from Middlefork Initial On-Line Calibration

Sample Number	Percent Solids	Percent Ash	Slurry Gray Level	Standard Gray Level	% Standard GL Change	% Slurry GL Change	Adjusted Slurry GL
1	4.0	74.3	74.1	199.0	-0.5	-1.2	75.0
2	5.0	72.6	73.4	199.2	-0.4	-0.9	74.1
3	5.3	70.1	74.9	200.0	0.0	0.0	74.9
4	2.8	77.2	77.2	200.7	0.3	0.8	76.6
5	2.1	78.7	79.1	200.2	0.1	0.2	78.9
6	2.6	76.0	76.4	200.8	0.4	0.9	75.7
7	3.3	76.4	77.6	201.1	0.5	1.3	76.6
8	2.5	78.9	80.5	200.4	0.2	0.5	80.1
9	1.9	77.7	79.9	200.6	0.3	0.7	79.3
10	2.6	76.4	78.9	202.1	1.1	2.4	77.0
11	3.0	75.0	75.6	199.8	-0.1	-0.2	75.8
12	3.6	70.0	75.3	199.8	-0.1	-0.2	75.5
13	2.3	77.1	92.1	211.1	5.5	12.7	80.4
14	2.8	75.4	92.8	212.7	6.3	14.6	79.2
15	2.1	78.4	96.0	214.8	7.4	17.0	79.7
16	1.3	81.5	99.4	215.6	7.8	17.9	81.6
17	0.8	68.4	91.3	215.4	7.7	17.7	75.1
18	1.0	68.0	90.0	216.6	8.3	19.1	72.8
19	1.0	68.6	91.2	217.6	8.8	20.2	72.7
20	1.0	69.4	82.0	211.2	5.6	12.9	71.4
21	1.1	67.4	81.4	211.9	6.0	13.7	70.3

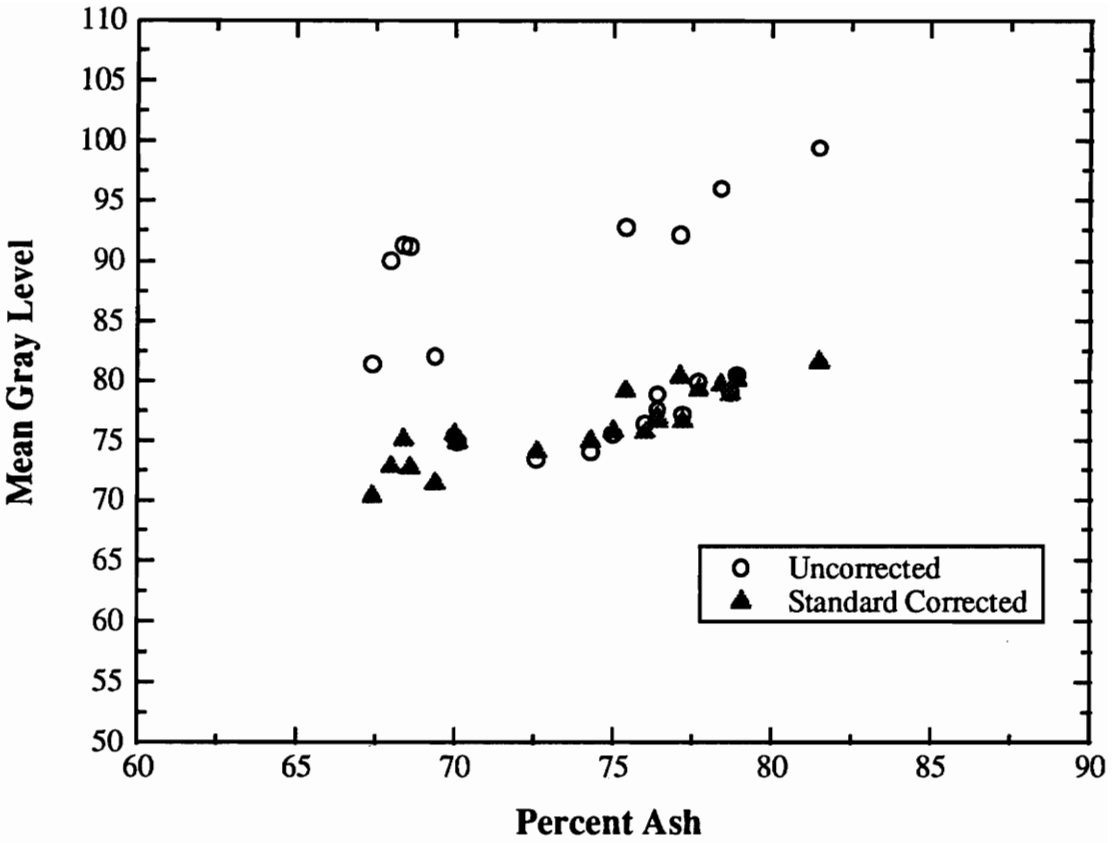

Figure 4.3 Mean Gray Level Versus Ash Content for Raw Data and Illumination Standard Corrected Data

Figure 4.4 shows these adjusted slurry gray level measurements plotted as a function of ash content. A linear regression fit to the data is also plotted in Figure 4.4. This linear fit was used as the initial on-line sensor calibration, with the slope and y-intercept values of 0.64 and 28.8 respectively, entered as inputs in the calibration portion of the ash analyzer software.

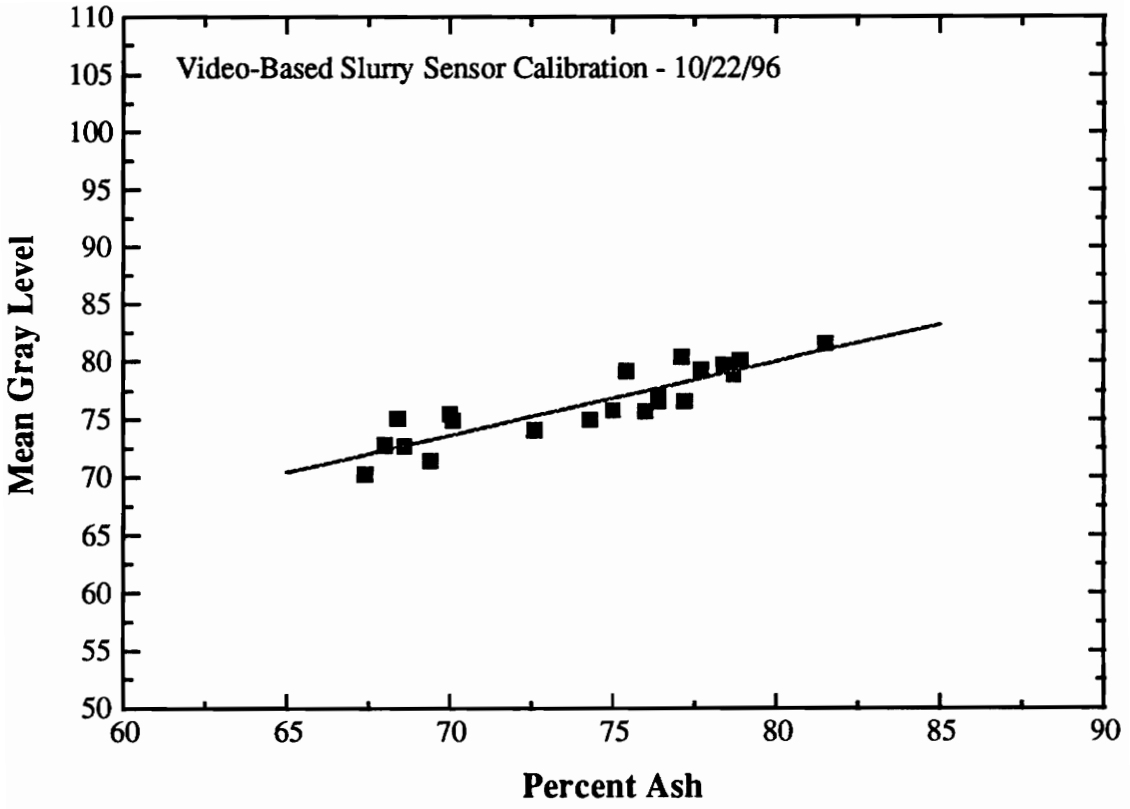

Figure 4.4 Initial On-Line Slurry Ash Analyzer Calibration

4.4 PERFORMANCE EVALUATION

At the writing of this thesis, the video-based slurry ash analyzer had only recently been installed on-line at the Middlefork plant site. Some preliminary test work has been carried out permitting the generation of an on-line calibration, and the continuous sensor operation has been initiated. Additional test work evaluating the sensor performance is underway. It is planned that the evaluation of the on-line performance of the sensor will be carried out in much the same manner as was described in the previous section for the determination of an initial sensor calibration. Samples are taken during sensor operation and analyzed for ash content. These actual ash content values can then be compared to the ash measurements that were predicted by the video-based ash analyzer and saved in the system log file. If deemed necessary, this approach will also allow for continual improvement of the sensor calibration.

In order to evaluate the on-line performance of the video-based ash analyzer, the data collected to date from continuous in-plant tests have been plotted in Figure 4.5 along with the 90% prediction interval. Prediction intervals are statistical parameters used to indicate the ability of a sensor to predict the next measurement. In other words, there is a 90% chance that any value predicted by the sensor will fall within the band illustrated in Figure 4.5.

As shown, the majority of the data points lie within the lines representing the 90% prediction interval. This corresponds to a sensor accuracy of 72.7% ± 4.1% ash. This method of reporting the accuracy of a sensor tends to lead to higher error values than

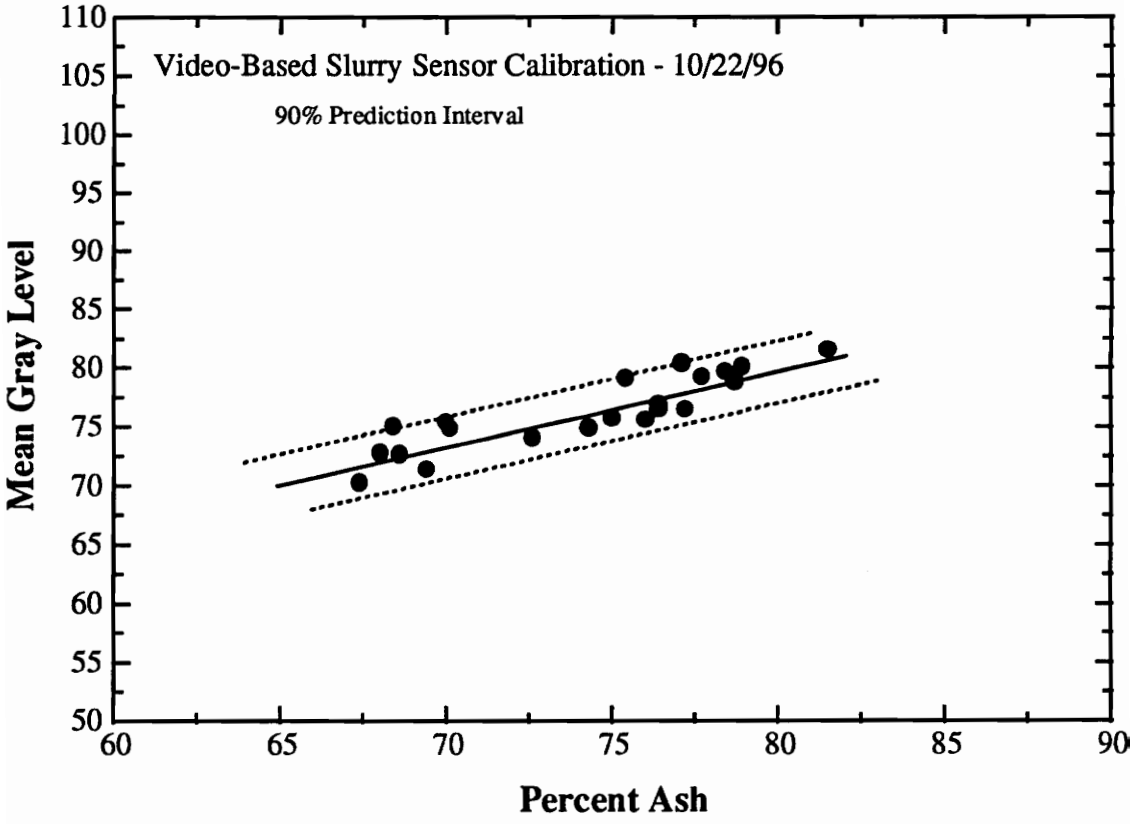

Figure 4.5 Slurry Ash Analyzer Calibration Plotted With a 90% Prediction Interval

normally found in the literature for other slurry ash analyzers. However, it is probably the most appropriate way to characterize sensor performance. In most work of this type, statistical analyses are carried out incorrectly. In the literature, for example, sensor accuracy is often represented by the standard deviations of the data set. This value is meaningless since it has little to do with how well the sensor can predict a given value. A 90% confidence interval may also be used to characterize sensor accuracy; however, this is also an inappropriate statistical measure. Confidence intervals only indicate how well a model or calibration line fits an existing data set. They are meaningless in determining how well the sensor can predict a given value.

Thus, prediction intervals are the appropriate statistical measures for determining the ability of a sensor to make an accurate measurement. Table 4.2 shows the 90% confidence and prediction intervals for the initial plant testing (Section 3.4.4) and the on-line testing (Section 4.3) of the video-based ash analyzer.

As shown, the sensor accuracy when measured in terms of a 90% confidence interval appears remarkable in both cases. These values are in fact ludicrous, and it must be reiterated that confidence intervals are a completely inappropriate format in which to evaluate the performance of a model or calibration curve. As seen, the prediction interval is a more realistic measure of the sensors ability to estimate ash content based on a given mean gray level measurement. Currently, the accuracy of the video-based ash analyzer, as determined by the 90% prediction interval, is 72.7% $\pm$ 4.1% ash. This is slightly less than the accuracy determined during developmental testing of the video-

Table 4.2 Calculated Confidence and Prediction Intervals at 72.7% Ash for Initial and On-Line Sensor Testing

	90% Confidence Interval	90% Prediction Interval
Initial Testing	72.7% ± 0.043% Ash	72.7% ± 3.5% Ash
On-Line Testing	72.7% ± 0.053% Ash	72.7% ± 4.1% Ash

based ash analyzer; however, the current on-line accuracy level was determined from a very small data set. This value is expected to improve over time as the on-line evaluation of the sensor performance continues. As the database of slurry gray level measurements and related slurry ash contents increases, it is expected that the sensor accuracy will match or surpass that shown for the initial calibration of the analyzer of 72.7% ± 3.5% ash based on a 90% prediction interval.

In the literature, the performance of slurry ash analyzers has traditionally been evaluated by comparing the statistical measurements of standard and relative error. As previously discussed, this method of determining the accuracy of a sensor is incorrect. For the sake of comparing the video-based ash analyzer accuracy to published values of nuclear-based ash analyzer accuracy, these statistical figures were calculated for the video-based sensor from the data obtained during the initial on-line testing. Table 4.3 shows the operating range, standard error, and relative error found in the literature for several tailings ash analyzers [6].

As shown, the Virginia Tech video-based performed very similarly to the nuclear based tailings ash analyzers. It should be noted that the data from the initial on-line testing of the sensor was used to calculate these sensor accuracy figures. The statistical measures of standard and relative error are greatly affected by the amount of data points considered, thus the Virginia Tech video-based sensor accuracy is remarkable when taking into account the small data set that was used in these calculations.

The video-based ash analyzer has been successfully installed on-line at the Middlefork plant site. Initial data from on-line testing indicate that the sensor performance is within the range of accuracy that is considered typical for the existing nuclear-based ash analyzers. It is believed that the ongoing testing of the sensor will allow the ash analyzer performance to be optimized, thus improving the ash prediction capability. Considering the ease of setup and use, operator acceptance, and comparable sensor accuracy, the video-based ash analyzer has easily proven itself to be a viable competitor with the nuclear-based devices.

Table 4.3 Performance Comparison of Coal Tailings Ash Analyzers

Ash Analyzer	Analyzer Type	Operating Range (% Ash)	Standard Error	Relative Error
Ashscan	Nuclear	40-80	4.4	7.3
Bergbau	Nuclear	5-65	1.6	4.6
Michigan Tech	Nuclear	56-78	0.7	1.1
MRDE	Nuclear	50-80	2.0	3.1
OSCAA	Nuclear	40-80	4.4	6.2
Virginia Tech	***Optical***	**65-90**	**4.8**	**6.6**

CHAPTER 5
SUMMARY AND CONCLUSIONS

This thesis has described the design, development, construction, testing and in-plant installation of a video-based slurry ash analyzer for fine coal tailings slurries. The major accomplishments of this work are summarized below:

1. A novel sample presentation system was developed which allows high quality images of slurry to be acquired continuously on-line. The system consists of a PVC tube, open at one end and containing a television camera and light source at the other end. The tube is inserted into a tank filled with slurry. Air pressure inside the tube is used to control the slurry level to the focal plane of the camera. Fresh slurry is drawn into the tube by pulsing the air pressure. As opposed to other optical slurry analyzers which have been proposed, this system requires no interface between the camera and the slurry which can become clouded over time.
2. A parametric study was carried out to identify those parameters which are responsible for influencing the correlation between slurry ash content and gray level. Laboratory tests indicated that, over the typical range of values encountered at the plant, the optical analyzer is relatively insensitive to percent solids, particle size distribution, sample presentation tube angle and incident light intensity. The camera was found to exhibit a warm-up period during which the resulting mean gray level of a given image gradually increases. As a result, a two-hour warm-up period is allowed before collecting any data. The number of images collected per

sample was also found to be a major contributor to data scatter. Laboratory tests indicate that 20 images should be collected per sample to ensure accurate gray-level readings.

3. Calibration tests were conducted on site at the Middlefork preparation plant (Pittston Coal Company). An excellent linear correlation between mean slurry gray level and ash content was obtained from these tests. After numerous plant visits, a consistent sensor calibration was obtained with approximately 90% of all samples analyzed falling within ± 2% ash of the best fit calibration line. The 90% prediction interval for this calibration yielded an accuracy of 72.7 ± 3.5% ash. This result was well within Pittston's desired sensitivity.

4. A method for identifying and automatically correcting for small variations in the sample illumination scheme was developed and incorporated into the operation of the video-based ash analyzer. An illumination standard was installed into the sample presentation tube and located within the field-of-view of the slurry image. When lighting conditions vary, changes are detected by analysis of the illumination standard, and corresponding adjustments are made to the slurry gray level measurement.

5. The video-based slurry ash analyzer has been successfully installed on-line at Pittston Coal Company's Middlefork preparation plant Preliminary evaluation of the ash analyzer's on-line performance indicates an accuracy of 72.7 ± 4.1% ash,

based on a 90% prediction interval. It is expected that sensor accuracy will improve as additional data points are added to the calibration set.

The video-based tailings ash analyzer has been successfully developed, tested, and installed at the Middlefork plant site. It is currently successfully operating on-line at the plant site. Realistically, it should be remembered however that there are limitations to the application of this sensor, and sensors of this type. As shown by the testing at the Maple Meadow plant site, this tailings ash sensor is not suitable for use with low ash content slurries (< 65% ash) or for tailings material that contains dark colored mineral matter such as shale. The successful implementation of this sensor and sensors of this type depends on the relationship that exists between visual appearance and quality. For applications where plant operators actively perform process control measures based on visual inspections of process streams, these types of sensors will be successful.

CHAPTER 6
FUTURE WORK

6.1 LONG TERM SENSOR PERFORMANCE

At the writing of this thesis, the video-based ash analyzer has only been running on-line at the Middlefork plant site for approximately 6 weeks. The transfer of knowledge and technology regarding the PC-based image analysis system is still underway, and the operation of the sensor is still being monitored closely. Periodic plant visits are planned to monitor the sensor performance, improve the sensor calibration, and update and improve the analysis software.

The software used to generate the user-friendly operator interface is currently being improved. Planned improvements include (i) a graphical display showing the trend of tailings ash content versus time, (ii) a light adjustment routine that activates if the gray level of the illumination standard falls outside a pre-determined range, and (iii) an alarm system to alert plant operators when the slurry ash content goes beyond a user-defined range. These changes are relatively simple in nature and are to be implemented as soon as possible.

6.2 INVESTIGATION OF ALTERNATIVE IMAGING SYSTEMS

The image analysis equipment used in the fabrication of this video-based sensor is standard and widely available commercially, while imaging and personal computer technology continues to develop at an unbelievable rate. A PC-based image analysis system was purchased recently that uses a 24-bit television camera for image acquisition at incredible speeds. It utilizes a frame-grabber with live VGA capabilities allowing the live image to be displayed on the PC monitor. This feature eliminates the need for a costly second monitor and greatly reduces the expense of the system. It is expected that such a reduction in cost may make the video-based sensor even more attractive to industry.

The use of digital cameras that can directly link to a PC without the use of a special frame-grabber board is also increasing. Digital camera information can be passed directly to the computer through existing data ports and be directly displayed on the PC monitor. The digital format of the image information eliminates the need for a frame-grabber board which is normally responsible for the conversion of the analog camera signal to a digital format. Currently, the speed of acquisition and the resolution that the digital camera provides is not cost effective; however, the current pace of technological advancements in the area of PC-based imaging will make the commercial use of high speed digital cameras a reality in a matter of a few years.

6.3 SENSOR-BASED CONTROL SYSTEM

Once the accuracy and reliability of the video-based slurry ash analyzer has verified in-plant over an extended period of time, it is likely that this sensor will be incorporated into a flotation column control system at the Middlefork site. Currently the column flotation cells are operated manually, and it is nearly impossible for plant operators to maximize coal recovery while maintaining a high coal yield. The tailings ash analyzer could be used along with other process sensors to permit automatic control of the column flotation circuit.

The tailings ash content can be a good indicator of several parameters including coal recovery and column circuit feed rate. Below normal tailings ash content signifies that coal recovery is being sacrificed, and possibly, that the column flotation cells are being overloaded. High tailings ash content ensures that coal recovery is maximized. However, when the tailings ash content gets abnormally high, it may signify that coal yield is low and that the columns may be underloaded. It is conceivable that a control system could use the column tailings ash content to control the amount of material that is fed to the column or, more likely, the amount of air or frother that are added.

6.4 ADDITIONAL APPLICATIONS

The development of a novel sample presentation system which allows clear images of moving slurry to be obtained and presented to image analysis systems could prove to be very valuable. In any field, in any application where plant operators are controlling processes by visual inspection of slurry or liquid appearance, a sensor of this type could prove helpful in maintaining consistent, effective process control. In the mineral processing industry, obvious opportunities exist for developing video-based sensors for slurry quality determination.

It has been shown that sulfide mineral, phosphate mineral, and kaolin slurries exhibit noticeable color differences as the slurry quality changes. These are just a few of the mineral processing systems where the color of the process streams can be directly related to the material quality. Image analysis of copper flotation froth surface and color has already been investigated as a means of developing video-based quality sensors, but due to the complex nature of the mineral systems and froth structures, these have not proven to be ultimately successful. By using the novel sample presentation system that was developed in this thesis work, clear images of the bulk slurry could be obtained. These images would be more representative of the flotation slurry, and would eliminate the problems associated with image analysis of froth surfaces. These clear slurry images would be a drastic improvement over those that have been used for analysis in mineral processing applications up to this point.

REFERENCES

[1] Kawatra, S.K., 1995, Foreword, *High Efficiency Coal Preparation: An International Symposium*, Littleton, CO, p. iii.

[2] Fonseca, A.G., 1995, "The Challenge of Coal Preparation," *High Efficiency Coal Preparation: An International Symposium*, Littleton, CO, pp. 3-22.

[3] Mikhail, M.W. and Humeniuk, O.E., 1980, "Automatic In-Line Ash Monitor For Coal Slurries," *IFAC Mining, Mineral and Metal Processing*, Montreal, Canada, pp. 389-400.

[4] Cierpisz, S., Mironowicz, W., and Mirkowski, C., 1980, "Instrumentation for Coal Preparation Plants," *IFAC Mining, Mineral and Metal Processing*, Montreal, Canada, pp.375-387.

[5] Kawatra, S.K., and Eisele, T.C., 1990, "Development of an Improved On-Stream Coal Slurry Ash Analyzer," *Control '90 - Mineral and Metallurgical Processing*, SME-AIME, pp. 151-162.

[6] Kawatra, S.K., 1992, "The Theory and Development of a Michigan Tech/Outokumpu Slurry Ash Analyzer," *Emerging Computer Techniques For The Mineral Industry*, pp. 259-270.

[7] Wills, B.A., 1992, Mineral Processing Technology, Pergamon Press, New York, New York.

[8] Meenan, G.F., and Oblad, H.B., 1992, "The Development of Optical Sensors for Coal Processing Applications," *Emerging Computer Techniques for the Minerals Industry*, pp. 195-200.

[9] Newman, T.S., and Jain, A.K., 1995, "A Survey of Automated Visual Inspection," *Computer Vision and Understanding*, Academic Press, pp. 231-262.

[10] Sanford, R.L., Meredith, D.L, and Spears, D.R., 1994, "Computer Vision Applications in Mineral Processing Research," *IEEE*, pp. 2013-2019.

[11] Adel, G.T., Yoon, R.H., and Ehrich, R.W., 1988, "Image Analysis Applications in Mineral Processing," *Proceedings of the Artificial Intelligence in Minerals and Materials Technology Conference*, pp. 19-31.

[12] O'Kane, K.C., Stanley, D.A., Meredith, D.L., and Davis, B.E., 1990, "Preliminary Evaluation of a Computer Vision Sensor for Analysis of Phosphate Tailings," *Control '90*, pp. 137-142.

[13] Adel, G.T, Chandler, M.A., Yoon, R.H., Gutierrez, E.C., and Richardson, J.N., 1992, "Phosphate Analysis by Optical Image Processing: Sensor Development and In-Plant Testing," *Emerging Computer Techniques for the Mineral Industry*, pp. 185-194.

[14] Grove, R.D., Elliot, M.F., and Wiegel, R.L., 1993, "Phosphate Process Stream Composition Measurement by an Image Analysis Technique," *SME Preprint Number 93-130*, Littleton, CO.

[15] Gebhardt, J.E., and Ahn, J.H., 1992, "Color Measurements of Minerals and Mineralized Froths," *SME Preprint Number 92-232*, Littleton, CO.

[16] Oestrich, J.M., Tolley, W.K., and Rice, D.A., 1994, "The Development of a Color Sensor System to Measure Mineral Compositions," *Minerals Engineering*, Vol. 8, Nos. 1/2, pp. 31-39.

[17] Moolman, D.W., Aldrich, C., Van Deventer, J.S.J., and Stange, W.W., 1994, "Digital Image Processing as a Tool for On-Line Monitoring of Froth Flotation Plants," *Minerals Engineering*, Vol. 7, No. 9, pp. 1149-1164.

[18] Moolman, D.W., Aldrich, C., and Van Deventer, J.S.J., 1995, "The Monitoring of Froth Surfaces on Industrial Flotation Plants Using Connectionist Image Processing Techniques," *Minerals Engineering*, Vol. 8, Nos. 1/2, pp. 23-30.

APPENDIX A
SENSOR SOFTWARE

This appendix contains a listing of the Optimas macro files that are currently being used to operate and interface with the video-based ash analyzer at Pittston Coal Company's Middlefork preparation facility. Software development was discussed in Section 4.2, and the work that is continuing with the software was described in Section 6.2. The files included in this appendix are "maindlg.mac", "recab.dlg", "sensor.dlg", and "sensor2.dlg".

MAINDLG.MAC

```
/* Description:
MAINDLG.MAC - Dialog Macro for Tailings Ash Video Sensor

** Purpose:
This macro displays the main dialog box of the system.

**  Loaded libraries:
        optdlg.oml

*/
hLib = LoadMacroLibrary( "optdlg.oml");

// Global Variables

        GLOBAL CHAR
                MacrosPath = PATHVARIABLE : "project/",
                DialogsPath =  PATHVARIABLE : "project/",
                LogPath =  PATHVARIABLE : "project/",
                CalibrationPath =  PATHVARIABLE : "project/",
                MainPath =  PATHVARIABLE : "project/";
        GLOBAL CHAR
                ashresult=NULL, boxtitle="PRESS START", sampgvtxt=NULL,
dskgvtxt=NULL, adjgvtxt=NULL, timlist[,];
        GLOBAL BOOLEAN
                loop=TRUE;
        GLOBAL INTEGER
                logash=0, StopAnalysis=-1, nrow=-1, sel, maxnimag=20;
        GLOBAL LONG
                timbetwsamp, totalnumbint;
        GLOBAL REAL
                avesampgv, avedskgv, adjgv;
        GLOBAL
                DLL_FUNCTION_SPEC SendVolt;


// Dialog Box Variables:
        GLOBAL CHAR      TA_Directory = MacroPathAndName[0, ];
        GLOBAL INTEGER  TA_hWndDlg;
        GLOBAL BOOLEAN          TA_IconOPTIMAS = FALSE;
```

```
// Defined Function

define AshCalc()
{

REAL calibdata[ ];
f2 = OpenFile("c:/optimas5/project/calib.dat");
PositionFile(f2,0,0);
ReadFile(f2,2,calibdata);
CloseFile(f2);
slope=calibdata[0];
intercept=calibdata[1];
calc_ash=(adjgv-intercept)/slope;

boxtitle="Ash Percentage";
ashresult=ToText(calc_ash);

}

define LogAshFunc()
{
        if (! OpenFile("c:/optimas5/project/ash.log", 0x4000)) {
                f = OpenFile("c:/optimas5/project/calib.dat", 0x1002);
                PositionFile(f, 0L, 0);
        }
        else {
                f = OpenFile("c:/optimas5/project/ash.log");
                PositionFile(f, 0L, 2);
        }
                LogDate = GetDateTime( );
                sampgvtxt=ToText(avesampgv);
                dskgvtxt=ToText(avedskgv);
                adjgvtxt=ToText(adjgv);
                OutString =
LogDate:'\t':sampgvtxt:'\t':'\t':dskgvtxt:'\t':'\t':adjgvtxt:'\t':'\t':ashresult:'\r\n';
                WriteFile(f, OutString);
                CloseFile(f);
                boxtitle="Assay Logged";
                DelayMS(5000);
        }
```

```
define GetImages( BOOLEAN dummy)
{
REAL allmeans=0, allmdsk=0;
OPTEnableControl(TA_hWndDlg,4,FALSE);
OPTEnableControl(TA_hWndDlg,5,FALSE);
//OPTEnableControl(TA_hWndDlg,6,FALSE);
//OPTEnableControl(TA_hWndDlg,9,FALSE);

boxtitle=NULL;
ashresult=NULL;
boxtitle="Flushing Tube";

SendVolt=Register("c:/windows/system/nidaq.dll","AO_VWrite","%d%d%d%f");

INTEGER device=1, channel=0;

INTEGER nimag;
REAL volt=0.0;

Acquire();
GainOffsetMonochrome [ 1 ] = 127;
GainOffsetMonochrome [ 0 ] = 255;

for (i=1;i<=2;++i)      // Flush tube
{
        volt=5.0;
        Call(SendVolt,device,channel,volt);

        DelayMS(2000);

        volt=0.0;
        Call(SendVolt,device,channel,volt);

        DelayMS(5000);
}

for (nimag=1;nimag<=maxnimag;++nimag)
{
Acquire();
GainOffsetMonochrome [ 1 ] = 127;
GainOffsetMonochrome [ 0 ] = 255;
```

```
volt=5.0;
Call(SendVolt,device,channel,volt);

DelayMS(2000);

volt=0.0;
Call(SendVolt,device,channel,volt);

DelayMS(5000);

Freeze();
boxtitle="Acquiring image No. ":ToText(nimag);
ImageMask (1, 4.653 : 11.107 ::
5.4741 : 8.3692 ::
6.9795 : 6.0543 ::
9.826 : 4.3849 ::
11.058 : 3.2943 ::
13.439 : 2.6265 ::
13.466 : 1.1129 ::
0.13685 : 1.0907 ::
0.054741 : 11.241 ::
4.653 : 11.107, 0); //  coal portion histogram

Histogram();

meangv=ArROIHistogramStats[0];
allmeans=allmeans+meangv;


ImageMask (1, 6.2678 : 11.174 ::
13.384 : 11.152 ::
13.357 : 6.8334 ::
11.961 : 6.8779 ::
9.7986 : 7.5234 ::
7.8553 : 8.9479 ::
6.3226 : 11.174 ::
6.2678 : 11.174, 0);  // constant disk portion ROI

Histogram();

mdskgv=ArROIHistogramStats[0];
```

```
allmdsk=allmdsk+mdskgv;

}

avesampgv=allmeans/maxnimag;
avedskgv=allmdsk/maxnimag;

adjgv=avesampgv-2.3*(avedskgv-200)/200*avesampgv;

boxtitle="Displaying results";
ashresult=NULL;
AshCalc();
if(logash==0)
{
LogAshFunc();
}

//OPTEnableControl(TA_hWndDlg,6,TRUE);
//OPTEnableControl(TA_hWndDlg,9,TRUE);

}



// Dialog Box Macros:


define TA_InitMacro( )
{
        OPTEnableControl(TA_hWndDlg,9,FALSE);
        timlist="5"::"10"::"15"::"20"::"30"::"45"::"60"::"90"::"120";
}

define TA1_TerminateMacro( )
{
        LoadMacroLibrary(TA_hLib);
        ObjectWildCardList ("TA_.*", 2);
}

define TA_Analyze( )
{
        if(nrow==-1)
        {
```

```
        boxtitle="Select sampling interval first";
        return;
        }
        OPTEnableControl(TA_hWndDlg,9,TRUE);
        GetImages(loop);
        while (StopAnalysis != 0) {
                boxtitle="Waiting to analyze next sample";
                DelayMS(totalnumbint-5000);
                if(StopAnalysis==0) {
                        break;
                }
                GetImages(loop);

        }
        boxtitle="Analysis stopped. Press Start to initiate sample analysis";
        OPTEnableControl(TA_hWndDlg,4,TRUE);
        OPTEnableControl(TA_hWndDlg,5,TRUE);
        OPTEnableControl(TA_hWndDlg,9,FALSE);
}


define TA_Recalibrate( )
{
 RunMacro(MacrosPath: "recalib.mac");
}

define TA_SelectInterval( )
{
        LONG minuts, min2sec=60L;
        nrow=SqueezeSelector(sel);
        CHAR interv=timlist[nrow, ];
        INTEGER found = FromText(interv, minuts);
        timbetwsamp=minuts*min2sec;
        totalnumbint=timbetwsamp*1000;
}


OBJECT_ID TA_Links[,5];
        TA_Links =
        3 : 0 : 0 : ObjectID (ashresult) : 0 ::
        4 : 0 : ObjectID (TA_Analyze) : 0 : 0 ::
        5 : 0 : ObjectID (TA_Recalibrate) : 0 : 0 ::
        6 : 0 : 0 : ObjectID (logash) : 0 ::
        7 : 0 : 0 : ObjectID (boxtitle) : 0 ::
```

```
        9 : 0 : 0 : ObjectID (StopAnalysis) : 0 ::
        10 : ObjectID (timlist) : ObjectID (TA_SelectInterval) : ObjectID (sel) : 0 ;



// .....Display Dialog Box.....

        TA_hLib = LoadMacroLibrary( "optdlg.oml");
        //RunMacro("c:/optimas5/macros/minimize.mac");
        OPTDialogBox(
                DialogsPath : "sensor2.dlg", TA_Links, TA_InitMacro,
TA1_TerminateMacro, hWndVideo, TA_hWndDlg,          ,                    );

//
.....
.....
```

RECAB.DLG

```
A_RESOURCE DIALOG DISCARDABLE LOADONCALL PURE MOVEABLE 23,
40, 362, 169

STYLE WS_POPUP | WS_DLGFRAME | WS_CAPTION | WS_SYSMENU

BEGIN
 CONTROL "Return to Main Window" 1, "BUTTON", WS_CHILD | WS_VISIBLE,
46, 121, 100, 12

 CONTROL "Save Values" 9, "BUTTON", WS_CHILD | WS_VISIBLE, 214, 121, 100,
12

 CONTROL "" 3, "EDIT", WS_CHILD | WS_VISIBLE | WS_BORDER | 0x80L, 57,
69, 65, 12

 CONTROL "" 4, "EDIT", WS_CHILD | WS_VISIBLE | WS_BORDER | 0x80L, 239,
69, 65, 12

 CONTROL "Line Slope" 5, "STATIC", WS_CHILD | WS_VISIBLE, 56, 45, 67, 12

 CONTROL "Line Intercept" 6, "STATIC", WS_CHILD | WS_VISIBLE, 237, 46, 67,
12

 CONTROL "" 7, "BUTTON", WS_CHILD | WS_VISIBLE | 0x7L, 31, 33, 301, 63

 CONTROL "RECALIBRATION SCREEN" 8, "STATIC", WS_CHILD |
WS_VISIBLE | 0x1L, 145, 5, 77, 18

END
```

SENSOR.DLG

```
101 DIALOG DISCARDABLE LOADONCALL PURE MOVEABLE 9, 22, 324, 227

STYLE WS_POPUP | WS_VISIBLE | WS_CAPTION | WS_SYSMENU | 0xC2L

CAPTION "Middlefork Column Tailings Ash Analyzer"
FONT 10, "MS Sans Serif"

BEGIN

 CONTROL "Cancel" 2, "BUTTON", WS_CHILD | WS_VISIBLE | WS_TABSTOP,
39, 194, 50, 14

 CONTROL "START" 4, "BUTTON", WS_CHILD | WS_VISIBLE | WS_TABSTOP,
234, 36, 55, 26

 CONTROL "Go to Calibration Screen" 5, "BUTTON", WS_CHILD | WS_VISIBLE |
WS_TABSTOP, 201, 193, 96, 11

 CONTROL "Ash Percentage:" -1, "BUTTON", WS_CHILD | WS_VISIBLE | 0x7L, 68,
47, 145, 97

 CONTROL "" 3, "STATIC", SS_CENTER | WS_CHILD | WS_BORDER | 0x1L, 113,
89, 59, 16

 CONTROL "Log" 6, "BUTTON", WS_CHILD | WS_VISIBLE | WS_TABSTOP, 244,
120, 41, 12

 CONTROL "mm/dd/yy" 7, "STATIC", WS_CHILD | WS_VISIBLE | WS_GROUP |
0x1L, 18, 16, 34, 10

 CONTROL "hh:mm:ss" 8, "STATIC", WS_CHILD | WS_VISIBLE | WS_GROUP |
0x1L, 18, 31, 34, 10

END
```

SENSOR2.DLG

```
101 DIALOG DISCARDABLE LOADONCALL MOVEABLE 9, 22, 324, 227
STYLE WS_POPUP | WS_VISIBLE | WS_CAPTION | WS_SYSMENU |
WS_DLGFRAME

CAPTION "Middlefork Column Tailings Ash Analyzer"
FONT 10, "MS Sans Serif"

BEGIN

 CONTROL "START" 4, "BUTTON", BS_PUSHBUTTON | WS_CHILD |
WS_VISIBLE, 251, 15, 47, 27

 CONTROL "Calibration Screen" 5, "BUTTON", BS_PUSHBUTTON | WS_CHILD |
WS_VISIBLE, 114, 193, 96, 13

 CONTROL "Ash Percentage:" -1, "BUTTON", WS_CHILD | WS_VISIBLE | 0x7L, 95,
67, 135, 61

 CONTROL "" 3, "STATIC", WS_CHILD | 0x1L, 133, 91, 65, 16

 CONTROL "" 7, "STATIC", WS_CHILD | WS_VISIBLE | 0x1L, 114, 15, 97, 18

 CONTROL "" 8, "STATIC", WS_CHILD | WS_VISIBLE | 0x1L, 11, 15, 93, 15

 CONTROL "Log Ash Values" 6, "BUTTON", WS_CHILD | WS_VISIBLE | 0x3L, 248,
112, 69, 16

 CONTROL "STOP SAMPLE ANALYSIS" 9, "BUTTON", WS_CHILD |
WS_VISIBLE | 0x3L, 116, 159, 97, 27

 CONTROL "" 10, "LISTBOX", WS_CHILD | WS_VISIBLE | WS_BORDER |
WS_VSCROLL | 0x1L, 24, 71, 28, 66

 CONTROL "Sampling Interval (minutes)" 11, "STATIC", WS_CHILD | WS_VISIBLE,
23, 41, 48, 26

END
```

APPENDIX B
SENSOR LOG FILE

This appendix is a partial listing of the log file that is constantly updated by the video-based ash analyzer during on-line operation. This file is used to monitor the performance of the ash analyzer, and yields information about how the column tailings material at the Middlefork site has changed over time. For each measurement that is recorded, the date and time, slurry gray level, illumination standard gray level, adjusted slurry gray level, and the predicted ash measurement that the analyzer software displays are all included. The following is partial listing of the log file that was generated during the first on-line testing of the ash analyzer.

ASH.LOG

Date and Time	Sample GV	Disk GV	Adjusted GV	Calculated Ash
Wed Oct 02 15:52:04 1996	85.9692	85.9878	170	211.061
Wed Oct 02 16:03:10 1996	85.9318	85.9491	170	211.061
Wed Oct 02 16:14:15 1996	85.9712	85.9802	170	211.061
Thu Oct 03 13:39:40 1996	93.5608	205.664	93	99.1
Thu Oct 03 14:06:22 1996	97.836	209.769	86.8445	90.1497
Thu Oct 10 10:02:24 1996	191.543	249.693	82.0814	83.2239
Thu Oct 10 10:13:27 1996	120.702	223.335	88.3121	92.2836
Thu Oct 10 10:53:34 1996	89.8078	199.276	90.5552	95.545
Thu Oct 10 11:01:29 1996	91.7341	200.651	91.0475	96.261
Thu Oct 10 11:12:32 1996	92.6085	199.92	92.6938	98.6548
Thu Oct 10 11:23:27 1996	94.4101	202.185	92.0377	97.7008
Thu Oct 10 11:34:30 1996	96.2962	204.142	91.7089	97.2226
Thu Oct 10 11:45:33 1996	98.6475	204.995	92.9807	99.0719
Thu Oct 10 11:56:36 1996	102.453	207.05	94.1466	100.767
Thu Oct 10 12:07:39 1996	105.616	209.191	94.4524	101.212
Thu Oct 10 12:18:42 1996	113.584	213.783	95.5812	102.853
Thu Oct 10 12:29:45 1996	116.964	216.484	94.7915	101.705
Thu Oct 10 12:40:48 1996	120.672	218.584	94.8823	101.837
Thu Oct 10 12:51:51 1996	124.665	220.643	95.0696	102.109
Thu Oct 10 13:02:54 1996	126.256	221.561	94.9505	101.936
Thu Oct 10 13:13:57 1996	127.056	221.746	95.2823	102.419
Thu Oct 10 14:05:10 1996	103.201	204.351	98.0373	142.55
Thu Oct 10 14:19:37 1996	101.514	204.172	96.6437	77.4183
Thu Oct 10 14:30:41 1996	103.086	205.362	96.7289	77.5423
Thu Oct 10 14:41:37 1996	102.135	204.95	96.3207	76.9487
Thu Oct 10 14:52:40 1996	102.034	205.191	95.9421	76.3983
Thu Oct 10 15:03:44 1996	104.249	205.974	97.0872	78.0633
Thu Oct 10 15:14:47 1996	105.216	206.158	97.7645	79.0481
Thu Oct 10 15:25:51 1996	102.163	202.773	98.9055	80.7071
Thu Oct 10 15:36:54 1996	101.009	202.14	98.5234	80.1515
Thu Oct 10 15:47:58 1996	101.154	202.259	98.5262	80.1556
Thu Oct 10 15:59:02 1996	100.194	201.361	98.6262	80.301
Thu Oct 10 16:10:05 1996	100.671	201.373	99.0814	80.9628
Thu Oct 10 16:21:02 1996	97.4268	199.779	97.675	78.9178
Thu Oct 10 16:38:52 1996	93.8663	198.13	95.8845	71.0799
Thu Oct 10 17:14:47 1996	96.3354	198.21	98.318	74.6184
Thu Oct 10 17:50:43 1996	99.9579	200.454	99.4365	76.2446
Thu Oct 10 18:26:39 1996	107.799	202.534	104.657	83.835
Thu Oct 10 19:02:35 1996	111.513	206.257	103.489	82.1372
Thu Oct 10 19:38:31 1996	99.1197	199.215	100.014	77.0846
Thu Oct 10 20:14:26 1996	95.7383	195.774	100.391	77.6323
Thu Oct 10 20:50:22 1996	98.7555	197.307	101.814	79.7014
Thu Oct 10 21:26:18 1996	97.2363	196.27	101.407	79.1097
Thu Oct 10 22:02:14 1996	92.2174	192.362	100.318	77.526
Thu Oct 10 22:38:10 1996	95.3452	194.876	100.963	78.4645
Thu Oct 10 23:14:05 1996	103.719	202.691	100.51	77.8054

Date and Time	Sample GV	Disk GV	Adjusted GV	Calculated Ash
Thu Oct 10 23:50:01 1996	106.167	205.385	99.5922	76.4711
Fri Oct 11 00:25:57 1996	107.42	206.948	98.8372	75.3733
Fri Oct 11 01:01:53 1996	109.277	208.449	98.6593	75.1146
Fri Oct 11 01:37:49 1996	109.205	208.214	98.8898	75.4498
Fri Oct 11 02:13:44 1996	109.693	208.768	98.6322	75.0751
Fri Oct 11 02:49:40 1996	110.496	209.158	98.8584	75.404
Fri Oct 11 03:25:35 1996	112.098	210.734	98.26	74.534
Fri Oct 11 04:01:31 1996	114.685	213.903	96.3479	71.7537
Fri Oct 11 04:37:26 1996	114.759	212.421	98.366	74.6881
Fri Oct 11 05:13:22 1996	99.8697	199.902	99.9818	77.0375
Fri Oct 11 05:49:17 1996	96.4419	197.743	98.9448	75.5297
Fri Oct 11 06:25:13 1996	98.8218	198.652	100.353	77.5775
Sat Oct 12 15:34:52 1996	102.949	188.573	116.477	101.022
Sat Oct 12 16:10:47 1996	104.613	190.856	115.613	99.7663
Sat Oct 12 16:46:43 1996	106.704	192.843	115.485	99.5803
Sat Oct 12 17:22:39 1996	108.182	194.372	115.184	99.1425
Sat Oct 12 17:58:35 1996	106.603	193.131	115.023	98.9085
Sat Oct 12 19:10:27 1996	105.438	192.69	114.301	97.8587
Sat Oct 12 19:46:23 1996	105.638	193.231	113.861	97.2189
Sat Oct 12 20:22:19 1996	105.064	193.757	112.607	95.3947
Sat Oct 12 20:58:15 1996	103.59	193.371	111.487	93.7659
Sat Oct 12 21:34:11 1996	101.742	193.15	109.757	91.2513
Sat Oct 12 22:10:06 1996	101.467	193.653	108.873	89.9656
Sat Oct 12 22:46:02 1996	100.161	192.319	109.008	90.1625
Sat Oct 12 23:21:58 1996	99.2418	191.56	108.874	89.9671
Sat Oct 12 23:57:54 1996	98.651	190.302	109.654	91.1009
Sun Oct 13 00:33:50 1996	97.5481	189.947	108.826	89.8971
Sun Oct 13 01:09:46 1996	96.5848	188.194	109.698	91.166
Sun Oct 13 01:45:42 1996	102.146	194.865	108.178	88.9554
Sun Oct 13 02:21:38 1996	100.918	194.612	107.172	87.4924
Sun Oct 13 02:57:34 1996	102.755	196.141	107.315	87.7006
Sun Oct 13 03:33:29 1996	103.586	196.913	107.264	87.6261
Sun Oct 13 04:09:25 1996	102.127	196.289	106.485	86.4928
Sun Oct 13 04:45:21 1996	102.261	195.992	106.975	87.2052
Sun Oct 13 05:21:17 1996	102.356	196.452	106.533	86.5632
Sun Oct 13 05:57:13 1996	104.871	199.2	105.836	85.5492
Sun Oct 13 06:33:09 1996	104.688	198.849	106.073	85.8943
Sun Oct 13 07:09:05 1996	100.976	195.557	106.136	85.9853
Sun Oct 13 07:45:00 1996	101.514	196.036	106.142	85.9948
Sun Oct 13 08:20:56 1996	100.177	195.413	105.462	85.006
Sun Oct 13 08:56:52 1996	102.342	197.551	105.225	84.6612
Sun Oct 13 09:32:48 1996	103.004	198.458	104.83	84.0872
Sun Oct 13 10:08:44 1996	97.2167	192.294	105.832	85.544
Sun Oct 13 10:44:40 1996	98.0138	193.614	105.212	84.6424
Sun Oct 13 11:20:35 1996	98.2835	194.424	104.586	83.7328
Sun Oct 13 11:56:31 1996	99.5436	195.409	104.799	84.0424
Sun Oct 13 12:32:27 1996	100.765	196.837	104.43	83.506
Sun Oct 13 13:08:23 1996	102.109	198.098	104.342	83.3779
Sun Oct 13 13:44:19 1996	104.011	199.265	104.89	84.1736

Date and Time	Sample GV	Disk GV	Adjusted GV	Calculated Ash
Sun Oct 13 14:20:14 1996	104.177	199.818	104.395	83.4543
Sun Oct 13 14:56:10 1996	103.849	200.423	103.343	81.925
Sun Oct 13 15:32:06 1996	105.342	201.522	103.498	82.1509
Sun Oct 13 16:08:02 1996	107.812	203.13	103.931	82.7799
Sun Oct 13 16:43:58 1996	107.445	203.078	103.642	82.3602
Sun Oct 13 17:19:53 1996	107.895	203.158	103.976	82.8451
Sun Oct 13 17:55:49 1996	106.867	202.525	103.763	82.5354
Sun Oct 13 18:31:45 1996	106.036	201.628	104.051	82.9544
Sun Oct 13 19:07:40 1996	105.337	201.327	103.73	82.488
Sun Oct 13 19:43:36 1996	104.721	200.497	104.122	83.058
Sun Oct 13 20:19:32 1996	104.789	200.546	104.131	83.0702
Sun Oct 13 20:55:28 1996	103.62	199.497	104.219	83.1988
Sun Oct 13 21:31:23 1996	102.805	198.74	104.295	83.3088
Sun Oct 13 22:07:19 1996	101.445	197.856	103.947	82.8029
Sun Oct 13 22:43:15 1996	100.356	196.903	103.93	82.7789
Sun Oct 13 23:19:11 1996	99.654	196.635	103.511	82.1685
Sun Oct 13 23:55:07 1996	98.6645	195.569	103.693	82.4331
Mon Oct 14 00:31:02 1996	98.2969	195.227	103.693	82.4333
Mon Oct 14 01:06:58 1996	99.0747	196.132	103.481	82.1261
Mon Oct 14 01:42:54 1996	103.544	200.289	103.2	81.7163
Mon Oct 14 02:18:50 1996	102.477	197.781	105.091	84.4668
Mon Oct 14 02:54:46 1996	101.832	192.293	110.858	92.8522
Mon Oct 14 03:30:42 1996	100.484	191.954	109.782	91.2868
Mon Oct 14 04:06:38 1996	101.34	192.857	109.664	91.116
Mon Oct 14 04:42:34 1996	99.8103	192.433	108.495	89.4167
Mon Oct 14 05:18:30 1996	100.251	192.39	109.025	90.186
Mon Oct 14 05:54:26 1996	99.5085	191.764	108.934	90.0538
Mon Oct 14 06:30:22 1996	99.4397	191.729	108.898	90.0021
Mon Oct 14 07:06:17 1996	99.5702	191.59	109.2	90.4409
Mon Oct 14 07:42:13 1996	99.6884	191.978	108.885	89.9834
Mon Oct 14 08:18:09 1996	98.6942	190.861	109.066	90.2467
Mon Oct 14 08:54:05 1996	95.1669	187.371	108.988	90.1329
Mon Oct 14 09:30:01 1996	94.9321	187.153	108.957	90.0878
Mon Oct 14 10:05:57 1996	95.0737	187.136	109.139	90.3525
Mon Oct 14 10:41:53 1996	93.9064	185.725	109.322	90.6192
Mon Oct 14 11:17:49 1996	92.7693	185.217	108.54	89.4817
Mon Oct 14 11:53:44 1996	94.1507	186.117	109.182	90.4155
Mon Oct 14 12:29:40 1996	94.9327	186.953	109.176	90.4067
Mon Oct 14 13:05:36 1996	96.1844	188.5	108.905	90.0126
Mon Oct 14 13:41:32 1996	98.077	189.99	109.367	90.6839
Mon Oct 14 14:17:28 1996	98.0607	189.529	109.869	91.4134
Mon Oct 14 14:53:24 1996	98.7469	190.139	109.945	91.5245
Mon Oct 14 15:29:20 1996	99.5489	191.057	109.786	91.2939
Mon Oct 14 16:05:16 1996	99.7907	191.335	109.734	91.2181
Mon Oct 14 16:41:12 1996	100.184	191.684	109.765	91.2632
Mon Oct 14 17:17:07 1996	100.464	191.759	109.984	91.5818
Mon Oct 14 17:53:03 1996	101.082	192.683	109.587	91.0044
Mon Oct 14 18:28:59 1996	101.027	192.621	109.6	91.0223
Mon Oct 14 19:04:55 1996	100.384	192.134	109.465	90.8266

Date and Time	Sample GV	Disk GV	Adjusted GV	Calculated Ash
Mon Oct 14 19:40:51 1996	98.3271	190.433	109.145	90.3619
Mon Oct 14 20:16:47 1996	98.2615	190.384	109.128	90.3361
Mon Oct 14 20:52:43 1996	97.9702	190.486	108.689	89.6982
Mon Oct 14 21:28:39 1996	97.3491	190.018	108.524	89.4588
Mon Oct 14 22:04:35 1996	97.3138	189.596	108.957	90.0878
Mon Oct 14 22:40:31 1996	96.3167	188.8	108.723	89.747
Mon Oct 14 23:16:27 1996	96.2861	188.943	108.529	89.4657
Mon Oct 14 23:52:23 1996	96.0628	188.679	108.57	89.5246
Tue Oct 15 00:28:18 1996	95.1651	188.004	108.294	89.1231
Tue Oct 15 01:04:14 1996	94.9829	187.941	108.155	88.9224
Tue Oct 15 01:40:10 1996	94.6297	187.587	108.138	88.8965
Tue Oct 15 02:16:06 1996	95.0412	187.672	108.515	89.4458
Tue Oct 15 02:52:02 1996	94.4909	187.344	108.243	89.0499
Tue Oct 15 03:27:58 1996	93.8953	186.969	107.967	88.6476
Tue Oct 15 04:03:54 1996	94.0008	186.859	108.207	88.9969
Tue Oct 15 04:39:50 1996	93.1895	186.244	107.932	88.5974
Tue Oct 15 05:15:45 1996	92.5662	185.891	107.585	88.093
Tue Oct 15 05:51:41 1996	91.931	185.046	107.741	88.3195
Tue Oct 15 06:27:37 1996	91.5593	184.736	107.632	88.1607
Tue Oct 15 07:03:33 1996	91.4726	184.385	107.899	88.5495
Tue Oct 15 07:39:29 1996	90.6194	183.934	107.362	87.7691
Tue Oct 15 08:15:25 1996	94.1604	187.483	107.715	88.2814
Tue Oct 15 08:51:21 1996	95.6379	188.965	107.775	88.3691
Tue Oct 15 09:27:17 1996	94.9167	188.273	107.717	88.2846
Tue Oct 15 10:03:13 1996	91.073	184.463	107.345	87.7442
Tue Oct 15 10:30:39 1996	89.8124	183.07	107.298	87.6755
Tue Oct 15 11:03:12 1996	108.591	198.898	109.967	73.5261
Tue Oct 15 11:14:08 1996	109.188	198.592	110.956	74.9641
Tue Oct 15 11:24:26 1996	109.681	199.013	110.926	74.9201
Tue Oct 15 11:35:23 1996	98.8957	186.141	114.657	80.3459
Tue Oct 15 11:46:20 1996	96.2757	183.764	114.252	79.7566
Tue Oct 15 11:57:17 1996	96.1789	183.473	114.459	80.0581
Tue Oct 15 12:15:12 1996	96.182	184.12	113.747	79.0225
Tue Oct 15 12:51:21 1996	102.866	189.588	115.182	81.1097
Tue Oct 15 13:02:16 1996	103.98	190.988	114.757	80.4906
Tue Oct 15 13:45:55 1996	118.499	202.675	114.854	80.6316
Tue Oct 15 13:56:49 1996	119.584	203.339	114.992	80.833
Tue Oct 15 14:07:43 1996	120.341	204.203	114.525	80.1533
Tue Oct 15 14:18:37 1996	120.461	204.591	114.101	79.538
Tue Oct 15 14:29:31 1996	120.846	204.726	114.279	79.7955
Tue Oct 15 14:50:20 1996	121.793	204.841	115.013	73.4477
Tue Oct 15 15:01:14 1996	121.876	204.906	115	73.4291
Tue Oct 15 15:12:08 1996	123.012	205.456	115.294	73.856
Tue Oct 15 15:23:02 1996	122.874	205.827	114.64	72.905
Tue Oct 15 00:28:18 1996	95.1651	188.004	108.294	89.1231
Tue Oct 15 01:04:14 1996	94.9829	187.941	108.155	88.9224
Tue Oct 15 01:40:10 1996	94.6297	187.587	108.138	88.8965
Tue Oct 15 02:16:06 1996	95.0412	187.672	108.515	89.4458
Tue Oct 15 02:52:02 1996	94.4909	187.344	108.243	89.0499

Date and Time	Sample GV	Disk GV	Adjusted GV	Calculated Ash
Tue Oct 15 03:27:58 1996	93.8953	186.969	107.967	88.6476
Tue Oct 15 04:03:54 1996	94.0008	186.859	108.207	88.9969
Tue Oct 15 04:39:50 1996	93.1895	186.244	107.932	88.5974
Tue Oct 15 05:15:45 1996	92.5662	185.891	107.585	88.093
Tue Oct 15 05:51:41 1996	91.931	185.046	107.741	88.3195
Tue Oct 15 06:27:37 1996	91.5593	184.736	107.632	88.1607
Tue Oct 15 07:03:33 1996	91.4726	184.385	107.899	88.5495
Tue Oct 15 07:39:29 1996	90.6194	183.934	107.362	87.7691
Tue Oct 15 08:15:25 1996	94.1604	187.483	107.715	88.2814
Tue Oct 15 08:51:21 1996	95.6379	188.965	107.775	88.3691
Tue Oct 15 09:27:17 1996	94.9167	188.273	107.717	88.2846
Tue Oct 15 10:03:13 1996	91.073	184.463	107.345	87.7442
Tue Oct 15 10:30:39 1996	89.8124	183.07	107.298	87.6755
Tue Oct 15 11:03:12 1996	108.591	198.898	109.967	73.5261
Tue Oct 15 11:14:08 1996	109.188	198.592	110.956	74.9641
Tue Oct 15 11:24:26 1996	109.681	199.013	110.926	74.9201
Tue Oct 15 11:35:23 1996	98.8957	186.141	114.657	80.3459
Tue Oct 15 11:46:20 1996	96.2757	183.764	114.252	79.7566
Tue Oct 15 11:57:17 1996	96.1789	183.473	114.459	80.0581
Tue Oct 15 12:15:12 1996	96.182	184.12	113.747	79.0225
Tue Oct 15 12:51:21 1996	102.866	189.588	115.182	81.1097
Tue Oct 15 13:02:16 1996	103.98	190.988	114.757	80.4906
Tue Oct 15 13:45:55 1996	118.499	202.675	114.854	80.6316
Tue Oct 15 13:56:49 1996	119.584	203.339	114.992	80.833
Tue Oct 15 14:07:43 1996	120.341	204.203	114.525	80.1533
Tue Oct 15 14:18:37 1996	120.461	204.591	114.101	79.538
Tue Oct 15 14:29:31 1996	120.846	204.726	114.279	79.7955
Tue Oct 15 14:50:20 1996	121.793	204.841	115.013	73.4477
Tue Oct 15 15:01:14 1996	121.876	204.906	115	73.4291
Tue Oct 15 19:17:51 1996	122.074	202.73	118.241	78.1409
Tue Oct 15 19:53:45 1996	121.483	202.796	117.577	77.1759
Tue Oct 15 20:29:39 1996	120.016	201.824	117.498	77.0615
Tue Oct 15 21:05:33 1996	118.904	201.196	117.269	76.7281
Tue Oct 15 21:41:27 1996	118.757	200.817	117.64	77.2677
Tue Oct 15 22:17:21 1996	117.403	199.957	117.461	77.008
Tue Oct 15 22:53:15 1996	116.361	198.962	117.75	77.4281
Tue Oct 15 23:29:09 1996	116.139	199.13	117.302	76.7761
Wed Oct 16 00:05:03 1996	118.128	199.212	119.199	79.5337
Wed Oct 16 00:40:57 1996	116.326	199.494	117.003	76.3412
Wed Oct 16 01:16:51 1996	118.036	199.915	118.152	78.012
Wed Oct 16 01:52:45 1996	118.965	200.698	118.01	77.8054
Wed Oct 16 02:28:39 1996	118.617	200.937	117.339	76.8296
Wed Oct 16 03:04:33 1996	117.086	200.591	116.29	75.3046
Wed Oct 16 03:40:27 1996	116.671	200.307	116.259	75.2596
Wed Oct 16 04:16:21 1996	116.321	199.718	116.698	75.8979
Wed Oct 16 04:52:14 1996	115.75	199.101	116.947	76.2594
Wed Oct 16 05:28:08 1996	115.762	199.049	117.028	76.3778
Wed Oct 16 06:04:02 1996	119.911	199.251	120.944	82.0716
Wed Oct 16 06:41:18 1996	115.811	199.708	116.199	75.1724

Date and Time	Sample GV	Disk GV	Adjusted GV	Calculated Ash	
Wed Oct 16 07:17:13 1996	114.736	198.176	117.143	76.5451	
Wed Oct 16 07:53:07 1996	115.752	198.845	117.29	76.7581	
Wed Oct 16 08:29:01 1996	118.194	198.748	119.895	80.5464	
Wed Oct 16 09:04:55 1996	117.132	199.369	117.982	77.7654	
Wed Oct 16 09:25:50 1996	118.765	199.677	119.207	79.5457	
Wed Oct 16 10:01:44 1996	118.104	199.018	119.439	79.8827	
Wed Oct 16 10:37:39 1996	117.307	197.399	120.816	81.885	
Wed Oct 16 11:13:33 1996	117.727	197.742	120.784	81.8389	
Wed Oct 16 11:49:27 1996	117.96	197.997	120.677	81.6829	
Wed Oct 16 12:25:22 1996	119.288	198.821	120.905	82.0148	
Wed Oct 16 13:01:16 1996	119.715	199.508	120.393	81.2702	
Wed Oct 16 13:37:11 1996	122.152	199.876	122.326	84.0805	
Wed Oct 16 14:13:05 1996	121.512	200.311	121.078	82.267	
Wed Oct 16 14:48:59 1996	122.702	200.381	122.165	83.8466	
Wed Oct 16 15:24:53 1996	124.239	201.82	121.639	83.0826	
Wed Oct 16 16:00:48 1996	127.681	202.294	124.314	86.9711	
Wed Oct 16 16:36:42 1996	125.355	201.104	123.763	86.1705	
Wed Oct 16 17:12:36 1996	126.447	202.196	123.254	85.4306	
Wed Oct 16 17:48:30 1996	126.621	202.471	123.022	85.0938	
Wed Oct 16 18:24:24 1996	126.468	202.262	123.179	85.3216	
Wed Oct 16 19:00:19 1996	125.852	202.265	122.574	84.4413	
Wed Oct 16 19:36:13 1996	124.281	201.2	122.565	84.4292	
Wed Oct 16 20:12:07 1996	123.87	200.912	122.57	84.4361	
Wed Oct 16 20:48:01 1996	118.998	193.544	127.833	92.0889	
Wed Oct 16 21:23:55 1996	117.631	192.137	128.268	92.7211	
Wed Oct 16 21:59:49 1996	116.59	191.459	128.041	92.3908	
Wed Oct 16 22:35:44 1996	115.709	190.683	128.107	92.4866	
Wed Oct 16 23:11:38 1996	114.92	190.512	127.46	91.546	
Wed Oct 16 23:47:32 1996	114.283	189.619	127.926	92.2233	
Thu Oct 17 00:23:26 1996	114.57	189.515	128.385	92.8917	
Thu Oct 17 00:59:21 1996	114.862	189.244	129.07	93.8869	
Thu Oct 17 01:35:14 1996	117.989	190.961	130.253	95.6073	
Thu Oct 17 02:11:09 1996	118.188	191.153	130.212	95.5471	
Thu Oct 17 02:47:03 1996	116.039	189.395	130.192	95.5186	
Thu Oct 17 03:22:57 1996	115.768	188.321	131.316	97.1531	
Thu Oct 17 03:58:52 1996	115.056	187.167	132.037	98.2009	
Thu Oct 17 04:34:46 1996	114.361	185.312	133.678	100.588	
Thu Oct 17 05:10:40 1996	112.693	183.446	134.147	101.269	
Thu Oct 17 05:46:34 1996	113.084	183.84	134.1	101.201	
Thu Oct 17 06:22:28 1996	112.73	183.94	133.55	100.402	
Thu Oct 17 06:58:22 1996	114.469	184.756	134.535	101.834	
Thu Oct 24 10:34:06 1996	98.5901	174.183	127.86	92.1285	1
Thu Oct 24 10:49:21 1996	110.672	195.052	116.97	53.7556	2
Thu Oct 24 11:18:54 1996	119.707	205.678	111.891	71.0891	3
Thu Oct 24 11:43:32 1996	117.95	205.006	111.16	70.0266	4
Thu Oct 24 11:59:35 1996	117.841	205.064	110.979	69.7632	5
Thu Oct 24 12:10:32 1996	117.99	204.86	111.395	70.3684	7
Thu Oct 24 12:21:28 1996	118.002	204.731	111.582	70.6398	8
Thu Oct 24 12:29:28 1996	110.786	201.066	109.427	67.5071	

Date and Time	Sample GV	Disk GV	Adjusted GV	Calculated Ash
Thu Oct 24 12:40:24 1996	107.218	199.086	108.345	65.9339
Thu Oct 24 12:51:20 1996	106.212	196.651	110.304	68.7812
Thu Oct 24 13:02:16 1996	105.281	195.015	111.316	70.2532
Thu Oct 24 10:34:06 1996	98.5901	174.183	127.86	92.1285 1
Thu Oct 24 10:49:21 1996	110.672	195.052	116.97	53.7556 2

VITA

Peter Lawrence Dunn was born November 21, 1972 in Baltimore, Maryland. He lived in Baltimore until 1983 when he moved to Woodbridge, Virginia. He attended Woodbridge Senior High School and graduated with honors in the spring of 1990. In the fall of 1990 he began his undergraduate studies at Virginia Tech. He received several scholarships and the A.P. Boxley Award during his undergraduate studies. He graduated from Virginia Tech in the spring of 1994 with a B.S. degree in Mining and Minerals Engineering. Following graduation Peter stayed at Virginia Tech, choosing to further his education in the area of mineral processing. He was married to Michelle Jane in the summer of 1996 and remained at Virginia Tech until earning his M.S. degree in Mining and Minerals Engineering in the fall of 1996. It is planned that he will join DuPont in Starke, Florida as a process engineer at their heavy minerals sands operation. He is a member of the Society for Mining, Metallurgy, and Exploration, and Tau Beta Pi.

Peter Lawrence Dunn